UNIVERSITY OF CALIFORNIA,
IRVINE

Drugs, Decisions, Desire, and DREADDs: Exploring Ventral Pallidum GABAergic Neuron Function in Motivated Behavior

DISSERTATION

submitted in partial satisfaction of the requirements
for the degree of

DOCTOR OF PHILOSOPHY

in Biological Sciences

by

Mitchell Farrell

Dissertation Committee:
Associate Professor Stephen V. Mahler, Chair
Professor Marcelo A. Wood
Associate Professor Christie D. Fowler

2022

DEDICATION

To

my partner, brothers, parents, grandparents, and friends—

graduate school was possible through you.

'*In order to understand bird flight, we have to understand aerodynamics; only then does the structure of feathers and the different shapes of bird's wings make sense.*'
-David Marr

'*Everybody wanna be a bodybuilder, but don't nobody wanna lift no heavy-ass weight.*'
-Ronnie Coleman

'*The true sign of intelligence is not knowledge but imagination.*'
-Albert Einstein

'*Never forget where you came from.*'
-Melanie Farrell

TABLE OF CONTENTS

List of Figures…..……..……..……iv

Acknowledgements……..……..……..……v

Vita…….....vi

Abstract of the Dissertation….....ix

Introduction……..……..……..……1

Chapter 1: Ventral pallidum is essential for cocaine relapse after voluntary abstinence…….……...12

Chapter 2: Ventral pallidum GABA neurons bidirectionally control opioid relapse across rat models..……..……..……..37

Chapter 3: Ventral pallidum GABA neurons mediate motivation underlying risky choice……..……...…….66

General Discussion..……..…….98

References…….……..113

LIST OF FIGURES

Figure		Page
1	Schematic of experimental timeline.	15
2	Viral expression in hM4Di misses and eGFP controls.	16
3	Punishment-resistant rats are more prone than punishment sensitive rats to cue-induced, but not cocaine-primed relapse.	24
4	Inhibitory DREADD localization in VP.	25
5	VP inhibition reduces relapse-like behavior, especially in punishment resistant rats.	27
6	VP inhibition decreases cocaine-induced rearing, but not distance traveled.	29
7	VP subregion Fos expression after relapse-like behavior.	31
8	Breakdown of self-administration, punishment resistance, and reinstatement by sex.	32
9	Behavioral testing schematic, training data, and vehicle-day reinstatement following punishment- versus extinction-induced abstinence.	49
10	Rostral, but not caudal, VP Fos correlates with remifentanil seeking.	51
11	VP^{GABA} DREADD localization and hM3Dq validation.	52
12	Following punishment, inhibiting or stimulating VP^{GABA} neurons bidirectionally controls remifentanil seeking.	54
13	Following extinction, stimulating VP^{GABA} neurons augments reinstatement in a cue- and context-dependent manner.	55
14	No impact of inhibiting or stimulating VP^{GABA} neurons on remifentanil self-administration.	57
15	Anatomical, cellular, and functional characterization of hM4Di DREADDs in VP^{GABA} neurons.	79
16	Inhibiting VP^{GABA} neurons reduces risky choice.	81
17	VP^{GABA} neuron inhibition increases latency to select the large/risky option, and trial omissions.	82
18	Inhibiting VP^{GABA} neurons spares the ability to choose between large and small rewards, while decreasing motivation.	84
19	Inhibiting VP^{GABA} neurons reduces responding for palatable food and chow in hungry rats, but only reduces responding for palatable food (not chow) in sated rats.	85
20	Inhibiting VP^{GABA} neurons reduces progressive ratio motivation for palatable food, without impairing free access palatable chocolate intake.	86
21	Inhibiting VP^{GABA} neurons increases avoidance latency, without affecting avoidance propensity or escape latency.	88
22	Motor and affective reactions to footshock unaffected by inhibiting VP^{GABA} neurons.	89

ACKNOWLEDGEMENTS

I would like to thank my mentors, Drs. Stephen Mahler and Dr. Margaret Martinetti, who molded me into the scientist I am today. Dr. Mahler invested heavily in me when I needed it most, and for that I am immensely grateful.

I would like to thank my committee members, Drs. Christie Fowler and Marcelo Wood, and my advancement committee members, Drs. Sean Ostlund and Georg Striedter, for guiding me over the years.

I would like to thank UC Irvine faculty that had a lasting impact on my thinking: Drs. Bruce McNaughton, Mike Yassa, and Norbert Fortin.

I would like to thank my collaborators for their support through the years: Drs. Lauren Faget, Tom Hnasko, and Stan Floresco.

I would like to thank Gary Roman for his consistently jovial spirit, northeastern sensibility, and authentic, humorous outlook on life.

I would like to thank Mahler Lab members, past and present, who have closely shared in the joys and tribulations of science: Hannah Schoch, Christina Ruiz, Erik Castillo, Iohanna Pagnoncelli, Stephanie Lenogue, Gagandeep Lal, Jeff Huang, Jenny Cevallos, Siyu Liu, Christine Khanbijian, Chrissy Perrone, Eden Harder, Jeanine Esteban, Yiyan Xie, Qiying Ye, Maricela Martinez, Kate Lawson, Sophie Levis, Drew Justeson, Erica Ramirez and others.

I would like to thank my funding sources including F31DA048578, R25GM055246, T32NS045540, and F99NS120641.

Chapter 1 of this dissertation is modified from a manuscript titled ‘Ventral pallidum is essential for cocaine relapse after voluntary abstinence in rats’ published in *Neuropsychopharmacology* with permission from Springer Nature, and was in collaboration with Christina M. Ruiz, Erik Castillo, Lauren Faget, Christine Khanbijian, Siyu Liu, Hannah Schoch, Gerardo Rojas, Michelle Y. Huerta, Thomas S. Hnasko, Stephen V. Mahler. Chapter 2 of this dissertation is modified from a manuscript titled ‘Ventral pallidum GABA neurons bidirectionally control opioid relapse across rat behavioral models’ published in *Addiction Neuroscience* with permission from Elsevier, and was in collaboration with Jeanine Sandra D. Esteban, Qiying Ye, Yiyan Xie, and Stephen V. Mahler. Chapter 3 of this dissertation is modified from a manuscript titled ‘Ventral pallidum GABA neurons mediate motivation underlying risky choice’ published in *Journal of Neuroscience* with permission from Society for Neuroscience, and was in collaboration with Stan B. Floresco, Jeanine Sandra D. Esteban, Lauren Faget, Thomas S. Hnasko, and Stephen V. Mahler.

VITA

Mitchell Farrell

EDUCATION

Fall 2016-Summer 2022
University of California Irvine, Department of Neurobiology & Behavior,
PhD, Stephen Mahler Lab, 3.97 GPA

Fall 2012-Spring 2016
The College of New Jersey, B.A. (Psychology, Magna Cum Laude)
Honors Program, Phi Beta Kappa, 3.79 GPA

GRANTS

NIH Blueprint Diversity Specialized Predoctoral to Postdoctoral Advancement in Neuroscience Award (D-SPAN/F99-K00; 2020-2026): Ventral Pallidum Circuits in Motivation, Risky Decision Making, and Opioid Addiction (1F99NS120641-01; $389,620)

National Institute on Drug Abuse Individual Predoctoral NRSA Fellowship (2019-2020): Ventral Pallidum GABA Circuits in Risky Decision Making (1F31DA048578; $104,929)

National Institute of Neurological Disorders and Stroke Epilepsy Research Training Program (2018; T32 5T32NS045540-15; $23,844)

National Institute of General Medical Sciences Education Projects (2016; R25 GM055246-25; $5,333)

PUBLICATIONS

Martinez MX, **Farrell MR**, Mahler SV (*in press*). Pathway-specific chemogenetic manipulation by applying ligand to axonally-expressed DREADDs, Book chapter: Vectorology for Optogenetics and Chemogenetics.

Farrell MR, Ye Q, Xie Y, Esteban JSD, Mahler SV (2022). Ventral pallidum GABA neurons bidirectionally control opioid relapse across rat behavioral models. *Addiction Neuroscience*, 100026(3).

Farrell MR, Esteban JSD, Faget L, Floresco S, Hnasko TS, Mahler SV (2021). Ventral pallidum GABA neurons mediate motivation underlying risky choice. *Journal of Neuroscience*, 41(20):4500–4513.

***Farrell MR**, Ruiz CM, Castillo E, Faget L, Khanbijian C, Liu S, Schoch H, Rojas G, Hnasko TS, Mahler SV. (2019). Ventral pallidum is essential for cocaine relapse after voluntary abstinence in rats. *Neuropsychopharmacology*, 44(13), 2174-2185.

*Featured in “Research Highlight” article: Ventral pallidum: a promising target for addiction intervention. McGovern DJ & Root DH, *Neuropsychopharmacology*.
*Cover Image (December 2019)

Bonaventura J, Eldridge MA, Hu F, Gomez JL, Sanchez-Soto M, Abramyan AM, Lam S, Boehm M, Ruiz CM, **Farrell MR**, Moreno A, Faress IMG, Andersen N, Lin JY, Moaddel R, Morris P, Shi

L, Sibley DR, Mahler SV, Nabavi S, Pomper MG, Bonci A, Horti AG, Richmond BJ, Michaelides M. (2019). High- potency ligands for DREADD imaging and activation in rodents and monkeys. *Nature Communications*.

Farrell MR, Schoch H, Mahler SV. (2018). Modeling cocaine relapse in rodents: Behavioral considerations and circuit mechanisms. *Progress in Neuropsychopharmacology & Biological Psychiatry*. pii: S0278-5846(17)30561-4.

Schoch H, Huerta MY, Ruiz CM, **Farrell MR**, Jung KM, Huang JJ, Campbell RR, Piomelli D, Mahler SV (2018). Adolescent cannabinoid exposure effects on natural reward seeking and learning in rats. *Psychopharmacology (Berl)*. 235(1), 121-134

HONORS AND AWARDS

Sheryl and Dan Tishman Postdoctoral Fellowship, Albert Einstein College of Medicine (2022)
Society for Neuroscience Trainee Professional Development Award (2021)
Top Data Blitz Award Center for the Neurobiology of Learning and Memory Spring Conference (2021)
Center for the Neurobiology of Learning and Memory Renée Harwick Advanced Graduate Student Award (2020)
Center for the Neurobiology of Learning and Memory John Haycock Memorial Travel Award (2018)
UC Irvine Diversity Recruitment Fellowship Award (2016)
Dean's List, The College of New Jersey (2012-2016)
Phi Kappa Phi Student Faculty Research Award (2015)
Phi Beta Kappa (2015)
Marshall P. Smith Scholarship (2015)
Psi Chi International Psychology Honor Society (2014)
Golden Key International Honor Society (2013)

INVITED TALKS

How Addiction Hijacks the Brain: What animal models can tell us about the neurobiology of drug abuse. Public Forum, Center for the Neurobiology of Learning and Memory at UC Irvine (2021).

F99/K00 (D-SPAN) Predoc-Postdoc Transition Awards. Academic Advancement Activity, GPS-STEM. Information Session University of California, Irvine (2021).

Rewiring the Addicted Brain: Insights from Preclinical Rodent Models. The College of New Jersey, Psychology Department Colloquia (2020).

"The DREADDed Weed: Chemogenetic Dissection of Dopamine Function after Adolescent Cannabinoid Receptor Stimulation" Gordon Research Conference: Cannabinoids in the CNS (Waterville Valley, NH, 2017).

POSTER PRESENTATIONS

Farrell MR, Ye Q, Xie Y, Esteban JSD, Mahler SV (2021). Ventral pallidum GABA neurons bi-directionally control remifentanil relapse following voluntary or imposed abstinence in rats. Society for Neuroscience. Chicago, IL.

Farrell MR, Ye Q, Xie Y, Esteban JSD, Mahler SV (2020). Ventral pallidum GABA neuron activity is necessary and sufficient for cue-induced reinstatement of opioid seeking after voluntary abstinence. American College of Neuropsychopharmacology, Zoom.

Farrell MR, Esteban JSD, Mahler, SV (2019). Roles for ventral pallidum GABA neurons in appetitive and aversive motivation during risky decision making. Society for Neuroscience. Chicago, IL

Farrell MR, Cevallos J, Ruiz CM, Huang J, Castillo E, Jung KM, Piomelli D, Mahler SV (2018). Chemogenetic ventral tegmental area dopamine stimulation reveals persistent prefrontal cortex endocannabinoid disruption after adolescent cannabinoid microdosing. American College of Neuropsychopharmacology. Hollywood, FL.

Farrell MR, Ruiz CM, Heyer J, Mahler SV (2018). Ventral pallidum GABA circuits in risky decision making. Society for Neuroscience. San Diego, CA.

Farrell MR, Ruiz C, Schoch H, Castillo E, Khanbijian C, Liu S, Mahler SV (2017). Ventral pallidum roles in mixed appetitive/aversive motivational states related to cocaine relapse. Society for Neuroscience. Washington, D.C.

Ruiz CM, **Farrell MR**, Schoch H, Huerta MY, Jung KM, Campbell RR, Piomelli D, Mahler SV (2017). Effects of adolescent cannabinoid exposure on conditioned and unconditioned natural reward and dopamine circuits. Society for Neuroscience. Washington, D.C.

Schoch H, Castillo E, **Farrell MR**, Mahler SV (2016). Ventral pallidum in context: Roles for VP and its inputs in appetitive and aversive motivation. Society for Neuroscience. Chicago, IL.

Farrell MR, Lansberry L, Caughron R, Martinetti MP (2016). The effect of environmental enrichment on behavioral economic demand for ethanol and sucrose in Long-Evans rats. Society for Neuroscience. Chicago, IL.

Farrell MR, Kutub N, Angulo J (2014). The effects of leptin on methamphetamine-induced caspase-3 activation in the rodent striatum. Leadership Alliance National Symposium. Stamford, CT.

TEACHING EXPERIENCE

Spring 2015 Instructional Internship (Undergraduate TA) at The College of New Jersey for Behavioral Pharmacology of Drugs of Abuse (PSY 343)

Winter 2018 Teaching Assistant for Advanced Neurobiology II (N115B, Georg Striedter, PhD)

Teaching Assistant for Upper Division Neurobiology Lab (N113L, Audrey Chen Lew, PhD)

Spring 2018 Instructor for Upper Division Neurobiology Lab (N113L, Audrey Chen Lew, PhD)

PROFESSIONAL AFFILIATIONS

Society for Neuroscience Phi Beta Kappa

Psi Chi International Psychology Honor Society Golden Key International Honor Society

ABSTRACT OF THE DISSERTATION

Drugs, Decisions, Desire, and DREADDs: Dissecting Ventral Pallidum GABAergic Neuron Function in Motivated Behavior

by

Mitchell Farrell

Doctor of Philosophy of Biological Sciences

University of California, Irvine, 2022

Professor Stephen V. Mahler, Chair

A fundamental function of the brain is to navigate a dynamic world and generate appropriate behaviors in pursuit of rewards (e.g., food, water) and avoidance of harm (e.g., predators). These fundamental functions go awry in psychiatric disorders like addiction, yet the particular neural circuits involved in balancing reward seeking and harm avoidance remain largely unresolved. Ventral pallidum (VP) has emerged as a convergence point of motivational information, and, as such, regulates motivation for diverse natural rewards as well as drugs of abuse. While most work in VP has assessed its function in appetitive motivation, emerging work has revealed that VP is critical for aversive motivation/learning. In part, VP supports both appetitive and aversive motivation via functionally distinct neurotransmitter-defined neuron populations. Specifically, VP GABAergic (VP^{GABA}) neurons are thought to be critical for appetitive processes, whereas VP glutamatergic neurons are important for aversive processes. However, most goals and actions are rife with potential consequences, and thus adaptive behavior must appropriately weigh these potential consequences when seeking rewards. Here, I explore the function of VP^{GABA} neurons under *motivational conflict*, as well as appetitive and aversive motivation. To do so, I employ a suite of decision making and relapse behavioral

models in rats accompanied by cell-type specific chemogenetics and immunohistochemical approaches to dissect the behavioral function of VP^{GABA} neurons. We found that 1) chemogenetic inhibition of VP^{GABA} neurons attenuates cocaine and remifentanil seeking across rat relapse models, 2) stimulating VP^{GABA} neurons augments remifentanil seeking in a 'dangerous' context in which rats had previously received footshock, and 3) inhibiting VP^{GABA} neurons diminishes an animals' willingness to exert risky behavior or exert effort to obtain valuable food rewards. These findings generally support the notion that VP^{GABA} neurons may control the deployment of cognitive resources to overcome obstacles, pursue goals in the face of adversity, and weigh whether a goal is worth pursuing. Further illuminating the neural circuits of motivation will potentially yield novel neuroscience-based interventions for treating psychiatric disorders like addiction in the future.

Introduction

Substance use disorder (drug addiction) is an insidious psychiatric disorder that results in nearly 100,000 overdose deaths and costs $600 billion dollars per year (Hedegaard et al.). According to the diagnostic and statistical manual (DSM-5), drug addiction a chronic, relapsing disorder characterized by drug use despite adverse consequences and persistent relapse risk (American Psychiatric, 2013). Though addicted individuals are often able to quit using drugs at least temporarily, exposure to 'triggers' can initiate strong bouts of craving and potentially lead to relapse. Such triggers are cues or contexts associated with past drug use, stressors, or small doses of the drug itself. Each trigger has the capacity to generate a strong 'drug seeking' state, leading addicted individuals to make poor decisions despite their best efforts to resist temptation. Indeed, in a severely addicted person, their decision-making becomes impaired such that an inordinate amount of time and resources becomes dedicated to the pursuit of drugs, at the expense of healthier alternatives. Drug addiction, indeed, might be considered a disorder of maladaptive decision making, in which one of several decision-making systems in the brain breaks down, producing persistent pathological choice (Lee, 2013). Understanding addiction through this lens—as failure modes in neural circuit computations that generate decisions—will shed light on how brains make poor decisions in the context of addiction (Redish et al., 2008).

Despite considerable efforts in developing treatments for addiction, few effective therapeutics exist to curb temptation in those suffering. Front-line therapies include anti-craving drugs like naltrexone for alcohol use disorder, replacement therapies including methadone and buprenorphine for opioid addiction or the nicotine patch for nicotine dependence, and aversion-based therapies like disulfiram which elicits malaise symptoms in the event of alcohol consumption (Blanco-Gandía and Rodríguez-Arias, 2018). Though helpful for some, such therapies are often coupled with negative side effects, low adherence, and lack lasting efficacy.

Such limitations in theory might be ameliorated by understanding how neural circuits operate, and how they breakdown in psychiatric disorders. Framing psychiatric disorders like addiction as brain disorders of aberrant circuit dynamics provides a lens through which to develop treatments based on neural circuit computation (Redish, 2004; Keiflin and Janak, 2015; Huys et al., 2016; Redish and Gordon, 2016). Indeed, current pharmacotherapeutics are designed to influence specific neurotransmitter systems in the brain, in essence amplifying or diminishing particular signaling pathways to curb psychiatric symptoms. However, such pharmacotherapies are relatively blunt approaches that fail to consider that massive functional and anatomical heterogeneity in nervous tissue. For these reasons, much clinical and preclinical work over the last few decades has sought to better understand the neural circuit basis of addiction in hopes of developing neuroscience-inspired treatments (Redish et al., 2008; Koob and Volkow, 2010; Lüscher, 2016).

Much work over the years has implicated a vast web of neural structures in addiction-like behavior including multiple elements of the brain's motivational circuitry including distributed regions of ventral basal ganglia and midbrain dopamine (DA) systems. Many studies have implicated ventral tegmental area (VTA) dopaminergic (DA) projections to nucleus accumbens (NAc) in the reinforcing effects of drugs of abuse (Pierce and Kumaresan, 2006). Indeed, a common thread that links all drugs of abuse is their capacity to boost DA levels in the NAc (Di Chiara and Bassareo, 2007). Blocking DA transmission systemically or in NAc reduces the reinforcing effects of drugs of abuse, strongly blunts motivation, and impacts decision making (Robinson and Berridge, 1993; Salamone and Correa, 2012; Floresco, 2015). NAc, and its DA afferents, are part of a wider ventral basal ganglia circuit that constitutes cortico-basal ganglia-cortical loops, which are critical for motivation, emotion, and decision making (Alexander et al., 1986; Parent and Hazrati, 1995). Much work in the addiction field has, for good reason, focused on VTA DA projections to NAc, though the wider ventral basal ganglia circuitry has come into focus in recent years. In particular, I focus on the emergence of the ventral pallidum (VP) as a

motivational hub-like structure embedded in ventral basal ganglia circuits—considered by some as a key node in a 'final common pathway' of natural and drug reward seeking behavior (Kalivas and Volkow, 2005; Smith et al., 2009).

Ventral pallidum anatomy: From substantia innominata and beyond. Historically a component of the substantia innominata (Reil, 1809), or 'unnamed substance', VP has emerged as a distinct brain region from the surrounding basal forebrain circuitry based on a number of anatomical, cytological, and histochemical features (Mogenson et al., 1980; Heimer et al., 1982; Haber and Nauta, 1983; Haber and Watson, 1985; Alheid and Heimer, 1988). VP is located ventral to the anterior commissure with a caudal, sublenticular extension ventral to the globus pallidus (Heimer et al., 1997). It is bordered rostrally by the NAc, and is caudally encapsulated by extended amygdala structures (Heimer et al., 1997; De Olmos and Heimer, 1999). Notably, VP expresses abundant substance P throughout its rostrocaudal extent which serves to demarcate VP borders from surrounding basal forebrain regions (Haber and Nauta, 1983). VP receives dense topographically organized GABAergic inputs from NAc medium spiny neurons (MSNs) (Kupchik et al., 2015; Creed et al., 2016), with the NAc shell innervating the neurotensin-rich ventromedial VP and the NAc core instead projecting to the calbindin-rich dorsolateral aspect of the VP (Cullinan, 1992; Zahm et al., 1996). NAc primarily consists of D1 DA receptor-expressing (D1R) and D2R- expressing MSNs (Surmeier et al., 2007; Gerfen and Surmeier, 2011), and these subpopulations are important for generating opposing behaviors, with D1-MSNs promoting behavioral activation (e.g., approach) while D2-MSNs instead promote behavioral inhibition (e.g., avoidance) (Kravitz et al., 2010; Lobo et al., 2010). Interestingly, both approach-related D1-MSNs and avoidance-related D2 MSNs send projections to VP (even single VP neurons) (Kupchik et al., 2015; Creed et al., 2016), suggesting that VP neurons integrates opposing types of motivational information from NAc and may help translate this information into adaptive behavioral output. This striatopallidal system is thought to be critical for translating motivation into action (Mogenson et al., 1980). Indeed, VP sends projections to

downstream regions involved in the generation of locomotion including the substantia nigra pars compacta, substantia nigra pars reticulata, and subthalamic nucleus (Root et al., 2015), thus positioning VP to modulate locomotor behavior in accordance with motivational demands.

Impact of VP circuits on midbrain dopamine systems. Of specific relevance to VP's role in addiction is its connectivity with midbrain DA systems. VP exerts control over both mesolimbic and nigrostriatal DA systems via direct and indirect projections to these midbrain sites (Root et al., 2015). VTA DA neurons are widely considered to be critical regulators of motivation—lesion or inactivation of these neurons dramatically reduces motivation for natural and drug rewards (Salamone and Correa, 2012). VP sends axonal projections directly to VTA (Haber et al., 1985; Zahm, 1989), that consist primarily of GABAergic (VP^{GABA}) neurons, with a minority of glutamatergic projections (Geisler et al., 2008). Since VP projections to VTA are largely GABAergic, it was originally posited that VP tonically inhibited VTA DA neurons. Consistent with this notion, pharmacological VP inactivation increases the number of spontaneously firing VTA DA neurons (Floresco et al., 2003). However, VP neurons also synapse on VTA GABAergic interneurons, in addition to VTA DA neurons themselves, and VP stimulation elicits inhibition in both types (Hjelmstad et al., 2013; Faget et al., 2016; Faget et al., 2018). This suggests that VP regulation of VTA is heterogeneous, potentially inhibiting VTA DA neurons directly or disinhibiting DA neurons by inhibiting local inhibitory interneurons.

VP can also indirectly impact DA neurons via the LHb or rostromedial tegmental nucleus (RMTg), whose collective activity is capable of potently inhibiting VTA DA neurons, which, in turn, constrains appetitively motivated behavior (Christoph et al., 1986; Jhou et al., 2009a; Hikosaka, 2010; Hong et al., 2011). LHb is an epithalamic structure that directly projects to VTA, where it synapses on GABAergic interneurons, providing feedforward inhibition on VTA DA neurons (Ji and Shepard, 2007; Omelchenko et al., 2009). Moreover, LHb sends indirect projections to VTA via the GABAergic hindbrain RMTg (Jhou et al., 2009a; Lammel et al., 2012) (also called tail of VTA (Perrotti et al., 2005; Kaufling et al., 2009)), which can potently inhibit

VTA DA neurons (Hong et al., 2011). VP can therefore influence VTA DA neurons by direct VTA projections or indirectly via LHb- or RMTg-mediated circuits (Jhou et al., 2009b; Bourdy and Barrot, 2012; Mahler et al., 2014; Stephenson-Jones et al., 2020), thus implying multiple inroads through which VP can impact DA-associated motivated behavior.

VP function in reward and motivation. VP has garnered much interest in the field of motivation and affective neuroscience over the last several years (Smith et al., 2009). Modern conceptions of VP function suggest that it is a motivation to motor interface (Mogenson et al., 1980; Heimer et al., 1982) and that is serves as a final common pathway of drug (Kalivas and Volkow, 2005) and natural reward seeking (Smith et al., 2009). As such, VP is involved in food and water intake, hedonics, sexual motivation, and drug seeking. Importantly, VP lesion or inhibition produces motivational deficits without eliminating the fundamental ability to move (Root et al., 2015), illustrating that it is more than a simple motor structure. With the aid of modern neuroscience tools, recent work has revealed a key role for neurotransmitter-defined subpopulations within VP in not just appetitive motivation, but also aversive motivation.

VP neurons increase their firing in response to Pavlovian reward-predictive cues and rewards themselves (Tindell et al., 2004). Not only does VP neuron activity encode cues or rewards, but their activity scales with the vigor or probability of pursuit of those rewards. Indeed, VP encoding of motivational vigor has been shown across species, including rats (Richard et al., 2016), monkeys (Tachibana and Hikosaka, 2012), and humans (Pessiglione et al., 2007). Overall, VP firing encodes the motivational value of reward-paired cues, and its firing relates to the likelihood that an action in pursuit of reward will occur. Consistent with recording data, disruption of VP circuits impairs a range of cue-associated behaviors. Disruption of NAc inputs to VP, and VP's outputs to VTA or mediodorsal thalamus (MD) all disrupt the ability of Pavlovian reward-associated cues to elicit food-seeking behavior (Leung and Balleine, 2013, 2015). Chemogenetic VP inhibition impairs learning about the incentive value of Pavlovian reward cues (Chang et al., 2015). Moreover, pharmacological, chemogenetic, or optogenetic disruption of VP

decreases cue-triggered motivated behavior across a range of models and species (Tachibana and Hikosaka, 2012; Richard et al., 2016; Chang et al., 2017). While much evidence has accrued indicating that VP inherits reward-related information from NAc, recent evidence suggests that VP encodes reward-related information at a shorter latency than NAc and that NAc-projecting VP neurons are key regulators of consummatory behavior (Ottenheimer et al., 2018; Vachez et al., 2021). These lines of evidence call into question the canonical information flow in ventral basal ganglia circuits and suggest a bidirectional role for VP and NAc in generating motivated behavior. Nevertheless, VP serves as a critical node in generating appetitive motivation in response to reward-related cues.

Rodent relapse models and VP's involvement. Persistent relapse risk even after lengthy periods of abstinence is a hallmark of addiction, and preventing relapse episodes remains a fundamental problem in treating addiction. In humans, craving and subsequent relapse are often precipitated by ingestion of a small priming dose of drug, experiencing acute stress, or encountering discrete or contextual cues previously paired with drug use (O'Brien et al., 1998; Sinha, 2001; Shaham et al., 2003). Rodent models of relapse, called reinstatement models, have been employed for decades to dissect the behavioral and neural underpinnings of relapse-like behavior. In intravenous self-administration-based relapse models, rats are trained to perform an operant response to gain access to an intravenous bolus of drug like cocaine. Following self-administration days (e.g., 2 weeks), rats generally undergo extinction training in which operant responses are met with no consequences, thereby leading to cessation of drug seeking. During subsequent relapse/reinstatement tests, rats are reintroduced to various triggers that reinitiate operant drug-seeking behavior—the number of operant responses emitted in pursuit of drug is the operational definition of relapse-like behavior. Notably, relapse triggers that elicit drug-seeking behavior in rodent models—cues, contexts, stressors, or priming doses—also can elicit craving and relapse in humans.

Such models have been instrumental in understanding the neural circuits of drug seeking after experimenter-imposed abstinence. Indeed, most work examining VP and related limbic neural circuits of relapse have used these classic reinstatement models in which relapse-like behavior is assessed after extinction training or a period of forced homecage abstinence (incubation of craving) (Bossert et al., 2013). However, abstinence in people with addiction is generally voluntarily initiated resulting from negative consequences like health or financial problems that ultimately lead to cessation of drug use (Marchant et al., 2013a). Recently developed preclinical rodent models have attempted to capture this feature of abstinence by incorporating negative consequences that accompany drug use to cause 'voluntary' abstinence (Marchant et al., 2013b; Farrell et al., 2018). These models generally employ an electrified floor in front of the drug-associated operant manipulandum, footshock contingent on drug seeking/taking, or bitter tastes in the case of oral self-administration (Vanderschuren et al., 2017). Such models may help advance our understanding of the brain circuits underpinning relapse-like behavior, especially since the brain circuits underpinning relapse-like behavior depend upon how abstinence was achieved (Fuchs et al., 2006; Pelloux et al., 2018a). For example, inhibiting basolateral amygdala (BLA) neurons *increases* drug seeking after punishment-induced abstinence, while the same manipulation *decreases* seeking after extinction training (Pelloux et al., 2018a). Such evidence leads to the notion that neural circuits are differentially recruited based on the form of abstinence and the specific triggers that led to relapse (Farrell et al., 2018). The development and use of these voluntary, punishment-induced abstinence-based relapse models, and examination of VP's role in these models, serve as a principal throughline of this dissertation.

A number of cortical and limbic structures are critical for reinstatement behavior in classic extinction-based relapse models, with VP considered by some as a final common pathway for reinstatement (Kalivas and Volkow, 2005). As such, it is implicated across reinstatement types (ie, cue/context, stress, and drug prime), and its outputs to VTA, lateral

hypothalamus, and MD are essential for driving some types of reinstatement (Mahler et al., 2014; Prasad and McNally, 2016; Farrell et al., 2018; Prasad et al., 2019). In particular, our lab has revealed a dissociation between rostral and caudal VP subregions in driving different reinstatement types. Specifically, rostral VP interactions with VTA are imperative for cue-induced relapse to cocaine-seeking behavior, whereas caudal VP is involved in reinstatement promoted by small priming doses of cocaine (Mahler et al., 2014). This dissertation expands upon our understanding of VP circuits in relapse-like behavior by examining how VP neural circuits are correlated with and causally implicated in cocaine and remifentanil seeking after punishment-induced, voluntary abstinence.

Importantly, though different classes of drugs of abuse may lead to addiction in susceptible individuals, each drug exerts distinct effects on neural reward systems. One commonality, however, among drugs of abuse is their ability to increase DA levels in NAc (Di Chiara and Bassareo, 2007). Drugs of abuse do so in different ways. For example, cocaine exerts its reinforcing effects as a dopamine reuptake inhibitor (Ritz et al., 1987), thus boosting the duration of action of these neuromodulators at the synapse. In contrast, μ opioid receptor agonists like remifentanil (discussed below) or heroin instead are thought to disinhibit VTA DA neurons by hyperpolarizing inhibitory interneurons in VTA that generally serve to inhibit DA neurons (Johnson and North, 1992). This reduction in interneuron activity in VTA will, in turn, elevate levels of DA in downstream targets like the NAc (Leone et al., 1991). Both cocaine and addictive opioids exert their effects beyond the brain's DA system, so furthering our understanding of how these drugs exert their effects in more widespread neural circuits might lead to pivotal insights about the process of addiction. Overall, the distinct pharmacological profiles of different drugs of abuse will likely be important for developing targeted treatments for addiction in the future, though such ideas are largely beyond the scope of this dissertation.

Neurotransmitter-defined VP neuronal populations in appetitive and aversive motivation. Though largely considered a reward-related structure, recent years have revealed a role for VP

in processing aversive stimuli and aversive motivation (ie, motivation to avoid bad things) (Wulff et al., 2018; Stephenson-Jones, 2019). Human fMRI studies have shown that presentation of disgusting images (e.g., rotten food) is associated with increased VP BOLD activity (Calder et al., 2007). In rodents, a taste that was previously paired with a nausea-inducing drug decreases VP activity, though, similar to the above fMRI study, some VP neurons were excited by the aversive taste (Itoga et al., 2016). Disruption of GABAergic neurotransmission in VP via microinjection of the GABAA receptor antagonist, bicuculline, impairs cued avoidance in monkeys (Saga et al., 2016), and μ opioid receptor agonist application elicits both appetitive eating and aversive 'defensive' treading behaviors in rats (Smith and Berridge, 2005).

Recent work has revealed subpopulations of genetically-defined VP neurons that govern distinct forms of motivated behavior—glutamate neurons appear to mediate aversive motivation while GABA neurons mediate reward motivation. Given that reward-related GABA neurons represent the predominant neuronal subtype in VP, it is perhaps not surprising that the smaller aversion-related glutamate subpopulation has been overlooked with standard pan-neuronal manipulations or monitoring techniques. GABA and glutamate neurons are intermingled throughout VP's rostrocaudal extent, though glutamate neurons are largely localized in the ventromedial and rostral aspect of VP (Faget et al., 2018). Anatomical tracing studies reveal that both GABA and glutamate neurons receive qualitatively similar inputs, with most afferents arising from NAc (Knowland et al., 2017; Tooley et al., 2018). Similarly, VP glutamate and GABA neurons send projections to the same downstream brain regions, including dense innervation of the VTA and LHb (Knowland et al., 2017; Faget et al., 2018). Cholinergic VP neurons, in contrast, project almost exclusively to BLA and cortical areas (Carlsen et al., 1985; Gritti et al., 1997; Faget et al., 2018), representing a stark divergence from GABA and glutamate projection patterns.

A surge of studies in the last few years has resulted in greater understanding of the function of VP^{GABA} and glutamate neurons. VP^{GABA} and glutamate cells are in seeming functional

opposition. In mice, optogenetic stimulation of VP^{GABA} neurons supports operant self-stimulation and mice will remain in a chamber in which these neurons are optogenetically stimulated (Knowland et al., 2017; Faget et al., 2018; Tooley et al., 2018). In contrast, mice will avoid a chamber paired with VP glutamate stimulation and accordingly refuse self-stimulation (Faget et al., 2018; Tooley et al., 2018). From these optogenetic stimulation studies, it appears that VP^{GABA} cells drive approach, while VP glutamate cells mediate avoidance (Faget et al., 2018; Tooley et al., 2018; Stephenson-Jones et al., 2020).

These simple photostimulation behavioral tests reveal opposing contributions of VP^{GABA} and glutamate neurons to motivated behavior, but what about more ethologically-relevant behaviors? Ablation of VP glutamate neurons, while leaving VP^{GABA} neurons intact, augments motivation to self-administer palatable rewards (Tooley et al., 2018). Moreover, VP glutamate neuron ablation impairs learning about an aversive outcome—mice lacking VP glutamate neurons fail to reduce their sucrose intake after sucrose was paired with a malaise-inducing lithium chloride injection (Tooley et al., 2018). Thus, it appears that VP glutamate neurons are involved in avoidance of potential harm and limiting of reward-seeking behavior.

A recent study in mice further examined the functionally opposed roles of VP^{GABA} and glutamate neurons (Stephenson-Jones et al., 2020). Optogenetically-tagged VP^{GABA} and glutamate neurons were recorded under appetitive and aversive circumstances, and under motivational conflict where both neuron subpopulations compete for behavioral control. Consistent with a role for VP^{GABA} neurons in appetitive motivation, these neurons were excited by water delivery or its predictive cues. Glutamate neurons, on the other hand, were activated by an aversive air puff to the face and cues that predicted the air puff. Consistent with VP encoding motivational value, as described above, VP^{GABA} neuron activity scales with the magnitude of the reward, exhibiting increased firing rates after a large reward or its predictive conditioned stimulus (relative to a small reward). VP glutamate neurons instead scale with the magnitude of the aversive air puff stimulus or its predictive cue, suggestive of encoding aversive

motivational value. Importantly, optogenetic inhibition of VP^{GABA} neurons decreased appetitive motivation (ie, operant licking to obtain a water reward) while this same manipulation had no effect on running to avoid an air puff, illustrating a specific role for VP^{GABA} neurons in reward motivation. The opposite was found with glutamate neuron inhibition—there was no effect on licking to obtain water, but a decrease in running to avoid air puff. Collectively, these data suggest that VP^{GABA} and glutamate neurons drive opposing motivated behaviors, with glutamate neurons being required for avoidance of harm and GABA neurons instead required for seeking rewards. Given the similar projection profiles of VP^{GABA} and glutamate neurons, an attractive hypothesis is that VP^{GABA} and glutamate neurons exist in functional balance—GABA neurons pushing towards obtaining rewards and glutamate neurons pushing towards avoiding harm via the same downstream targets.

Despite VP^{GABA} neurons acting to stimulate appetitive motivation, how such circuits contribute to behavior under motivational conflict remains unclear. To address this question, I employ a host of complex behavioral models of decision making, harm avoidance in the absence of reward, and reward seeking in the absence of potential harm. Moreover, I employ punishment-based relapse models that pit cocaine- or opioid-seeking motivation against aversive motivation to avoid contingent footshock punishment. Through the application of cell-specific chemogenetic approaches and a suite of behavior models, I shed light on the behavioral function of VP^{GABA} neurons in hopes that better understanding these circuits may yield deeper understanding of psychiatric disorders that involve maladaptive motivation like addiction.

CHAPTER 1: Ventral pallidum is essential for cocaine relapse after voluntary abstinence in rats

Introduction

Addiction is characterized by persistent drug use despite negative consequences, and a lasting vulnerability to relapse after protracted periods of abstinence (Hunt et al., 1971; Wikler, 1973; O'Brien et al., 1992). Typically, individuals with addiction eventually recognize the negative consequences of their behavior, and choose to cease using drugs—a decision they usually renege upon when tempted by drug cues, small doses of drug, or stressors (Shaham et al., 2003). In rodent relapse models, reinstatement of seeking is triggered by analogous stimuli, usually following a period of imposed abstinence from drug (incubation), or explicit extinction training. Recently, voluntary abstinence-based rodent relapse protocols have emerged, modeling people with addiction who choose to stop using drugs due to mounting negative life consequences, rather than ceasing use due to extinction training, or external forces (Panlilio et al., 2003; Economidou et al., 2009; Marchant et al., 2013b; Marchant et al., 2013a; Venniro et al., 2016). This is important because in rodents, the neural substrates underlying reinstatement differ based upon how abstinence was achieved, be it experimenter-imposed, through extinction training, or through voluntary cessation due to punishment or availability of more attractive reinforcers (Fuchs et al., 2006; Venniro et al., 2017; Marchant et al., 2018; Pelloux et al., 2018a; Venniro et al., 2018; Golden et al., 2019). If the brain substrates of human relapse similarly depend upon why a person stopped using drugs, then considering these factors in preclinical models will be essential for developing effective interventions to treat addiction.

A hallmark of addiction is an inability to limit drug intake in the face of negative life consequences. This can be modeled in rodents by training them to self-administer drugs, then introducing consequences to continued use, such as co-delivered footshock (Panlilio et al., 2003; Deroche-Gamonet et al., 2004; Belin et al., 2009; Marchant et al., 2013b; Vanderschuren et al., 2017; Pelloux et al., 2018b; Smith and Laiks, 2018). As in humans, most rodents readily

suppress their drug intake when negative outcomes begin to result from continued use. However, a subset of rodents show punishment-resistant drug intake (Deroche-Gamonet et al., 2004; Vanderschuren and Everitt, 2004; Everitt et al., 2008; Chen et al., 2013), similar to the proportion of humans who use drugs and ultimately become addicted (Anthony et al., 1994). Punishment-resistant rats also exhibit elevated reinstatement of cocaine and methamphetamine seeking (Deroche-Gamonet et al., 2004; Torres et al., 2017), suggesting that compulsive use and relapse liability involve common underlying neural mechanisms. Indeed, the circuitry underlying compulsive cocaine intake overlaps with the limbic substrates of reinstatement behavior, at least when tested following extinction training (Ersche et al., 2011; Bock et al., 2013; Chen et al., 2013; Farrell et al., 2018; Yager et al., 2019).

One brain region that has emerged as being crucial for motivated behavior is the VP, the main efferent target of NAc (Swanson and Cowan, 1975; Williams et al., 1977; Saga et al., 2016; Faget et al., 2018; Tooley et al., 2018). VP is thought to help translate motivation into action (Mogenson et al., 1980; Heimer et al., 1982; Kalivas and Volkow, 2005; Smith et al., 2009), and accordingly, VP neural activity encodes reward motivation in rodents, monkeys, and humans (Pessiglione et al., 2007; Tachibana and Hikosaka, 2012; Richard et al., 2016), including for cocaine (Root et al., 2013). VP is also required for seeking of several abused drugs (Hubner and Koob, 1990; Rogers et al., 2008a; Perry and McNally, 2013; Mahler et al., 2014; Prasad and McNally, 2016, 2019), and for cocaine reinstatement triggered by cues, stress, or cocaine following extinction training (McFarland and Kalivas, 2001; McFarland et al., 2004; Mahler et al., 2014). Notably, VP is a heterogeneous structure, with functionally- and anatomically-distinct rostral/caudal and dorsolateral/ventromedial subregions that mediate distinct aspects of reward seeking (Groenewegen et al., 1993; Churchill and Kalivas, 1994; Smith and Berridge, 2005; Beaver et al., 2006; Calder et al., 2007; Smith and Berridge, 2007; Root et al., 2013; Stefanik et al., 2013; Mahler et al., 2014; Root et al., 2015). Specifically, rostral VP mediates cue-induced, whereas caudal VP mediates primed reinstatement of cocaine

seeking following extinction training (Mahler et al., 2014). The NAc shell input-receiving ventromedial, and NAc core-receiving dorsolateral VP subregions are also differentially involved in cocaine-taking behaviors (Zahm and Heimer, 1990; Churchill and Kalivas, 1994; Root et al., 2013). Given these results, and recent findings that VP contains phenotypically distinct populations of reward- and aversion-related neurons (Knowland et al., 2017; Faget et al., 2018; Tooley et al., 2018; Wulff et al., 2018; Stephenson-Jones, 2019; Stephenson-Jones et al., 2020), VP's role in drug seeking under translationally-relevant mixed motivation circumstances was of interest to us.

Here we explore effects of transiently and reversibly inhibiting VP neurons of punishment-resistant or punishment-sensitive rats with designer receptors (DREADDs) (Armbruster et al., 2007), determining effects on punished cocaine seeking, context-, discrete cue-, and primed-reinstatement after voluntary abstinence, and cocaine-induced locomotion. We also assessed relapse-related Fos in VP subregions. We found that chemogenetic VP inhibition reduced cue-, cocaine primed-, and context-induced relapse to cocaine seeking, and VP subregions are robustly Fos-activated during exposure to cocaine- or cocaine + punishment contexts. These studies shed light on the functions of this essential, but understudied nucleus within cocaine addiction-related neural circuits.

Methods

Subjects. Male (*n* = 50; mean ± SEM body weight = 345 ± 6 g at start of self-administration) and female (*n* = 36; mean ± SEM = 226 ± 4 g) Long-Evans rats were bred at the University of California, Irvine or obtained from Envigo, and were pair housed on a 12 hr reverse light/dark cycle (testing in dark phase), with *ad libitum* food and water throughout experiments. Procedures were approved by the UCI Institutional Animal Care and Use Committee, and are in accordance with the NIH Guide for the Care and Use of Laboratory Animals (National Research, 2010).

Surgery. Rats were anesthetized with ketamine (56.5 mg/kg) and xylazine (8.7 mg/kg), administered the non-opioid analgesic meloxicam (1.0 mg/kg), and implanted with indwelling jugular catheters exiting the dorsal back. In the same surgery, they also received bilateral viral vector injections (250-300 nL) into VP (mm from Bregma; AP: 0.3, ML: +/-1.8, DV: -8.2 mm) with pressure injections using a Picospritzer and glass micropipette. **Fig. 1** describes procedures.

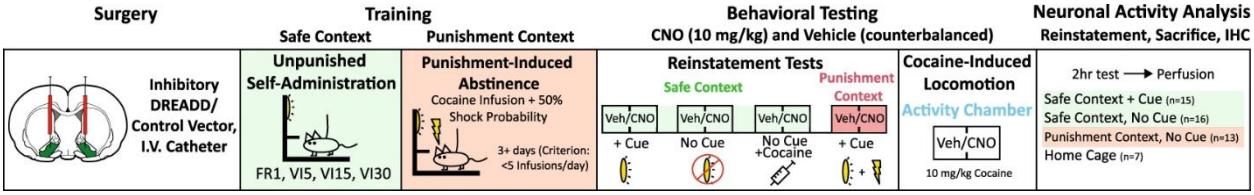

Figure 1. Schematic of experimental timeline. Following DREADD or control AAV injection, rats underwent cocaine self-administration, punishment training, followed by reinstatement and cocaine-induce locomotor testing. A final relapse test preceded sacrifice for neuronal activity (Fos) analysis. Light/green shading = safe context, dark/red shading = punishment context.

Viral constructs. To transduce VP neurons with hM4Di inhibitory DREADDs, we used a human synapsin (hSyn) promoter-driven AAV with mCitrine (*n* = 44; U North Carolina vector core: *AAV2-hSyn-HA-hM4D(Gi)-IRES-mCitrine*; titer = $2.6x10^{12}$ virus particles/mL) or mCherry (*n* = 16; Addgene: *AAV2-hSyn-hM4D(Gi)-mCherry*; titer = $7x10^{12}$ vg/mL) reporter. To control for non-specific impact of viral transduction and clozapine-N-oxide (CNO) in the absence of DREADDs, an eGFP-only reporter without DREADDs (*n* = 7; Addgene: *AAV2-hSyn-eGFP*; titer = $3x10^{12}$ vg/mL), was employed in a group of control rats (MacLaren et al., 2016; Gomez et al., 2017; Mahler and Aston-Jones, 2018).

Anatomical analysis of DREADD expression. hM4Di DREADD/reporter expression was visualized with immunofluorescent amplification, and Substance P co-stain demarcating VP borders. Histological quantification was performed by an observer blind to group and behavioral results. Rats with at least 40% of VP volume expressing DREADDs/reporter, and at least 40% of virus expression localized within VP borders were considered hits (*n* = 46; male = 26; female = 20). Some leakage into the adjacent lateral preoptic area and horizontal limb of the diagonal band was detected in most rats, but if rats had more than 60% of DREADD expression localized

outside VP, they were considered “misses” (*n* = 13). Since rats with extra-VP DREADD expression did not behaviorally differ from fluorophore-only rats (no main effect of group or CNO treatment on reinstatement of any kind, *Fs* < 1.29, *ps* > 0.27; **Fig. 2**), they were combined into a single control group (*n* = 20; male = 10; female = 10) for subsequent analyses of CNO effects in the absence of VP DREADDs.

RNAscope analysis of DREADD expression in VP neurons. PFA-fixed brains from cocaine-naïve male rats were serially cut (16 µm) on a cryostat and mounted directly onto glass slides. Sections were stored at –80° C until processing for RNAscope Multiplex Fluorescent assay (Advanced Cell Diagnostics). Briefly, sections were warmed on a hot plate for 30 minutes at 60° C then boiled at 100° for 6 min in target retrieval solution. Sections were then dehydrated in 100% ethanol and treated with protease (pretreatment reagents, cat. No. 322380). RNA hybridization probes included antisense probes against rat *Gad1* (316401-C1) and *Slc17a6* (317011-C3), respectively labeled with alexa-488 and atto-647 fluorophores. Slides were then incubated with rabbit anti-DsRed primary antibodies (1:2000, Catalog #: 632496, Clontech) and donkey anti-rabbit AlexaFluor 594 secondary antibodies (1:400, #711-585-152, Jackson ImmunoResearch), counterstained with DAPI, and coverslipped using Fluoromount-G mounting medium. Images for cell counting were taken at 63x (1.4 NA) magnification using a Zeiss AxioObserver Z1 widefield Epifluorescence microscope with a Zeiss ApoTome 2.0 for structured illumination and Zen Blue

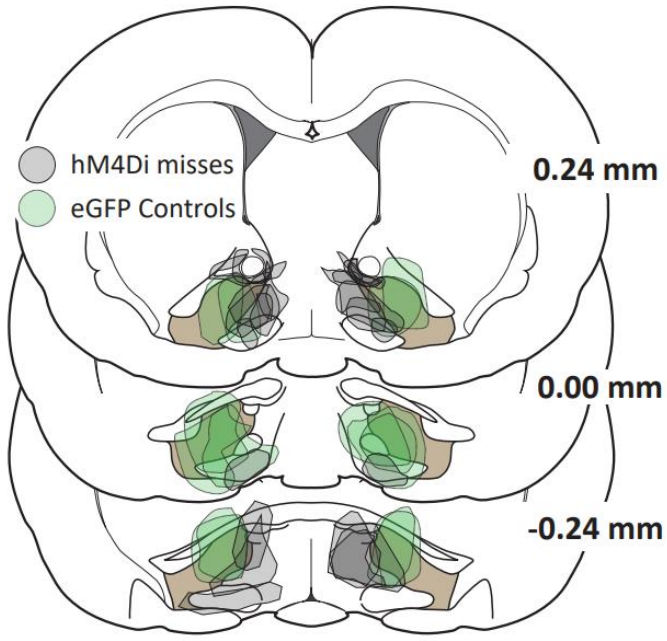

Figure 2. Viral expression in hM4Di misses and eGFP controls. hM4Di misses (thin solid border) and eGFP controls (thick dotted border) depicted on rostrocaudal VP sections relative to bregma.

software. An average of 177 ± 9 cells positive for AAV-hSyn-hM4D(Gi)-mCherry were counted per brain (*n* = 3 rats).

Drugs. Cocaine HCl (NIDA) was dissolved in 0.9% saline, and was available for self-administration at 0.2 mg/50 µL infusion for male rats (~0.58 mg/kg/infusion), and 0.15 mg/50µL infusion for female rats (~0.66 mg/kg/infusion) (Zhou et al., 2014; Kohtz and Aston-Jones, 2017). Cocaine (10 mg/kg) was used for primed reinstatement and locomotion testing. CNO was dissolved in a vehicle of 5% DMSO in 0.9% saline, and injected i.p. at 10 mg/kg, 30 min prior to behavioral testing.

Behavioral testing apparatus. Self-administration training and testing took place in Med Associates operant chambers within sound-attenuating boxes, equipped with two retractable levers with white lights above them, and a tone generator. Cocaine-induced locomotion testing was conducted in 43×43×30.5 cm Med Associates locomotor testing chambers.

Behavioral training summary. We employed a model of punishment-induced abstinence from self-administered cocaine, followed by repeated reinstatement testing. Rats initially self-administered cocaine in a 'safe context,' then in a distinct 'punishment context,' where they learn to abstain from cocaine due to co-administration of footshock with 50% of cocaine infusions. After voluntary abstinence was achieved in all rats, a series of reinstatement tests in the safe and punishment contexts were conducted, each tested after vehicle and CNO on separate days, 48 hr apart.

Self-administration training in safe context. We employed a punishment-induced abstinence/relapse protocol modeled after previous reports (Panlilio et al., 2003; Economidou et al., 2009; Marchant et al., 2013b; Krasnova et al., 2014; Marchant et al., 2014; Marchant et al., 2016; Pelloux et al., 2018b; Pelloux et al., 2018a). Initial 2 hr self-administration sessions occurred in a 'safe context,' signaled by presence of a white or red house light, peppermint or orange scent, and plain or polka dot pattern walls (randomly assigned). Rats received five daily sessions of fixed-ratio 1 (FR1) training where an active lever press delivered a 3.6 s intravenous

cocaine infusion, and concurrent stimulus light + 2.9 kHz tone. A 20 s timeout period (signaled by dimming of the house light) followed each infusion/cue presentation, during which additional lever presses did not yield cocaine delivery. Following FR1 training to criterion (> 10 infusions/day), rats then completed 3 days of variable-interval 5 schedule (VI5), on which an active lever press initiated a timer with an average duration of 5 s, and another press after that interval delivered a cocaine infusion + light/tone cue. The VI schedule was increased to VI15 for the next 3 days, then VI30 for an additional 3-6 days until performance stabilized. VI schedules promote resistance to extinction (Ferster and Skinner, 1957), providing a high baseline of responding in relapse tests, so we followed methods of prior reports using this procedure (Marchant et al., 2013b; Marchant et al., 2014; Marchant et al., 2016; Pelloux et al., 2018b; Pelloux et al., 2018a). Pressing on an inactive lever was recorded but had no consequences.

Punishment context testing and training. Following safe context self-administration training, rats (n = 35) began punishment training in a distinct chamber, with different cues from those of the safe context. A VI30 schedule was still used, but 50% of cocaine infusions/cues were now accompanied by a 0.3 mA foot shock (0.5 s). Although sex can impact sensitivity to footshock in other operant suppression models (Orsini et al., 2016), shock intensity was not titrated here, and sex-differences in suppression of cocaine intake were not observed (active lever presses change from baseline self-administration: $t_{11} = 0.095$, $p = 0.92$). To test effects of inhibiting VP upon punished cocaine intake, a subset of rats were injected with either CNO (n = 22) or vehicle (n = 13) prior to each of the first two daily shock punishment training sessions. In a crossover design, these rats were administered the opposite treatment (vehicle/CNO) prior to a third punished intake session 48 hr later, then additional punished cocaine intake training session with no vehicle or CNO injections was conducted. Another group of rats (n = 31) received no injections during punished training. After 3-4 days of shock training at 0.3 mA, shock intensity was increased by 0.15 mA every 2 subsequent training days, up to 0.75 mA, or until voluntary abstinence criterion was met by each rat (< 5 active lever presses for 2 consecutive days). `

Punishment sensitivity classification. Sensitivity to punishment was determined in two ways. A suppression ratio (infusions on day 1 punishment/infusions on last day unpunished; (Deroche-Gamonet et al., 2004; Pelloux et al., 2007)) was calculated as a measure of initial punishment sensitivity, with high ratios reflecting relative insensitivity of cocaine intake to shock. Rats were classified as relatively punishment-resistant or punishment-sensitive based on the maximum level of shock they tolerated before meeting abstinence criterion. Punishment resistant rats were defined for analyses as those exceeding 5 active lever presses for 2 consecutive sessions at 0.45 mA footshock intensity, therefore requiring higher shock intensities (0.60-0.75 mA) to achieve voluntary abstinence. As previously reported (Marchant et al., 2013b; Marchant et al., 2014; Marchant et al., 2016), punishment resistant rats underwent more shock training sessions (mean ± SEM, 7.62 ± 0.24) than punishment sensitive rats (mean ± SEM, 4.25 ± 0.15; t_{51} = 11.16, $p < 0.0001$). All rats eventually suppressed their intake to criterion levels by day 9 of punished training.

Measuring mixed motivations during punished cocaine intake: "Abortive lever pressing". During punished cocaine intake training sessions, rats displayed a previously characterized, species-typical risk assessment behavior 'abortive lever pressing' (Hunt and Brady, 1955; Blanchard et al., 1990; Blanchard et al., 2011), in which they stretch their trunk and extend their forepaw towards the active or inactive lever, but rapidly retract it without completing the press to deliver cocaine + chance of shock. Aborted presses of the active and inactive levers were quantified by blinded video analysis of the final day of safe context self-administration, and the first day of punishment context self-administration (after VP inhibition or control).

Relapse tests. A series of 2hr reinstatement tests commenced 48 hr after rats met abstinence criterion, with 48 hr elapsing between each test, during which time rats remained in their home cages. Reinstatement tests occurred in: safe context with response-contingent cues (n = 66; vehicle/CNO administered on separate consecutive test days, in counterbalanced order), then the safe context without cues (vehicle/CNO, n = 31), safe context with a cocaine priming

injection (10 mg/kg; vehicle/CNO, *n* = 38), punishment context with cues (vehicle/CNO, *n* = 35), and punishment context without cues (vehicle only, *n* = 24). Reinstatement testing order was chosen to limit carryover effects from previous reinstatement tests, e.g., by conducting cocaine-primed tests after cue tests to limit impact of non-contingent cocaine on conditioned responding (Kruzich and See, 2001; Mahler et al., 2019). Though expected extinction-related order effects on cocaine-free cue reinstatement tests were seen (first versus second reinstatement test: $t_{65} = 4.23$, $p < 0.0001$), CNO and vehicle tests were counterbalanced within each reinstatement type, limiting the impact of test order on overall behavior (Fuchs et al., 2005; Bossert et al., 2012; Mahler et al., 2013a; Mahler et al., 2014; Mahler et al., 2019). For reinstatement tests with response-contingent cues, active lever presses yielded cocaine-associated discrete cues (but no cocaine or shock), delivered on a VI30 schedule, each followed by a 15 s timeout period. For tests without discrete cues, lever presses were without consequence, but recorded.

Cocaine induced-locomotion. Following reinstatement tests, a subset of rats (*n* = 51) habituated to a locomotor testing chamber for 2 consecutive days, followed by two counterbalanced 2 hr locomotor tests, 48 hr apart. Next, rats were placed in the chamber for 30 min after vehicle/CNO, injected with cocaine, then returned to the chamber for 90 min. Horizontal distance travelled, and number of vertical rears were recorded via infrared beam breaks.

Relapse-related Fos. To examine VP neuronal activity during reinstatement, some rats underwent a final drug-free 2 hr reinstatement test, 48 hr after their last vehicle/CNO reinstatement test. They were tested in: the safe context with cues (*n* = 15), safe context without cues (*n* = 16), punishment context without cues (*n* = 13), or no reinstatement (removed directly from their home cage after equivalent self-administration/reinstatement training, *n* = 7). To capture neural activity occurring during the entire 2 hr test, rats were returned to their home cages for 90 min, then perfused with saline (0.9%) and paraformaldehyde (4%; 210 min after

the start of behavioral testing) (McReynolds et al., 2018). Brains were then sectioned (40 μm) following cryoprotection in 20% sucrose azide.

Fos quantification. To allow quantification of neural activity within anatomically-defined VP subregions, we stained for Fos, and substance P to define VP borders. Ventromedial, ventrolateral, and dorsolateral subregions of substance P-defined VP were delineated with reference to adjacent sections stained for substance P and neurotensin, defining ventromedial VP (Zahm and Heimer, 1988; Root et al., 2015). Dorsolateral and ventrolateral VP were defined by the relative absence of neurotensin immunoreactivity (Zahm and Heimer, 1988; Root et al., 2015). Images of VP were taken at 5x magnification, and one section/rat was quantified bilaterally in rostral VP (+0.12 to +0.60 mm relative to Bregma), and another in caudal VP (-0.48 to -0.24 mm; (Paxinos and Watson, 2006)), squarely within the rostral and caudal zones defined in our previous work (Mahler et al., 2014). Fos+ neurons were identified using the Stereoinvestigator (Microbrightfield) particle counter tool, with thresholding parameters incorporating particle size (> 2 μm^2 and < 200 μm^2), minimum distance between nuclei (150 μm), and color relative to background. Fos density (Fos/mm^2) was computed for each VP subregion on each slice (average of both hemispheres) of each rat. All structure delineation and quantification was performed blind to experimental conditions, and imaging/analysis settings were consistent across rats.

Data analysis. Graphpad Prism software was used for statistical analyses. Effects of punishment on self-administration were examined with repeated measures ANOVAs, including day (last unpunished plus 3 initial punished days) and behavioral output (active lever, inactive lever, infusions) factors. Punishment sensitive versus resistant groups were compared on reinstatement using two-way ANOVA of punishment sensitivity group X reinstatement modality factors. Pearson correlation was used for assessing relationships between aborted lever presses and completed lever presses. Effects of punishment sensitivity group on unpunished cocaine intake and cocaine-induced locomotion were examined with unpaired *t*-tests. Effects of

CNO in control and VP-hM4Di rats on abortive lever pressing were computed with one-way ANOVA. Effects of CNO versus vehicle on each reinstatement modality were examined using separate repeated measures ANOVAs for VP-hM4Di and control rats, with drug (vehicle/CNO) and lever (active/inactive) factors. Effects of VP inhibition on reinstatement in punishment resistant and punishment sensitive rats were computed as change from vehicle day behavior (CNO-vehicle), and analyzed with unpaired *t*-test. Separate one-way ANOVAs compared behavioral groups on Fos density in each VP subregion. Impact of rostrocaudal VP location on Fos was examined with a two-way ANOVA on rostral/caudal site, and reinstatement modality factors. Separate two-way ANOVAs were used to compare CNO effects on cocaine-induced horizontal distance and rearing in control and VP-hM4Di rats. Tukey and Bonferroni corrected *t*-tests were used for posthoc comparisons as appropriate. Two-tailed tests with a significance threshold of $p < 0.05$ were used for all analyses.

Results

Unpunished self-administration. Rats readily discriminated between the inactive and active lever (lever: $F_{(1, 130)} = 55.3$, $p < 0.0001$), and daily cocaine intake was stable by the final 3 days of training ($F_{(2, 130)} = 0.87$, $p = 0.42$). Male and female rats did not differ in active lever presses, or (sex-adjusted) cocaine doses self-administered during the last 3 days of training (no main effect of sex (lever: $F_{(1, 64)} = 1.8$, $p = 0.19$, infusions: $F_{(1, 64)} = 0.29$, $p = 0.59$) or day X sex interaction (lever: $F_{(2, 128)} = 1.0$, $p = 0.37$, infusion: $F_{(2, 128)} = 0.48$, $p = 0.62$).

Individual differences in cocaine seeking under punishment. As expected, cocaine-coincident shock (50% of infusions) in the punishment context suppressed cocaine self-administration overall (day: $F_{(3, 585)} = 30.1$, $p < 0.0001$, **Fig. 3A**). Most rats (79.2%; $n = 42$) reached suppression criterion at the two lowest shock intensities (0.30-0.45 mA: 'punishment sensitive' rats), but a subset of rats (20.8%, $n = 11$) persisted in responding up to higher shock intensities (0.60-0.75 mA: 'punishment resistant' rats; **Fig. 3B-C**). In addition, punishment resistant rats had higher suppression ratios (infusions on the first day in the punishment

context/infusions on the last day in the safe context (Deroche-Gamonet et al., 2004; Pelloux et al., 2007); mean ± SEM = 0.48 ± 0.09) than punishment sensitive rats (mean ± SEM = 0.25 ± 0.02; t_{64} = 4.4, p < 0.0001). Notably, of the 11 punishment resistant rats in this study, 7 were female (30.4% of tested females), while 4 were male (13.3% of tested males).

Punishment resistant rats reinstated more. Punishment resistant rats, once they received shock intensities high enough to suppress even their seeking, showed greater cue-induced reinstatement than punishment sensitive rats. However, this was only true when response contingent cues were delivered, and not for cocaine primed reinstatement (punishment sensitivity x reinstatement type interaction: $F_{(1, 87)}$ = 2.92, p = 0.091; Bonferroni corrected t-test, punishment resistant vs. sensitive in safe context with cues: t_{87} = 3.43, p = 0.0019; **Fig. 3D**; note: **Fig. 3D** shows vehicle-day reinstatement data). Punishment resistance was unrelated to total prior cocaine self-administered (punishment resistant vs. sensitive total unpunished infusions: t_{51} = 0.51, p = 0.61; **Fig. 3E**), or to cocaine's locomotor stimulating or relapse-promoting effects (horizontal distance traveled: t_{36} = 1.34, p = 0.19; **Fig. 3F**; rearing: t_{36} = 1.69, p = 0.10; cocaine prime reinstatement active lever presses: t_{36} = 0.83, p = 0.41), indicating that punishment resistance and cue-induced relapse likely involve common underlying individual differences in addiction-like compulsivity, rather than sensitivity to cocaine's effects per se.

DREADD expression in VP neuronal populations. Robust hM4Di-DREADD expression was observed throughout the rostrocaudal extent of VP (**Fig. 4A-B**). Fluorescent *in situ* hybridization (RNAscope) revealed a predominant colocalization of hM4Di expression with Gad1 (80.8 $\pm$ 4.4 % of hM4Di$^+$ cells), and a smaller percentage colocalizing with Vglut2 (18.1 $\pm$ 2.4 % of hM4Di$^+$ cells; **Fig. 4C-E**). A small fraction of the cells expressed both transcripts (12.3 $\pm$ 3.2 % of hM4Di$^+$ cells). We note that co-localization of Gad1 and Vglut2 transcripts is not sufficient to establish the co-release of glutamate and

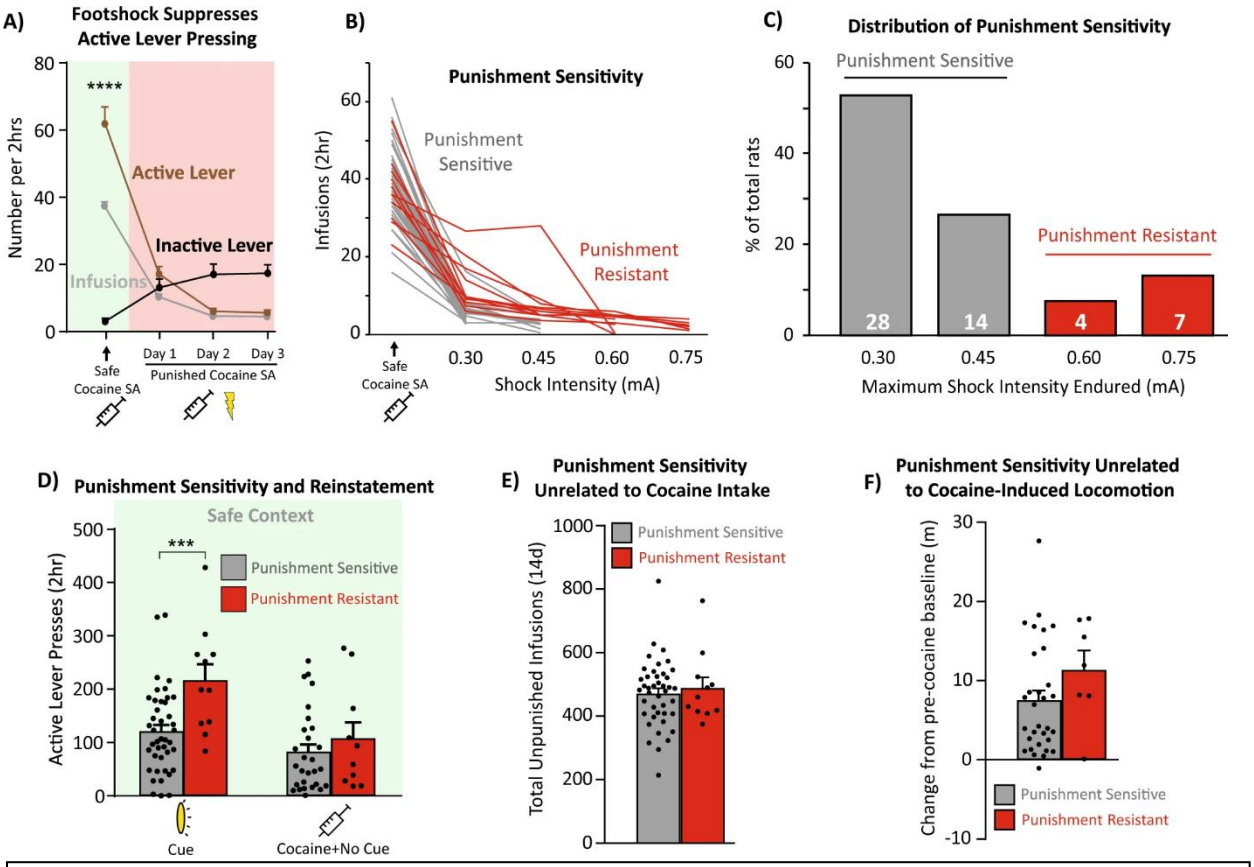

Figure 3. Punishment-resistant rats are more prone than punishment sensitive rats to cue-induced, but not cocaine-primed relapse. A) Probabilistic footshock reduces active lever pressing across all rats, while increasing the number of inactive presses. SA = self-administration. **B)** Individual variation in punishment sensitivity. Rats that reached at least 0.60 mA footshock were considered punishment resistant (dark/red shading). Punishment sensitive rats (light/green shading) stopped taking cocaine at < 0.60 mA footshock intensities. **C)** Most rats cease cocaine intake at low shock levels (punishment sensitive: light/green shading): 42/53 rats, 79.2%), but a subset reached the highest shock levels (punishment resistant: dark/red shading): 11/53 rats, 20.8%). **D)** Punishment resistant rats cue-reinstated more in the safe context, relative to punishment sensitive rats on vehicle day reinstatement tests (the same vehicle-day data are also depicted in **Fig. 4**). This effect was specific to cue-induced, but not cocaine primed relapse. **E-F)** Punishment resistant rats were no different than sensitive rats on unpunished cocaine intake (**E**) or cocaine-induced locomotion (**F**). ***$p < 0.001$.

GABA by these neurons, especially since the Vglut2 signal was weak compared to the Gad1 signal. hM4Di+ neurons lacking either Gad1 or Vglut2 (13.3 $\pm$ 4.8 %, **Fig. 4E**) may represent cholinergic neurons (Root et al., 2015; Faget et al., 2018). These DREADD expression results are consistent with unbiased transduction of all VP neurons, as GABA neurons represent the predominant neuronal phenotype in VP (Faget et al., 2018).

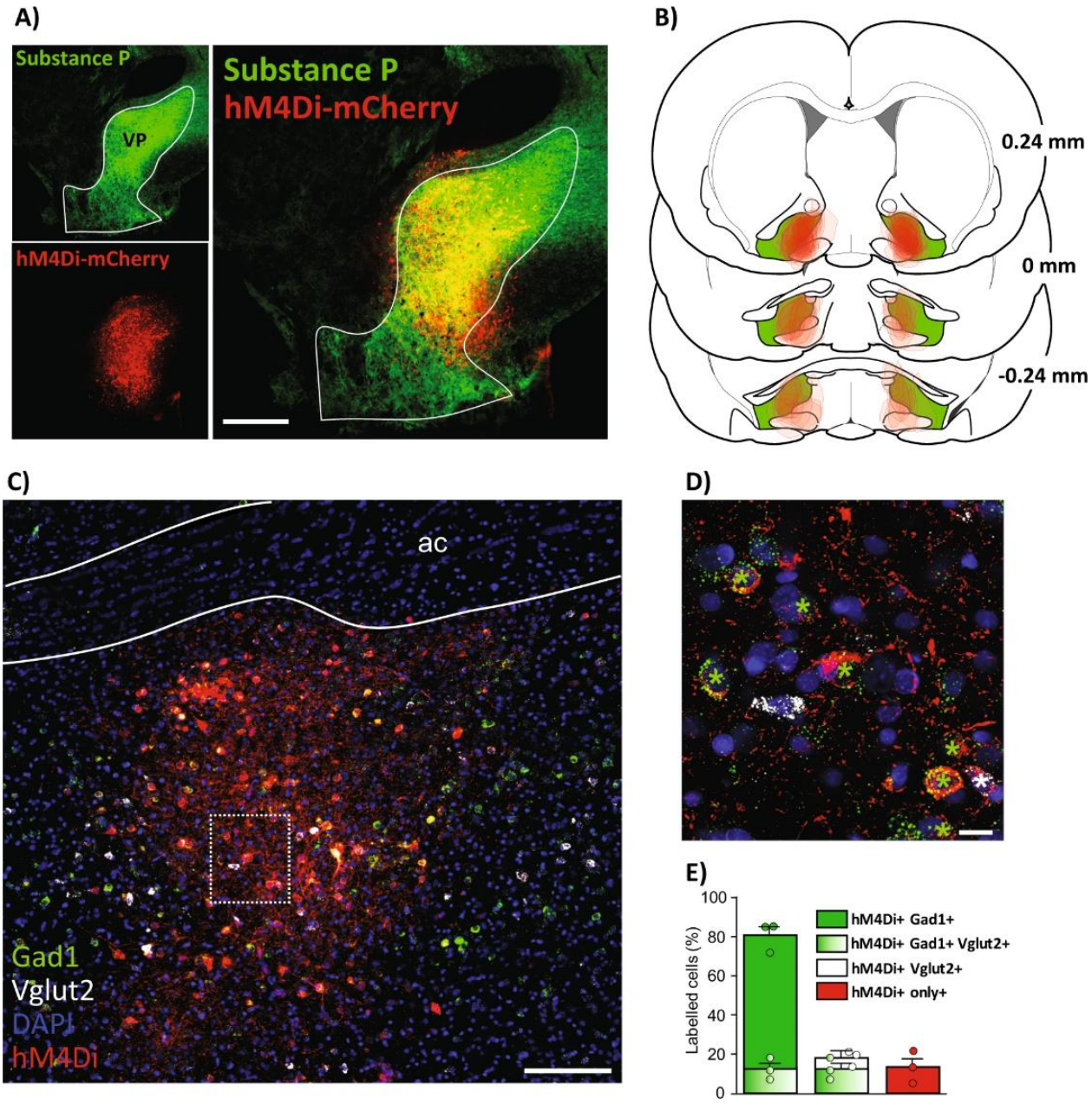

Figure 4. Inhibitory DREADD localization in VP. **A)** Immunofluorescent co-stain for hM4Di-mCherry (red) within Substance P-expressing VP borders (green). **B)** Bilateral hM4Di expression sites in individual animals on VP's rostrocaudal axis relative to bregma. **C**) Wide-field and **D)** high magnification images of fluorescent *in situ* hybridization for Gad1 (green) and Vglut2 (white), combined with immunofluorescence for hM4Di-mCherry (red). $hM4Di^+/Gad1^+$ cells are labeled with green stars, and $hM4Di^+$ /$Vglut2^+$ cells are labeled with white stars. **E)** 80.8 +/- 4.4 % of $hM4Di^+$ cells are co-positive for Gad1 (green bar). 12.3 +/- 3.2 % of $hM4Di^+$ cells are co-labeled for both Gad1 and Vglut2 (green gradient bar). 18.1 +/- 2.4 % of $hM4Di^+$ cells are co-labeled for Vglut2 (white bar). 13.3 +/- 4.8 % of hM4Di+ cells are negative for both Gad1 and Vglut2 (red bar) (*n*=3 rats, total of 531 $hM4Di^+$ cells counted). ac = anterior commissure. Scale bars = 500μm (B), 200μm (C), and 20μm (D).

CNO effects on punishment-induced suppression of cocaine intake in VP-hM4Di rats. On day 1 of punished self-administration, CNO in VP-hM4Di rats modestly, but non-significantly, decreased the number of active and inactive lever presses relative to control rats (treatment: $F_{(1, 33)} = 3.41$, $p = 0.073$; **Fig. 5A**), with no interaction of treatment x lever ($F_{(1, 33)} = 0.27$, $p = 0.61$). CNO had no further effects on lever pressing on day 2, though all rats decreased their responding relative to day 1 (day: $F_{(1, 33)} = 20.56$, $p < 0.0001$), indicating a likely floor effect due to prior punishment training. When vehicle and CNO treatments were reversed on punishment day 3, no further changes were observed (ps > 0.05).

Footshock + cocaine also increased abortive pressing of the active and inactive levers, relative to the low levels of abortive pressing seen during unpunished self-administration in the safe context ($F_{(2, 40)} = 7.93$, $p = 0.0013$; self-administration vs. vehicle day punishment: $p = 0.0022$; **Fig. 5B**). Aborted lever presses were most prevalent in rats with the most punished active lever presses (correlation of aborted lever presses and completed presses after both CNO; $r = 0.61$, $p = 0.027$; and vehicle; $r = 0.61$, $p = 0.016$), suggesting that abortive lever pressing may be a sensitive measure of deliberation about pursuing the now-dangerous cocaine. Interestingly, CNO strongly suppressed aborted lever presses, returning them to unpunished levels in VP-hM4Di rats ($p = 0.0013$; Tukey test, CNO vs. self-administration: $p = 0.93$), but not in controls (controls vs. self-administration: $p = 0.0082$; **Fig. 5B**).

VP DREADD inhibition suppresses cocaine relapse after voluntary abstinence. CNO in VP-hM4Di rats robustly suppressed context only-, cue-, and cocaine-induced relapse in the safe context, but failed to do so in control rats without VP DREADDs. In VP-hM4Di rats, CNO (compared to vehicle) reduced cue-induced active, but not inactive lever pressing in the safe context (drug x lever interaction: $F_{(1, 45)} = 18.53$, $p < 0.0001$; **Fig. 5C**). VP-hM4Di rats with the most specific DREADD localization (> 60% in VP; $n = 13$) exhibited stronger decreases in cue-induced reinstatement relative to rats with less specific DREADD localization (40-60% in VP; $n = 33$; $t_{44} = 2.01$, $p = 0.05$), suggesting that behavioral effects are primarily due to VP inhibition,

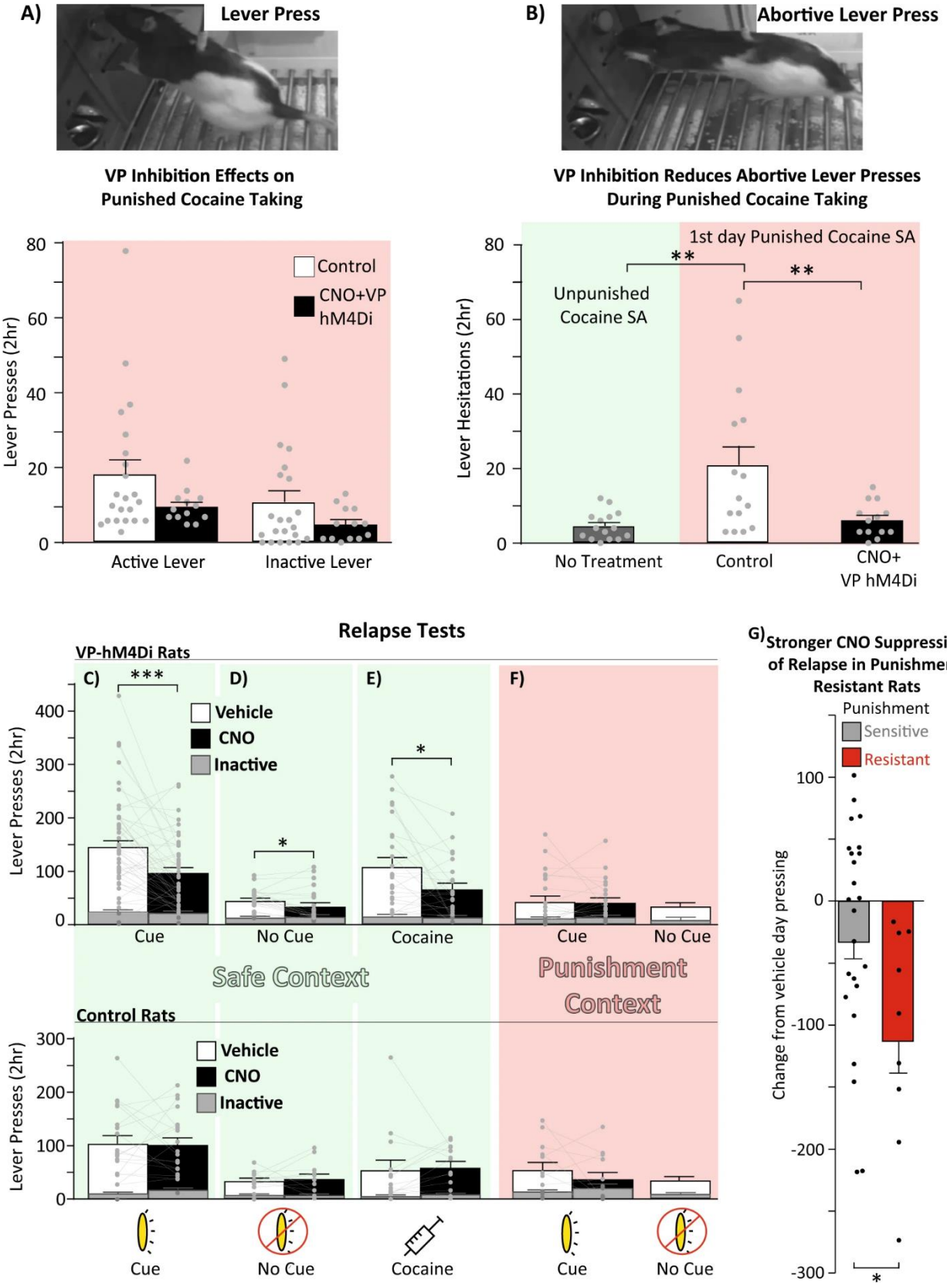
A)
Lever Press
B)
Abortive Lever Press
VP Inhibition Effects on Punished Cocaine Taking
Lever Presses (2hr)
Control
CNO+VP hM4Di
Active Lever
Inactive Lever
VP Inhibition Reduces Abortive Lever Presses During Punished Cocaine Taking
Lever Hesitations (2hr)
1st day Punished Cocaine SA
Unpunished Cocaine SA
No Treatment
Control
CNO+ VP hM4Di
Relapse Tests
VP-hM4Di Rats
C)
D)
E)
F)
Vehicle
CNO
Inactive
Cue
No Cue
Cocaine
Safe Context
Punishment Context
Control Rats
G)
Stronger CNO Suppression of Relapse in Punishment Resistant Rats
Punishment
Sensitive
Resistant
Change from vehicle day pressing

Figure 5. VP inhibition reduces relapse-like behavior, especially in punishment resistant rats. A) Top panel: Example picture of a completed lever press. Bottom panel: CNO in VP-hM4Di rats modestly reduces active and inactive lever pressing for cocaine under threat of punishment on day 1 of punishment training. Control = vehicle-injected rats and CNO-injected VP misses. **B)** Top panel: Example of an aborted press, in which the rat stretches its trunk towards the lever and extends its paw, without depressing the lever. Bottom panel: Active and inactive abortive lever pressing, quantified during safe (light/green shading) and punished (dark/red shading) intake sessions. CNO in VP-hM4Di rats reduced abortive lever pressing relative to control rats, returning abortive pressing to unpunished self-administration levels. Control = vehicle-injected rats, and CNO-injected VP misses. **C-F)** Within subjects comparisons of reinstatement for VP-hM4Di rats (top panels) in safe (light/green shading) and punishment (dark/red shading) contexts. CNO in VP-hM4Di rats reduced reinstatement in the safe context with cues **(C)**, without cues **(D)**, and with cocaine and no cues **(E)**, but not in the punishment context with cues **(F)**. CNO in control rats did not affect reinstatement under any condition (bottom panels). Control = eGFP-only rats, and rats with hM4Di expression primarily outside VP. **G)** CNO in VP-hM4Di punishment resistant rats (dark/red bars) elicited a greater decrease in cued reinstatement, relative to VP inhibition in punishment sensitive rats (light/green bars). Data presented as change from vehicle test baseline. *$p < 0.05$, **$p < 0.01$, ***$p < 0.001$.

rather than inhibition of nearby structures. Moreover, CNO failed to alter cue-induced reinstatement in rats with selective DREADD expression in the VP-adjacent horizontal limb of the diagonal band (HLDB; $n = 5$), a region that was usually partially penetrated in VP-hM4Di rats (no effect of treatment: $F_{(1, 4)} = 0.47$, $p = 0.53$; or treatment x lever interaction: $F_{(1, 4)} = 0.47$, $p = 0.53$).

CNO administration in VP-hM4Di rats suppressed safe context pressing without response-contingent cues (drug x lever interaction: $F_{(1, 20)} = 4.31$, $p = 0.05$; **Fig. 5D**). Cocaine primed reinstatement (no cues) in the safe context was also suppressed by CNO in VP-hM4Di rats (drug x lever interaction: $F_{(1, 23)} = 7.94$, $p = 0.01$; **Fig. 5E**). Effects of VP inhibition on cocaine primed reinstatement in the punishment context were not examined here, but warrant future study. Although we previously showed that rostral and caudal VP differentially mediate cue- and primed reinstatement using a spread-limiting lentiviral vector (Mahler et al., 2014), AAV2 viral infection here spanned most of the rostrocaudal axis of VP. In contrast to the safe context, CNO in VP-hM4Di rats failed to reduce cue reinstatement in the punishment context (drug x lever interaction: $F_{(1, 21)} = 0.19$, $p = 0.66$; **Fig. 5F**). This null finding was unlikely to have resulted from a floor effect, since pressing was similar in the punishment context with cues and the safe

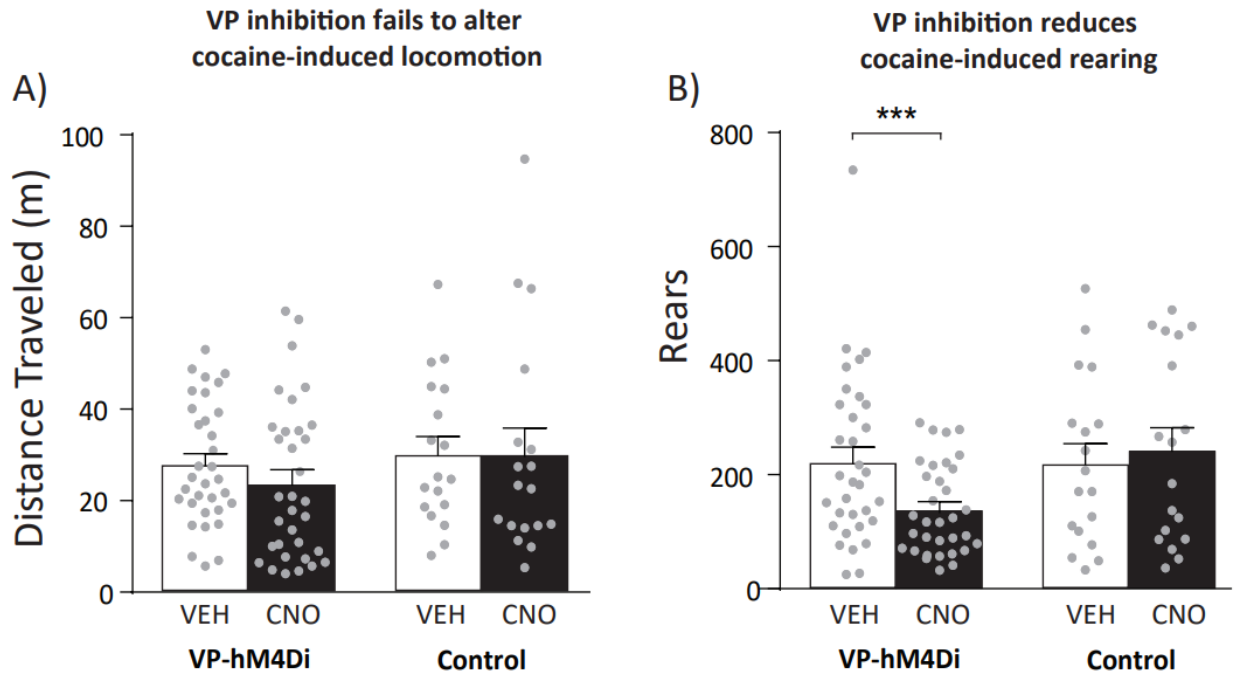

Figure 6. VP inhibition decreases cocaine-induced rearing, but not distance traveled. **A)** Within-subject tests showed that CNO in VP-hM4Di rats and controls fails to alter cocaine-induced horizontal locomotion. **B)** CNO decreases rearing in VP-hM4Di rats, but not controls. Control = extra-VP hM4Di and eGFP-only rats. ***$p < 0.001$.

context without cues, yet VP inhibition suppressed only the latter. In control rats without VP DREADDs, CNO had no effects on lever pressing in any reinstatement test (*ps* > 0.05; **Fig. 5C-F**), suggesting that CNO effects here, as previously shown (Mahler et al., 2014; Chang et al., 2015; Prasad and McNally, 2016; Mahler et al., 2019), were specific to VP inhibition.

VP inhibition suppressed relapse most in punishment-resistant rats. VP inhibition reduced safe context cue-induced reinstatement more in punishment-resistant rats than punishment-sensitive rats ($t_{44} = 2.23$, $p = 0.031$; **Fig. 5G**). This effect was specific to the safe context with cues, as there was no such effect on other reinstatement types (*t* values < 1.26, *ps* > 0.22). Importantly, DREADD expression was identical in punishment sensitive and resistant groups (% of VP infected: $t_{31} = 1.16$; $p = 0.25$; % of expression within VP borders: $t_{31} = 0.85$, $p = 0.40$). This finding suggests that VP plays an especially important role in relapse after punishment-imposed abstinence for the individual rats showing the most addiction-like behavior.

VP inhibition did not affect cocaine-induced locomotion. CNO failed to affect the locomotor-activating effects of cocaine in either VP-hM4Di or control groups (treatment: $F_{(1, 49)} = 0.63$, $p = 0.43$; treatment x group interaction: $F_{(1, 49)} = 0.58$, $p = 0.45$; **Fig. 6A**), though it did reduce rearing behavior after cocaine in VP-hM4Di rats, but not controls (treatment x group interaction: $F_{(1, 49)} = 10.24$, $p = 0.0024$; **Fig. 6B**). Moreover, CNO did not differentially reduce horizontal locomotion or rearing in punishment-sensitive versus -resistant VP-hM4Di rats (group x treatment interaction; locomotion: $F_{(3, 93)} = 0.70$, $p = 0.55$; rearing: $F_{(3, 93)} = 0.61$, $p = 0.61$). These results indicate that VP mediates cocaine-induced motivation, but not all cocaine-induced behaviors.

VP subregion Fos recruited during relapse. Relative to cocaine/shock-experienced rats sacrificed from their homecages, VP subregions showed strong Fos activation during all tested reinstatement conditions ($F_{(3, 47)} = 3.93$, $p = 0.014$; Tukey: punishment + no cues, $p = 0.013$; safe + cues, $p = 0.019$; safe + no cues, $p = 0.043$). Ventromedial VP was selectively activated (relative to home cage) by the punishment context without cues, but not by either of the safe context reinstatement tests ($F_{(3, 47)} = 2.67$, $p = 0.05$; Tukey: punishment + no cues: $p = 0.048$; safe + cues: $p = 0.28$; safe + no cues: $p = 0.09$; **Fig. 7A-C**). In contrast, ventrolateral and dorsolateral VP were activated in all reinstatement conditions, relative to homecage controls (ventrolateral: $F_{(3, 47)} = 5.98$, $p = 0.0015$; Tukey: safe + cues: $p = 0.0051$; safe + no cues: $p = 0.0011$; punishment + no cues: $p = 0.0049$; **Fig. 7D**; dorsolateral**:** $F_{(3, 47)} = 4.63$, $p = 0.006$; Tukey: safe + cues: $p = 0.0043$; safe + no cues: $p = 0.017$; punishment + no cues: $p = 0.021$; **Fig. 7E**). We then examined Fos expression based on rostral and caudal sections position within VP, given known rostrocaudal functional and anatomical differences (Smith and Berridge, 2005, 2007; Mahler et al., 2014; Root et al., 2015). Overall, rostral VP had greater Fos density than caudal VP ($F_{(3, 47)} = 4.8$, $p = 0.0051$), though this did not significantly differ between reinstatement types (no reinstatement type x rostrocaudal position interaction; $F_{(3, 47)} = 1.42$, $p = 0.25$; **Fig. 7F**).

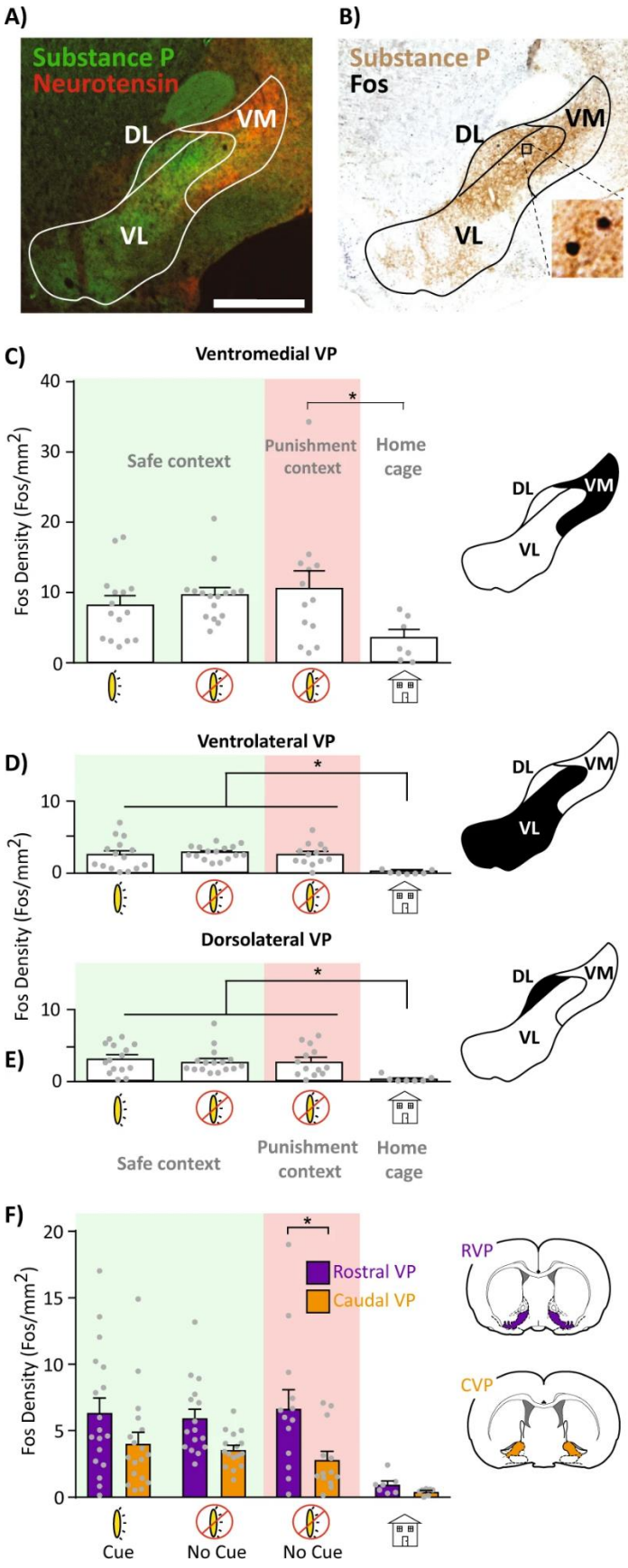

Figure 7. VP subregion Fos expression after relapse-like behavior. **A)** Representative image of substance P (VP borders) and neurotensin (ventromedial VP marker) immunofluorescent co-stain. **B)** Representative image of substance P and Fos co-staining used for Fos quantification. **C-E)** Comparison of VP ventromedial **(C)**, ventrolateral **(D)**, and dorsolateral **(E)** Fos density across reinstatement conditions. Light/green shading = safe context, dark/red shading = punishment context, no shading = home cage controls. **F)** Fos density across the VP rostrocaudal axis after reinstatement tests (collapsed across mediolateral subdivisions). Rostral VP had greater Fos density than caudal VP only in the punishment context + no cues condition; VM = ventromedial, VL = ventrolateral, DL = dorsolateral. AC = anterior commissure. Scale bar = 1000μm. $p < 0.05$*.

Sex differences. Few sex differences in VP manipulation effects were detected. Male and female rats exhibited comparable levels of punishment-induced suppression of cocaine self-administration (suppression ratio: $t_{64} = 1.65$, $p = 0.10$) and comparable levels of cocaine self-administration (**Fig. 8A**). Notably, female rats represent 63.6%

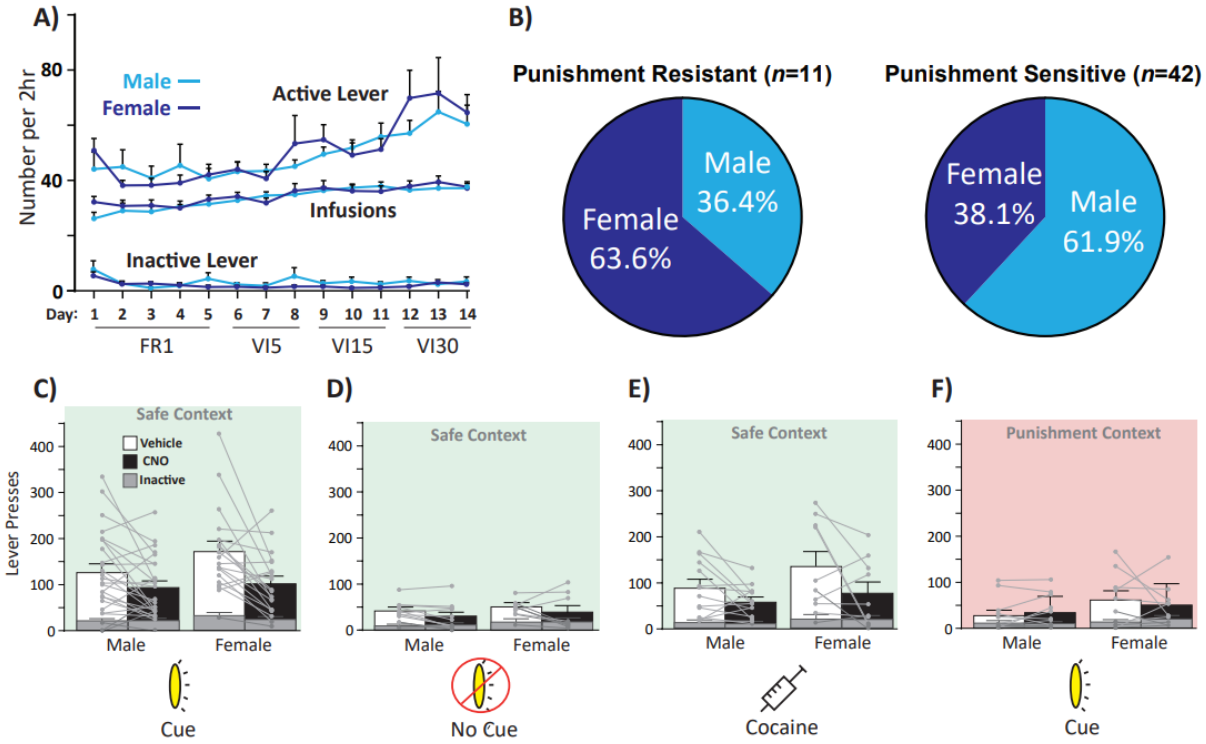

Figure 8. Breakdown of self-administration, punishment resistance, and reinstatement by sex. A) Active lever (top lines), cocaine infusions (middle lines), and inactive lever (bottom lines) shown for 14d self-administration training in male (light blue) and female (dark blue) rats. **B)** Punishment sensitivity classification for male (light blue) and female (dark blue) rats. 63.6% of total punishment resistant rats were female (left panel), whereas 38.1% of punishment sensitive rats were female (right panel). **C-F)** Reinstatement testing for male and female VP-hM4Di rats. White bars = vehicle test, black bars = CNO test, gray bars = inactive lever presses, gray circles = individual rat active lever presses. Reinstatement testing data presented for: **C)** safe context with response contingent cues, **D)** safe context with no response contingent cues, **E)** safe context with cocaine prime, and **F)** punishment context with response contingent cues.

of the punishment resistant rats (7/11 rats), while females represent 38.1% of the punishment sensitive rats (16/42 rats; **Fig. 8B**). As previously reported (Van Haaren and Meyer, 1991), females exhibited more cocaine-induced locomotion than males (sex; $F_{(1, 31)} = 4.91$, $p = 0.034$,), though CNO in VP-hM4Di rats did not sex-dependently impact locomotion (sex x treatment interaction; $F_{(1, 31)} = 0.33$, $p = 0.57$) or any type of reinstatement (Fs < 2.5, ps > 0.13; **Fig. 8C-F**). Despite greater cocaine-induced locomotion in females, no sex differences in cocaine-primed reinstatement were seen ($F_{(1, 22)} = 2.06$, $p = 0.17$), suggesting that cocaine's arousing and incentive motivational effects are differentially impacted by sex.

Discussion

These findings point to a crucial role for VP in cocaine relapse following voluntary abstinence, a translationally-relevant model of humans who relapse after quitting drugs due to mounting negative life outcomes. Indeed, we found that VP plays an especially important role in the most compulsive cocaine-seeking individuals, i.e., the ~20% of rats that here tolerated significant footshock punishment to continue taking cocaine. We also found robust relapse-related activity in anatomically defined VP subregions. Our results suggest that unlike connected limbic nuclei, VP plays a critical role in reinstatement regardless of how abstinence was achieved or how relapse was initiated, thereby placing it amongst the most essential nodes within the neural circuits of cocaine addiction.

VP is essential for addiction-like compulsive seeking and relapse. Persistent drug use despite negative consequences, and long-lasting relapse propensity are cardinal features of addiction in humans (American Psychiatric, 2013). Though compulsive drug intake despite punishment is common following extended drug access in rodents (Vanderschuren and Everitt, 2004; Pelloux et al., 2007; Chen et al., 2013), some rats seem to transition to compulsive use even after short access to cocaine. Here, we observed such a subset of compulsive rats, and found that these same animals were also most sensitive to cue + context reinstatement after voluntary abstinence, similar to prior findings (Deroche-Gamonet et al., 2004; Torres et al., 2017; Yager et al., 2019). Importantly, VP inhibition in these compulsive rats had a greater relapse-suppressing effect than in punishment sensitive rats, suggesting that VP plays a particularly important role in those rats which most pathologically seek drug. VP inhibition only modestly reduced punished cocaine self-administration, but selectively reduced abortive pressing of the cocaine/shock and inactive levers, which we interpret as reflecting motivation to pursue cocaine tempered by motivation to avoid being shocked. These results highlight the sensitivity of this novel assay of conflicting motivations during cocaine seeking, as well as the

importance of careful ethological analysis of complex drug-seeking behaviors during such neural circuit manipulation experiments.

Relapse is not a unitary phenomenon, since brain circuits underlying drug reinstatement depend on the drug of choice, mode of abstinence, and relapse trigger (Shalev et al., 2002; Bossert et al., 2005; Fuchs et al., 2006; Badiani et al., 2011; Mantsch et al., 2016; Farrell et al., 2018; Marchant et al., 2018; Pelloux et al., 2018a). This said, we show that even under maximally human-relevant conditions VP is broadly implicated in reinstatement regardless of trigger, or mode of abstinence. In contrast, other VP-connected limbic regions seem to be engaged differentially during reinstatement after different modes of abstinence. For example, inhibition of BLA *decreases* reinstatement after extinction training, whereas the same manipulation during reinstatement following punishment-induced abstinence *increases* drug seeking (Pelloux et al., 2018a). These results are consistent with the idea that VP serves as a 'final common pathway' of drug seeking (Kalivas and Volkow, 2005; Smith et al., 2009). Therefore, VP holds promise as a potential therapeutic target for suppressing relapse in humans, especially since a prior human fMRI report found that activity in the vicinity of VP predicts relapse propensity in humans (Li et al., 2015).

Interestingly, in the unpunished safe context, VP inhibition attenuated reinstatement with or without cues, and also cocaine primed reinstatement, yet VP inhibition did not reduce cue reinstatement in the punishment context. As expected, conditioned suppression of cue-induced seeking was observed in the punishment context relative to the safe context, but response-contingent cues nonetheless supported some pressing, and this was not affected by VP inhibition. We therefore speculate that VP promotes conditioned drug seeking in a context-gated manner (Bouton, 2019), consistent with prior reports that VP is necessary for context-induced reinstatement of alcohol seeking (Perry and McNally, 2013; Prasad and McNally, 2016, 2019; Prasad et al., 2019).

Heterogeneities in VP circuits underlying relapse. VP is a heterogeneous structure, with rostrocaudally- and mediolaterally-located subregions, and genetically-distinct, functionally-opposing neuronal subpopulations (Root et al., 2015; Knowland et al., 2017; Faget et al., 2018; Tooley et al., 2018; Prasad et al., 2019; Stephenson-Jones et al., 2020). We observed broad recruitment of Fos in VP subregions after exposure to both the safe and punishment context, and in the safe context when response-contingent cues were presented. This homecage-relative Fos recruitment was more pronounced in rostral than caudal VP, yet there was broad activation of ventromedial, dorsolateral, and ventrolateral subregions under all reinstatement conditions. We note that VP DREADD expression here spanned rostrocaudal VP subregions, potentially obscuring the distinct roles these subregions may play in cocaine seeking (Mahler et al., 2014). Though we found no effect of selective inhibition of a VP-adjacent region (HLDB), and reinstatement suppression effects were strongest in the rats with the most selective VP DREADD expression, the dissociable roles of VP subregions, and of other nearby basal forebrain structures (e.g., lateral preoptic area) should be further investigated.

Our results suggest a global recruitment of VP subregions during safe context- and safe context + cue-induced relapse, and also during mere exposure to the punished context, though global VP inhibition failed to suppress cue-induced cocaine seeking in this dangerous context. One possible explanation for this puzzling pattern of effects is that functionally opposed VP cells are engaged in the safe- and punished-contexts, such as the intermingled VP^{GABA} and glutamate neurons which drive appetitive and aversive behavior, respectively (Faget et al., 2018; Tooley et al., 2018; Wulff et al., 2018). Our pan-neuronal chemogenetic approach primarily targeted reward-related VP^{GABA} neurons (~80%), which likely mediate reinstatement in the safe context, when aversion-related glutamate neuron activity may be less relevant. We speculate that in the punishment context, glutamate and GABA neurons are both recruited (explaining Fos results), but inhibiting both populations concurrently with DREADDs suppressed motivation as well as aversion, resulting in a null effect. More work is clearly needed to parse

the specific behavioral roles for VP subregions and neuronal subpopulations in addiction-related behaviors.

The circuit mechanisms by which VP inhibition reduces reinstatement remain puzzling, given that VP's strongest afferent is from NAc GABA neurons, in which neural activity would be expected to inhibit VP cells—yet this activity appears to promote motivation similarly to activity in VP itself (Carelli et al., 2000; McFarland et al., 2003; Day et al., 2006; Salamone et al., 2007; Ambroggi et al., 2008; Fuchs et al., 2008; Floresco, 2015). Clearly, there is more complexity to the network-level interactions of VP and NAc than is currently appreciated. Future work should explore the motivation-related roles of NAc/VP subregional communication, functional distinctions between VP and/or NAc cell subpopulations, and also the major reciprocal projection from VP back to NAc (Smith and Berridge, 2007; Stefanik et al., 2013; Richard et al., 2016; Chang et al., 2018; Ottenheimer et al., 2018; Smedley et al., 2019).

Conclusion. The present report firmly establishes VP as an essential node in the neural circuits of translationally-relevant cocaine reinstatement behavior, especially in the most compulsive, addicted-like rats. By better understanding how addiction-relevant behaviors map onto defined neural circuits in the addicted brain, we may reveal neural signatures that could facilitate diagnosis and treatment of addiction in a personalized manner. These results join others which suggest that VP plays a pivotal role in relapse, spanning specific relapse triggers and modes of abstinence, making it a promising target for future interventions to treat addiction.

CHAPTER 2: Ventral pallidum GABA neurons bidirectionally control opioid relapse across rat models

Introduction

Pan-neuronal chemogenetic VP inhibition strongly attenuated reinstatement of cocaine seeking after punishment-imposed abstinence (Farrell et al., 2019). Here, we expand upon these findings by selectively chemogenetically inhibiting or stimulating VP^{GABA} neurons during reinstatement to remifentanil seeking—a potent μ opioid receptor agonist.

Opioid addiction is a disorder characterized by persistent drug use despite adverse consequences, and chronic risk of relapse after quitting. Though addicted individuals frequently quit drug use due to mounting negative consequences, they often still relapse despite their desire to remain abstinent (O'Brien et al., 1992; Sinha and Li, 2007; American Psychiatric, 2013). In particular, exposure to drug-associated cues or contexts often elicit cravings and promote relapse (Serre et al., 2015).

Much preclinical work has examined the neural circuits of cue-, stress-, or drug-induced relapse-like behavior in rodents, especially using models involving experimenter-imposed abstinence or extinction training prior to reinstatement of drug seeking (Shaham et al., 2003). Yet these conventional models do not capture the voluntary initiation of abstinence that is typical of people with addiction seeking to control their use in the face of mounting negative life consequences—rats in these experiments have little disincentive to pursue drugs when they may be available (Ahmed et al., 2013; Venniro et al., 2020). It has been argued that the presence of such disincentives to drug use might be important for preclinically modeling addiction (Belin et al., 2016; Vanderschuren et al., 2017; Lüscher et al., 2020), especially since the neural substrates underlying reinstatement differ when rats previously chose to stop taking drugs, rather than undergoing extinction training (Panlilio et al., 2005; Pelloux et al., 2018a). Furthermore, no single rodent model captures all aspects of the human use-cessation-relapse cycle, so to maximize likelihood of translational relevance, we propose that putative addiction

interventions should be tested in multiple rodent behavioral models including those optimizing human relevance (Epstein et al., 2006). We hope that by understanding the converging neural circuits underlying relapse across animal models that capture distinct features of the human disorder, we can identify more promising candidates for targeting brain-based psychiatric interventions in humans struggling to control their drug use.

Many prior rodent reinstatement studies have examined the brain substrates of relapse following experimenter-imposed homecage abstinence (such as incubation of craving), or extinction training (De Wit and Stewart, 1981; Shaham et al., 2000; Grimm et al., 2001; Fuchs and See, 2002; Pickens et al., 2011; Reiner et al., 2019; Kruyer et al., 2020; Fredriksson et al., 2021). Fewer studies have used models in which rodents instead voluntarily cease their drug use, for example due to delivery of punishing shocks co-administered with drug. For opioid drugs, this is partly due to the methodological consideration that the analgesic properties of opioid drugs can diminish the ability of shock to suppress drug seeking. Here, we circumvented this problem by using the short-acting, but highly reinforcing μ opioid receptor agonist remifentanil, similar to a model presented by Panlilio and colleagues (Panlilio et al., 2003, 2005). Since remifentanil is rapidly metabolized (Burkle et al., 1996), we were able to develop a shock-based voluntary abstinence/reinstatement procedure, allowing for direct comparison of opioid reinstatement following either voluntary punishment-induced abstinence, or extinction training.

Specifically, we examined the role of VP, a brain region tightly embedded within mesocorticolimbic motivational circuits, where opioid signaling plays important roles in reward-related processes (Napier and Mitrovic, 1999; Smith et al., 2009). Locally applied μ opioid receptor agonists in VP induce robust food intake and locomotion, and enhance pleasure-like reactions to sweet tastes (Austin and Kalivas, 1990; Smith et al., 2009). Systemically administered heroin or morphine decrease extracellular GABA levels in VP (Caillé and Parsons, 2004, 2006), and lesioning or inactivating VP neurons diminishes high-effort responding for

heroin (Hubner and Koob, 1990), and the ability of heroin priming injections to reinstate heroin seeking following extinction training (Rogers et al., 2008b). VP is also required for high-effort intake of remifentanil, since local application of an orexin receptor antagonist attenuates remifentanil motivation in both behavioral economic and cue-induced reinstatement tasks (Mohammadkhani et al., 2019). Therefore, VP is a key node in the circuits underlying the rewarding and relapse-inducing effects of addictive opioid drugs.

This said, VP is a heterogeneous structure, and little is known about how this functional heterogeneity impacts relapse-like behavior for opioids. VP contains subpopulations of neurons with different neurotransmitter profiles and behavioral functions (Geisler et al., 2007; Root et al., 2015; Faget et al., 2018; Tooley et al., 2018; Heinsbroek et al., 2020; Stephenson-Jones et al., 2020), and rostrocaudal as well as mediolateral functional heterogeneity are also apparent (Heimer et al., 1991; Johnson et al., 1993; Churchill and Kalivas, 1994; Panagis et al., 1995; Zahm et al., 1996; Calder et al., 2007; Smith and Berridge, 2007; Kupchik and Kalivas, 2013; Root et al., 2013; Mahler et al., 2014). For example, the rostral portion of VP is critical for cue-induced cocaine seeking, whereas its caudal aspect is instead required for cocaine-primed reinstatement (Mahler et al., 2014). Caudal VP also contains a 'hedonic hotspot' wherein local application of a selective μ opioid receptor agonist (or orexin$_A$ peptide (Ho and Berridge, 2013)) selectively enhances taste pleasure (Smith and Berridge, 2005, 2007).

VP^{GABA} neurons, which span both rostral and caudal VP zones, appear to play a specialized role in reward-related processes, in contrast to intermingled VP glutamate neurons, which instead mediate aversive salience processes (Geisler et al., 2007; Faget et al., 2018; Tooley et al., 2018; Stephenson-Jones et al., 2020; Wang et al., 2020). For example, mice find optogenetic stimulation of VP^{GABA} neurons reinforcing, and these neurons show endogenous firing patterns consistent with the encoding of incentive value of rewards and reward-predictive cues (Zhu et al., 2017; Faget et al., 2018; Stephenson-Jones et al., 2020). Stimulation of a subset of VP^{GABA} neurons expressing enkephalin also increases reinstatement of cocaine

seeking in mice following extinction training (though broadly stimulating VP^{GABA} neurons did not affect reinstatement) (Heinsbroek et al., 2020), and inhibiting VP^{GABA} neurons suppresses context-induced alcohol seeking after extinction training in rats (Prasad et al., 2020). Though these findings point to an important role for VP^{GABA} neurons in highly motivated and relapse-relevant behaviors, no studies have yet examined their roles in opioid seeking, nor compared their functions in relapse models capturing dissociable addiction-relevant behavioral processes.

Here we address this gap by determining how VP^{GABA} neurons regulate remifentanil intake and seeking using two distinct models of relapse-like behavior, including a newly adapted voluntary abstinence-based reinstatement task. Using DREADDs (Armbruster et al., 2007), we found that inhibiting VP^{GABA} neurons decreased opioid relapse after voluntary abstinence, whereas stimulating VP^{GABA} neurons strongly increased opioid seeking regardless of the way in which abstinence was achieved prior to reinstatement. Moreover, chemogenetic effects largely relied on the presence of response-contingent cues, suggesting that VP^{GABA} neurons may play a special role in discrete cue-induced opioid seeking. Consistent with these findings, VP Fos expression correlated with opioid reinstatement behavior in individual animals, but only in its rostral, but not caudal, subregion. Further, we found that neither inhibiting nor stimulating VP^{GABA} neurons influenced unpunished remifentanil self-administration, highlighting a selective role for these neurons in relapse-like drug seeking, rather than in the primary reinforcing effects of remifentanil. Together, these results point to a fundamental and specific role for VP^{GABA} neurons in opioid drug relapse-like behavior in rats, regardless of the behavioral model employed. These results beg the question of whether VP is similarly involved in human drug relapse, and if so, whether such circuits might be a promising future target for clinical treatment of opioid or other addictions (Farrell et al., 2018; Farrell et al., 2019; McGovern and Root, 2019).

Methods

Subjects. GAD1:Cre transgenic rats (*n* = 32 males, *n* = 9 females) and wildtype littermates (*n* = 22 male, *n* = 12 female) were used in these studies. They were pair-housed in temperature,

humidity, and pathogen-controlled cages under a 12:12 hr reverse light/dark cycle, and were provided *ad libitum* food and water in the homecage throughout all experiments. Experiments were approved by University of California Irvine's Institutional Animal Care and Use Committee, and were conducted in accordance with the NIH Guide for the Care and Use of Laboratory Animals (National Research, 2010).

Surgery. Procedures for GAD1:Cre-dependent DREADD viral injections in VP were conducted as previously described (Farrell et al., 2021). Briefly, anesthetized GAD1:Cre rats and wildtype littermates were injected with one of three AAV2 viral constructs obtained from Addgene: hSyn-DIO-hM4D(Gi)-mCherry (*n* = 11 males, 9 females), hSyn-DIO-hM3D(Gq)-mCherry (*n* = 36 males, 12 females), or hSyn-DIO-mCherry (*n* = 7 male, 0 female) (~0.3 µL/hemisphere, titers: ~1.2 x 10^{13} GC/mL). During the same surgery, rats were implanted with indwelling, back-mounted right jugular vein catheters for chronic drug self-administration as previously described (Mahler and Aston-Jones, 2012; Mahler et al., 2014; Farrell et al., 2019; Mahler et al., 2019).

Drugs. Frozen powder aliquots of clozapine-N-oxide (CNO; NIDA) were diluted in 5% dimethyl sulfoxide (DMSO; Sigma-Aldrich), vortexed for 10 s, then diluted with sterile 0.9% saline to a concentration of 5 mg/mL. CNO was mixed fresh on each test day, and injected at 5 mg/kg (i.p.) 30 min prior to the start of behavioral testing in all experiments. Vehicle solutions were 5% DMSO in saline, injected at 1 mL/kg. Rats were surgically anesthetized with ketamine (56.5 mg/kg) and xylazine (8.7 mg/kg), and given the non-opioid analgesic meloxicam (1 mg/kg). Remifentanil hydrochloride was dissolved in sterile 0.9% saline to a concentration of 38 µg/mL for self-administration.

Group^{Punish} training.

Self-administration phase.

Following recovery from surgery, hM4Di (*n* = 8 males, 5 females), hM3Dq (*n* = 13 male, *n* = 0 female) and control rats (*n* = 9 males, 8 females) were initially trained in a distinct Context A (peppermint odor, white light, and bare walls) during 2 hr daily sessions. They learned to

press an active lever for intravenous infusions of remifentanil (1.9 µg/50 µL/ infusion), a short-acting µ opioid receptor agonist (Egan, 1995; Burkle et al., 1996), accompanied by a light + tone cue (3.6 s stimulus light + 2.9 kHz tone). Infusions/cues were followed by a 20 s timeout period, signaled by dimming of the houselight, during which lever presses were unreinforced, but recorded. Presses of an inactive lever positioned on the opposite side of the chamber were without consequence. Training in Context A proceeded on the following schedules of reinforcement: 5-6 days of fixed-ratio 1 (FR1), 2 days of variable interval 5 (VI5), 2 days of VI15, and finally 5 days of VI30.

*Punishment training***.**

Next, Group^{Punish} rats were moved to a distinct Context B (orange odor, red light, and polka dot walls), where active lever presses (on a VI30 schedule) yielded the same dose of remifentanil and the same light + tone cue as delivered in Context A. However, in Context B, infusions were accompanied by a 50% probability of footshock, delivered concurrently with the start of the infusion/cue. All rats were initially given one drug-free punishment training day in Context B (0.30 mA footshock intensity), in order to determine the degree of punishment-induced suppression of self-administration in each individual. An initial cohort (*n* = 7 hM4Di, *n* = 5 hM3Dq, *n* = 4 controls) was then used to examine effects of inhibiting or stimulating VP^{GABA} neurons during punished remifentanil self-administration. This group was administered CNO (5 mg/kg) or vehicle on each subsequent daily punishment training day according to the following protocol: 2 days with 0.30 mA shocks, followed by 2 days each at footshock intensities increasing by 0.15 mA on each step, up to a maximum of 1.65 mA, to suppress pressing. Punishment training ceased in all rats upon reaching voluntary abstinence criterion (< 25 AL presses on 2 consecutive days, days to criterion mean ± SEM: 16.8 ± 0.53). 48+ hours after abstinence criterion was reached in these rats, they were given a final Context B punished self-administration test without CNO/vehicle, to measure maintenance of abstinence in the absence of VP manipulation.

Since no signs of CNO effects were observed on punished drug seeking in this cohort (data not shown), subsequent cohorts of rats (n = 20 males, 7 females) received a modified protocol aimed at more rapidly inducing voluntary abstinence, without daily CNO/vehicle treatment. These rats were trained on the Context B punished self-administration procedure according to the following protocol: 1 day of 0.30 mA shocks, followed by 1 day each at 0.45, 0.60, 0.75, 0.90, and 1.05, 1.20, and 1.35 mA. Rats trained with both protocols reached the same voluntary abstinence criterion (< 25 AL presses on 2 consecutive days) and showed similar levels of pressing by the end of training (average active lever presses on last 2 days in the 2 cohorts: $t_{41} = 0.15$, $p = 0.88$). Both cohorts also showed similar levels of subsequent reinstatement behavior (two-way ANOVA on reinstatement type x cohort; no main effect of cohort: $F_{(1, 121)} = 0.28$, $p = 0.60$; or reinstatement type x cohort interaction: $F_{(2, 121)} = 1.68$, $p = 0.19$). Therefore, groups were collapsed for subsequent analyses of DREADD effects on reinstatement in Group^{Punish}.

Reinstatement testing.

After achieving abstinence criterion in Context B, all Group^{Punish} hM4Di, hM3Dq, and control rats were then administered a series of reinstatement tests to determine how inhibiting or stimulating VP^{GABA} neurons affected reinstatement in Contexts A and B, with or without response-contingent cues (and without further remifentanil or shocks). Counterbalanced vehicle and CNO injections were administered using a within subjects design prior to each reinstatement test with 48 hrs between each test: 1) Context B with response-contingent cues (n = 42) and 2) with no cues (n = 42) and 3) Context A with (n = 43) and 4) with no cues (n = 27). Note that a subset of rats (n = 16) did not undergo the Context A with no cues tests, due to a Spring of 2020 COVID-19 shutdown. Active/inactive lever presses were recorded.

Remifentanil self-administration retraining and testing.

Following reinstatement testing, a subset of Group^{Punish} rats (n = 5 male, n = 1 female hM4Di, n = 8 male, n = 0 female hM3Dq, n = 6 male, n = 6 female controls) were retrained to

self-administer remifentanil and light + tone cue in a distinct chamber (ie, neither Context A nor B) on a VI30 schedule, identical to initial training. Counterbalanced vehicle and CNO tests were administered upon achieving stability criterion (< 25% change in active lever presses on 2 consecutive days), with at least one day of restabilization between tests.

Group^{Ext} training. A separate cohort of hM3Dq rats (*n* = 8 males, 4 females) and controls (*n* = 11 males, 4 females) were trained to self-administer remifentanil/cues exactly as was Group^{Punish}: 14 daily 2 hr sessions up to VI30, occurring in Context A. Next, Group^{Ext} was also moved to Context B, but for this group active lever presses delivered no drug infusions, cues, or shocks (extinction conditions), unlike in Group^{Punish} where Context B active lever presses yielded all three. Extinction training continued in Context B for Group^{Ext} rats until the extinction criterion was met (< 25 active lever presses on 2 consecutive sessions). After lever pressing was extinguished, Group^{Ext} rats then underwent CNO/vehicle tests on each of the 4 reinstatement types, as described for Group^{Punish} rats above: 1) Context B with cues (*n* = 27) and 2) with no cues (*n* = 27) and 3) Context A with cues (*n* = 27) and 4) with no cues (*n* = 27).

hM3Dq-DREADD Fos validation. Our prior work validated the function of hM4Di-DREADDs in VP^{GABA} neurons of GAD1:Cre rats (Farrell et al., 2021). Here, we confirmed the function of hM3Dq-DREADDs in this model, using Fos as a marker of neural activity. To do so, two experimentally-naïve groups were first tested. The first group expressed mCherry in VP^{GABA} neurons (mCherry-only, *n* = 3), and the second group instead expressed hM3Dq-mCherry in VP^{GABA} neurons (*n* = 3). Both groups were injected with CNO before returning to the homecage for 2.5 hrs, then were perfused for analysis of Fos in mCherry-expressing VP^{GABA} neurons.

Further, we also asked whether hM3Dq-induced Fos was affected by the behavioral situation the rat was in. In a final 2 hr session following reinstatement testing described above, we stimulated VP^{GABA} neurons of hM3Dq-mCherry Group^{Ext} rats prior to perfusion. These rats were injected with CNO, then 30 min later we noncontingently presented 66 evenly spaced remifentanil-paired cues (*n* = 3), or no cues (*n* = 4) over 2 hrs in a novel operant chamber (ie,

neither Context A nor B), without levers extended. This number of cues was selected as it was the average number of cues delivered by rats during self-administration training. Rats were perfused immediately after this final cue/no-cue session
for analysis of Fos in mCherry-expressing VP^{GABA} neurons.

Experimental Procedures. $Group^{Punish}$ and $Group^{Ext}$ rats were trained on self-administration in Context A, followed by punishment/extinction in Context B, then were tested in a series of reinstatement tests in both contexts, each following counterbalanced vehicle and CNO injections. Some $Group^{Punish}$ rats (*n* = 26) were re-trained on remifentanil self-administration following reinstatement to test effects of CNO on self-administration. These rats also underwent a final reinstatement test without CNO, held in Context A or B with cues, to examine behavior-related Fos expression in rostral or caudal VP (neuron type not determined). Some hM3Dq- and mCherry-expressing $Group^{Ext}$ rats (*n* = 7) and non-behaviorally tested rats (*n* = 6), following reinstatement tests, were used to validate DREADD stimulation of Fos.

Immunofluorescent and immunohistochemical staining.

Immunofluorescent visualization of DREADD expression.

To visualize DREADD localization in each behaviorally tested subject, VP sections were stained for substance P, which delineated VP borders from surrounding basal forebrain (Zahm and Heimer, 1988; Root et al., 2015), and mCherry, which labeled DREADD-expressing GABA neurons. Rats were perfused with 0.9% saline and 4% paraformaldehyde, brains were postfixed for 16 hrs, then cryoprotected in 20% sucrose-azide. Brains were sectioned at 40 µm using a cryostat, and 6-8 sections spanning VP's rostrocaudal axis (from bregma +0.7 to bregma -0.6) were collected and stained, as described previously (Farrell et al., 2021). Briefly, sections were first blocked in 3% normal donkey serum (NDS), then incubated overnight in rabbit anti-substance P (ImmunoStar; 1:5000) and mouse anti-mCherry antibodies (Clontech; 1:2000) in PBST-azide with 3% NDS. Finally, sections were incubated for 4 hrs in Alexafluor donkey anti-Rabbit 488 and donkey anti-Mouse 594 (Thermofisher). Sections were mounted, coverslipped

with Fluoromount (Thermofisher), and imaged at 5x magnification with a Leica DM4000 with StereoInvestigator software (Microbrightfield). Viral expression sites were mapped in each rat referencing a rat brain atlas (Paxinos and Watson, 2006) and observed VP borders.

Endogenous reinstatement-related VP Fos visualization.

A subset of Group^{Punish} rats were perfused following a final 2 hr reinstatement test (Context A with cues: *n* = 9, Context B with cues: *n* = 8), in the absence of CNO/vehicle injection. To quantify reinstatement-related neural activity in VP cells of any type, we stained a set of slices throughout VP for Fos protein, and co-stained the same samples for substance P to define VP borders on each section. Tissue was blocked in 3% NDS, incubated overnight in rabbit anti-Fos primary antibody (Millipore, 1:10000), then for 2 hrs in biotinylated donkey anti-rabbit secondary antibody (Jackson Immuno, 1:500), followed by 90 min amplification in avidin-biotin complex (ABC; Vector Lab, 1:500). Sections were then reacted in 3,3′-Diaminobenzidine (DAB) with nickel ammonium sulfate, to reveal a black nuclear stain for Fos protein. After washing, sections were incubated overnight in mouse anti-substance P (Abcam, 1:10000), then donkey anti-mouse biotinylated secondary antibodies (Jackson Immuno, 1:500), then amplified with ABC. Another DAB reaction without nickel ammonium sulfate was conducted, yielding a light brown product visualizing substance P-immunoreactive processes and neuropil (i.e. VP borders).

Validating hM3Dq-induced Fos in VP^{GABA} neurons.

From separate experimentally-naïve (*n* = 6) and Group^{Ext} (*n* = 7) Cre+ rats expressing mCherry in VP^{GABA} cells, sections were stained using double DAB immunohistochemistry to visualize neurons expressing Fos (black nuclei) and mCherry (brown soma). Procedures mirrored above, except after the Fos stain, a mouse anti-mCherry primary antibody (Takara Bio, 1:5000) was used instead of the substance P primary antibody to visualize hM3Dq-mCherry or mCherry-expressing cells.

Fos quantification.

Endogenous reinstatement-related VP Fos quantification.

To examine reinstatement-related Fos within defined VP borders, stained sections were mounted, coverslipped, and imaged at 10x magnification, and two observers blind to experimental conditions manually counted all Fos+ nuclei within the substance-P defined VP borders on 4 sections/rat, using ImageJ. These sections spanned the rostrocaudal extent of VP, from bregma +0.7 to bregma -0.6. Fos counts from the left and right hemisphere were averaged for each section, and these section averages were averaged to generate a per-rat mean Fos value, which was used for statistical analyses. In addition, sections were divided into rostral and caudal bins (1-3 sections/bin) in accordance with their location relative to bregma (rostral VP > 0 AP relative to bregma, caudal VP ≤ 0 AP relative to bregma). An inter-rater reliability measure showed a strong positive correlation between the two observers' per-rat average Fos quantification (Pearson's correlation: $r = 0.94$, $p < 0.0001$).

Quantifying hM3Dq-induced Fos in VP^{GABA} neurons.

To examine hM3Dq-induced Fos in VP^{GABA} cells, stained sections were mounted, coverslipped, and imaged at 10x magnification. mCherry+ cells, Fos+ cells, and mCherry+/Fos+ cells within VP borders (estimated based on (Paxinos and Watson, 2006)) were counted in ImageJ. Two sections per rat were quantified from near the center of VP virus expression sites, and counts from the left and right hemisphere of each section were averaged. The two section averages were then combined to generate a per-rat mean, which was used for statistical analyses of group effects.

Data analysis. Data were analyzed in Graphpad Prism, and figures were generated in Adobe Illustrator. Repeated measures two-way ANOVAs with lever (inactive, active) and treatment (vehicle, CNO) were conducted for each set of reinstatement and self-administration tests, accompanied by Sidak post hoc tests. One-way or two-way ANOVAs were used to examine differences in lever pressing among vehicle-treated rats during their reinstatement tests, coupled with Sidak post hoc tests. Repeated measures two-way ANOVAs with DREADD type

(Gi, Gq, control) and treatment (vehicle, CNO) were used to compare active lever pressing for each reinstatement condition to confirm DREADD-specificity of CNO effects. Three-way repeated measures ANOVAs with treatment (vehicle, CNO), context (Context A, Context B), and cues (cues, no cues) as factors were conducted for each DREADD group. Between subjects three-way ANOVAs with DREADD group (hM4Di, hM3Dq, Control), context (Context A, Context B), and cue (cues, no cues) as factors were performed for vehicle-day reinstatement active lever pressing. A one-way ANOVA was used to compare Fos across reinstatement conditions, coupled with Sidak or Dunnett's post hoc tests. Paired *t*-tests were used to compare final-day self-administration behavior to first day punishment behavior. Pearson's correlations were used to examine the relationship between VP Fos and active lever pressing on a final reinstatement test, as well as inter-rater reliability between blinded observers. Log-rank (Mantel-Cox) test compared the number of days required to reach abstinence criterion for $Group^{Punish}$ versus $Group^{Ext}$. One rat in $Group^{Ext}$ and 1 in the substance P/Fos reinstatement experiment were removed from reinstatement and Fos analyses, respectively, as outliers (> 3 standard deviations from the mean). Statistical significance thresholds for all analyses were set at $p < 0.05$, two-tailed.

Results

Training in Context A, and response suppression in Context B via punishment or extinction training. During Context A training, $Group^{Punish}$ and $Group^{Ext}$ exhibited comparable levels of remifentanil self-administration (infusions obtained throughout training: $t_{68} = 1.30$, $p = 0.20$). In $Group^{Punish}$, as we previously saw using an analogous cocaine model (Farrell et al., 2019), shifting from unpunished Context A to Context B where 50% of infusions were met with contingent footshock decreased active lever responding (**Fig 9A**, last day Context A vs. 1st day Context B: active lever, $t_{42} = 2.61$, $p = 0.022$), and increased inactive lever pressing ($t_{42} = 2.70$, $p = 0.0098$). In $Group^{Ext}$, shifting from Context A to Context B also decreased active lever responding (**Fig 9C**, last day self-administration vs. 1st day extinction active lever: $t_{26} = 3.16$, $p =$

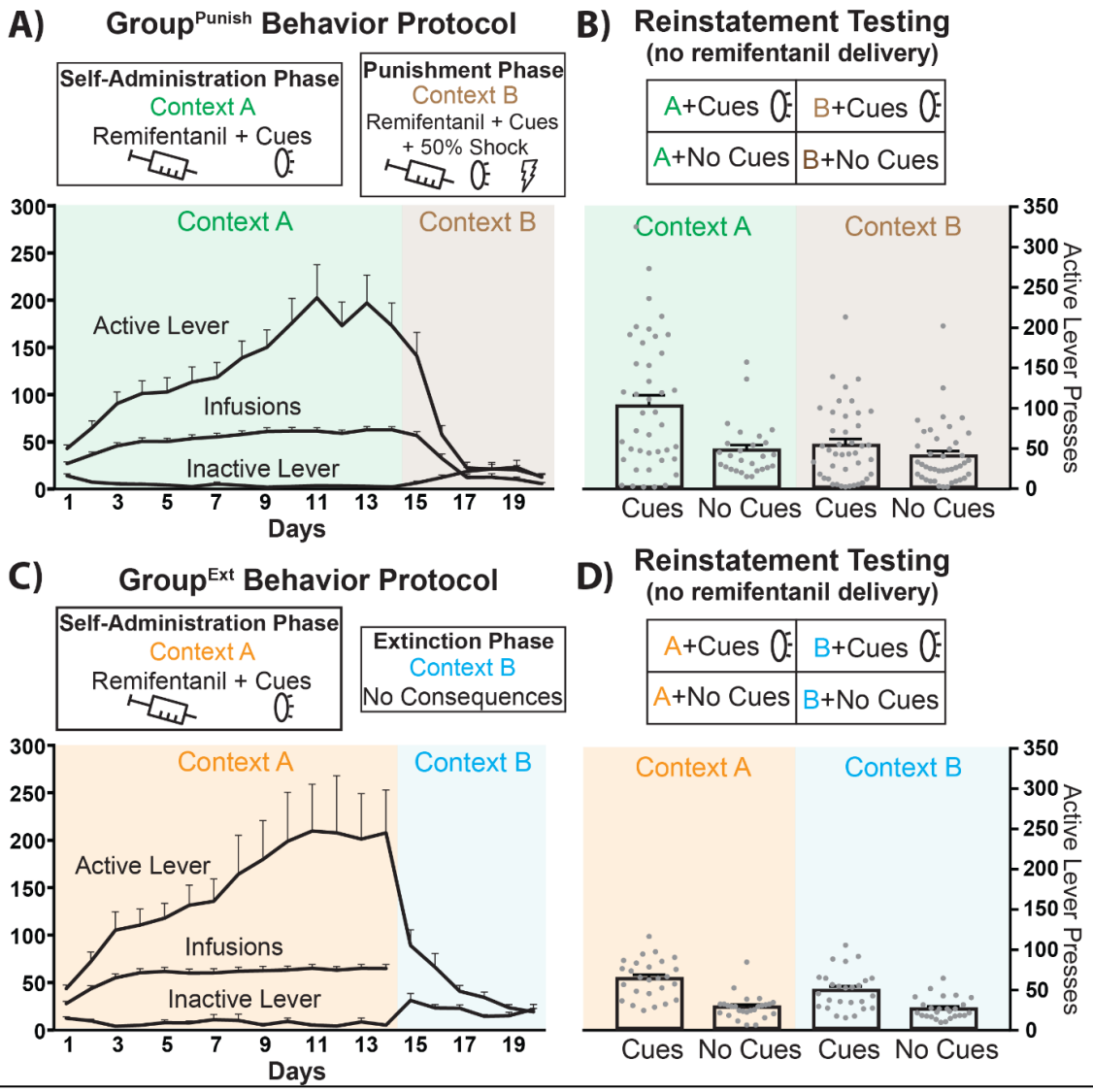

Figure 9. Behavioral testing schematic, training data, and vehicle-day reinstatement following punishment- versus extinction-induced abstinence. A) Schematic of the behavioral training for Group^{Punish} rats undergoing self-administration in Context A (green shading) and punishment in Context B (brown shading). Infusions and active/inactive lever presses depicted. **B)** In Group^{Punish} rats, active lever pressing in Context A (green) and punishment Context B (brown), with or without response-contingent discrete cues is shown for vehicle test days, with accompanying test schematic (top). **C)** Schematic of the behavioral training for Group^{Ext} rats undergoing self-administration in Context A (orange shading) and extinction in Context B (blue shading). Infusions and active/inactive lever presses depicted. **D)** In Group^{Ext} rats, active lever pressing in Context A (orange) or extinction Context B (blue), with or without discrete cues is shown for vehicle test days, with associated test schematic (top). All training and testing sessions were 2 hr in duration. Individual rats shown as gray dots. Data presented as mean + SEM.

0.004) and increased inactive lever responding (t_{26} = 5.22, p < 0.0001). Across Context B training, Group^{Punish} rats suppressed their active lever pressing to criterion in fewer days than

Group^{Ext} rats (Log-rank Mantel-Cox survival analysis test, $\chi^2 = 18.52$, $p < 0.0001$).

Cues and contexts gate remifentanil reinstatement in both Group^{Punish} and Group^{Ext} rats. In Group^{Punish} rats, opioid reinstatement was impacted by both context and the presence or absence of discrete, response-contingent cues (**Fig 9B,** two-way ANOVA (cues and context as factors) on vehicle test day active lever pressing; cues main effect: $F_{(1, 150)} = 14.3$, $p = 0.0002$; context main effect: $F_{(1, 150)} = 9.23$, $p = 0.0028$; cues x context interaction: $F_{(1, 150)} = 5.13$, $p = 0.025$). In Context A, more seeking was seen with cues than without (Sidak post hoc: $p = 0.0005$), and cues elicited more pressing in Context A than they did in Context B ($p = 0.0006$). Context A with cue reinstatement was also greater than in Context B without cues ($p < 0.0001$). Pressing was similar in Context A without cues to pressing in Context B, with or without cues (ps > 0.83). In Group^{Ext} rats, opioid reinstatement was also impacted by both context and discrete, response-contingent cues (**Fig 9D,** two-way ANVOA (cues and context as factors); cues main effect: $F_{(1, 100)} = 55.67$, $p < 0.0001$; context main effect: $F_{(1, 100)} = 4.43$, $p = 0.038$; cues x context interaction: $F_{(1, 100)} = 2.57$, $p = 0.11$). Pressing was greater in the Context A with cues test than in either context without cues (Sidak post hocs; Context A with cues versus no-cue tests in Context A: $p < 0.0001$; or Context B: $p < 0.0001$), and cue-elicited pressing trended toward being greater in Context A than in Context B ($p = 0.059$). In Context B, pressing was greater with cues than without them ($p = 0.0004$). Overall, reinstatement in Group^{Punish} was greater than reinstatement in Group^{Ext} (vehicle day data; two-way ANOVA with group (Group^{Punish}, Group^{Ext}) and reinstatement condition (Context A with/without cues, Context B

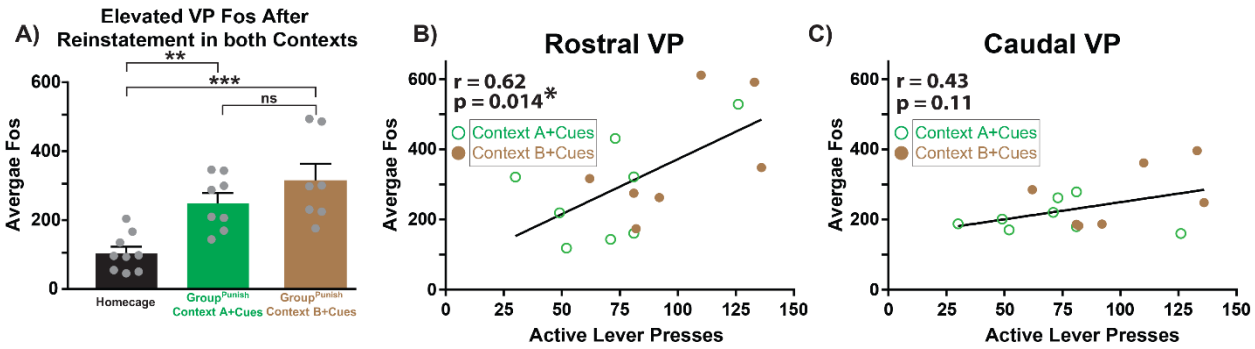

Figure 10. Rostral, but not caudal, VP Fos correlates with remifentanil seeking. A) Elevated Fos in VP neurons in Context A with cues (green bar) and Context B with cues (brown bar), relative to homecage control (gray bar). No difference in VP Fos was detected between Context A with cues and Context B with cues. Individual rats shown as gray dots. Data presented as mean + SEM. **B)** In Group^{Punish} rats, Fos in rostral VP (anterior of bregma) positively correlates with cue-induced opioid reinstatement (active lever presses). Green circles represent rats tested with cues in Context A, brown dots represent those tested with cues in Context B. **C)** Fos in caudal VP (posterior of bregma) was uncorrelated with opioid reinstatement. Pearson correlation: $p^* < 0.05$. One-way ANOVA, Dunnett's post hoc: $p^{**} < 0.01$, $p^{***} < 0.0001$.

with/without cues) as factors: $F_{(1, 250)} = 11.44$, $p = 0.0008$). This effect was in part due to high levels of pressing of Group^{Punish} rats in Context A with cues, as there was greater reinstatement in Context A with cues relative to all other reinstatement conditions in both Group^{Punish} and Group^{Ext} (Sidak post hocs: ps < 0.016). These results indicate that response-contingent cues reinstate seeking following either punishment or extinction training, but the modulation of this by context may be greater in Group^{Punish}, relative to Group^{Ext}.

Rostral VP neural activity is positively correlated with cue-induced reinstatement. To determine whether VP Fos (any neuron type) was associated with reinstatement behavior, a subset of GAD1:Cre and wildtype Group^{Punish} rats, following all 8 reinstatement tests with vehicle and CNO, were sacrificed following a final reinstatement test in Context A with cues, Context B with cues, or directly from their homecage. Greater Fos expression in all VP neurons was found

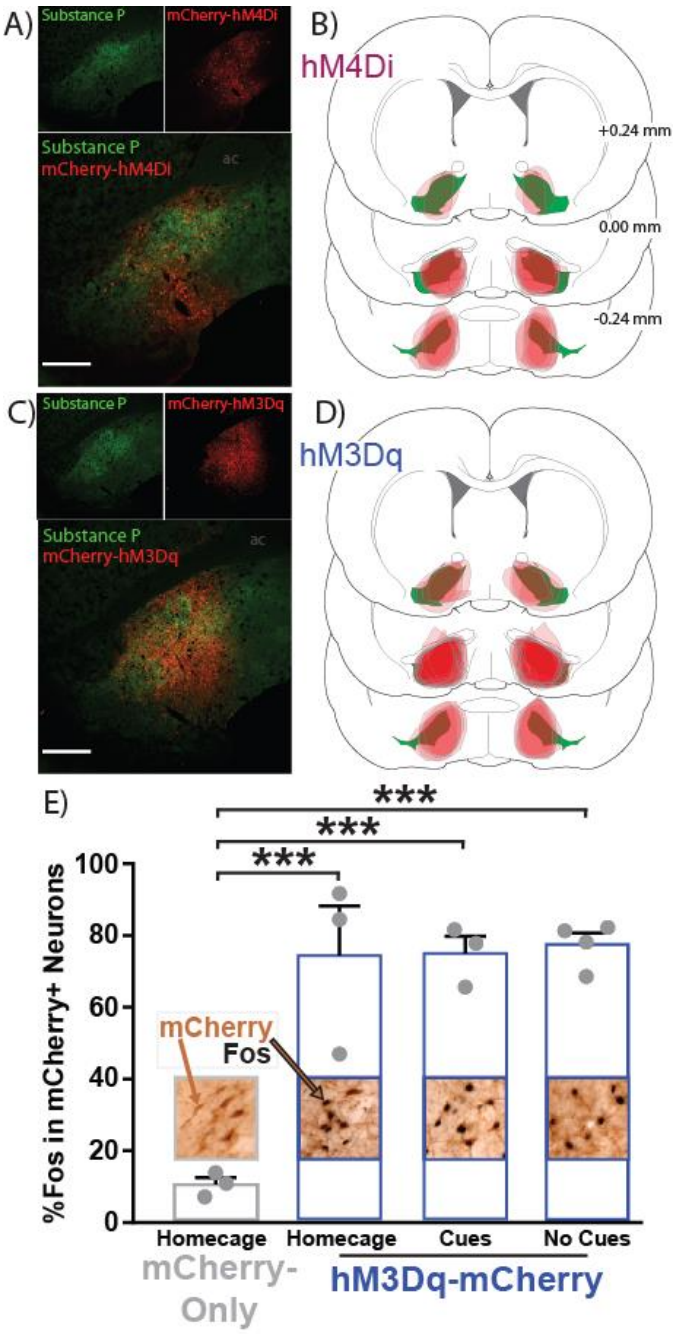

Figure 11. VP^{GABA} DREADD localization and hM3Dq validation. A) Expression of hM4Di-mCherry (red) localized largely within VP borders defined by substance P (green). **B)** Coronal sections depicting the center of hM4Di-mCherry expression (red) for each rat along VP's rostrocaudal axis relative to bregma (substance P-defined VP borders = green). **C)** Expression of hM3Dq-mCherry (red) is similarly localized within VP borders (green). **D)** Coronal sections similarly depicting the center of hM3Dq-mCherry expression (red) for each rat is shown. **E)** CNO treatment in hM3Dq-mCherry rats tested in the homecage exhibited greater Fos in mCherry+ neurons (2nd bar, blue), than in homecage mCherry-only rats treated with CNO (1st bar, gray). CNO-treated hM3Dq-mCherry rats exposed to remifentanil-paired cues (3rd bar, blue) or no cues (4th bar, blue) had more Fos+ mCherry neurons homecage rats (1st bar, gray). However, the hM3Dq stimulation of Fos was no different in the presence or absence of cues. Images above/embedded within bars depict 10x images of immunohistochemical staining of mCherry (brown) within VP borders, and Fos+ nuclei (black). Example mCherry-only and mCherry+Fos double-labeled neuron indicated with brown and brown/black arrows, respectively. Individual rat data shown as gray dots on top of bars. One-way ANOVA, Dunnett's post hoc: $p^{***} < 0.001$. Data presented as mean + SEM.

in both Context A- and Context B-tested rats, relative to homecage-tested controls (**Fig 10A**, one-way ANOVA, $F_{(2, 21)} = 12.25$, $p = 0.0003$; Dunnett's post hoc: Context A with cues vs. homecage, $p = 0.005$; Context B with cues vs. homecage, $p = 0.0002$). No difference in VP Fos expression was detected between Context A with cues and Context B with cues (Sidak post hoc: $p = 0.43$). Fos in rostral (**Fig 10B**), but not caudal (**Fig 10C**) VP correlated with total active

lever presses during the final reinstatement test (r = 0.62, p = 0.014), similar to our prior report showing that rostral VP Fos is associated with cue-induced cocaine seeking (Mahler et al., 2014).

hM4Di- and hM3Dq-DREADD expression in VP^{GABA} neurons. GAD1:Cre rats expressing DREADDs with at least 50% within VP borders (defined by substance P) were included for analyses, for a total of 13 GAD1:Cre hM4Di-expressing (hM4Di) rats (**Fig 11A-B**, Group^{Punish}: n = 8 males, 5 females) and 25 GAD1:Cre hM3Dq-expressing (hM3Dq) rats (**Fig 11C-D**, Group^{Punish}: n = 13 males, 0 females; Group^{Ext}: n = 8 males, 4 females). Control rats were designated as those with DREADD expression outside of VP (n = 2), mCherry expression (n = 8), or Cre- rats with no expression (n = 10), which were combined for analyses.

CNO increases Fos immunoreactivity in hM3Dq-expressing neurons. CNO treatment induced more Fos in hM3Dq-expressing neurons, relative to mCherry-only neurons (**Fig 11E**, one-way ANOVA: $F_{(3, 9)}$ = 20.56, p = 0.0002). Equivalent Fos induction was seen regardless of the behavioral circumstance in which CNO was administered, with similar homecage mCherry-relative increases in hM3Dq rats tested in homecage (Dunnett's post hoc, p = 0.0005), or in a novel operant chamber with (p = 0.0004) or without (p = 0.0002) cues. hM3Dq rats tested in home- or test-cages did not differ in Fos expression (Sidak post hoc: ps > 0.99). These results collectively show that 1) hM3Dq stimulation augments neural activity as expected and 2) hM3Dq stimulation enhanced neural activity similarly regardless of the behavioral context in which the stimulation occurred.

Inhibiting VP^{GABA} neurons suppresses remifentanil reinstatement after punishment. In Group^{Punish} rats expressing hM4Di DREADDs, a lever (active, inactive) x treatment (vehicle, CNO) ANOVA revealed a significant main effect of lever across all conditions (p < 0.01). Active lever presses in Context A with cues were suppressed by CNO treatment in hM4Di rats (**Fig 12A,** treatment x lever interaction: $F_{(1, 24)}$ = 6.53, p = 0.017; active lever Sidak post hoc: p = 0.0047), but this was not the case in Context A without cues (**Fig 12D,** treatment: $F_{(1, 10)}$ = 0.43,

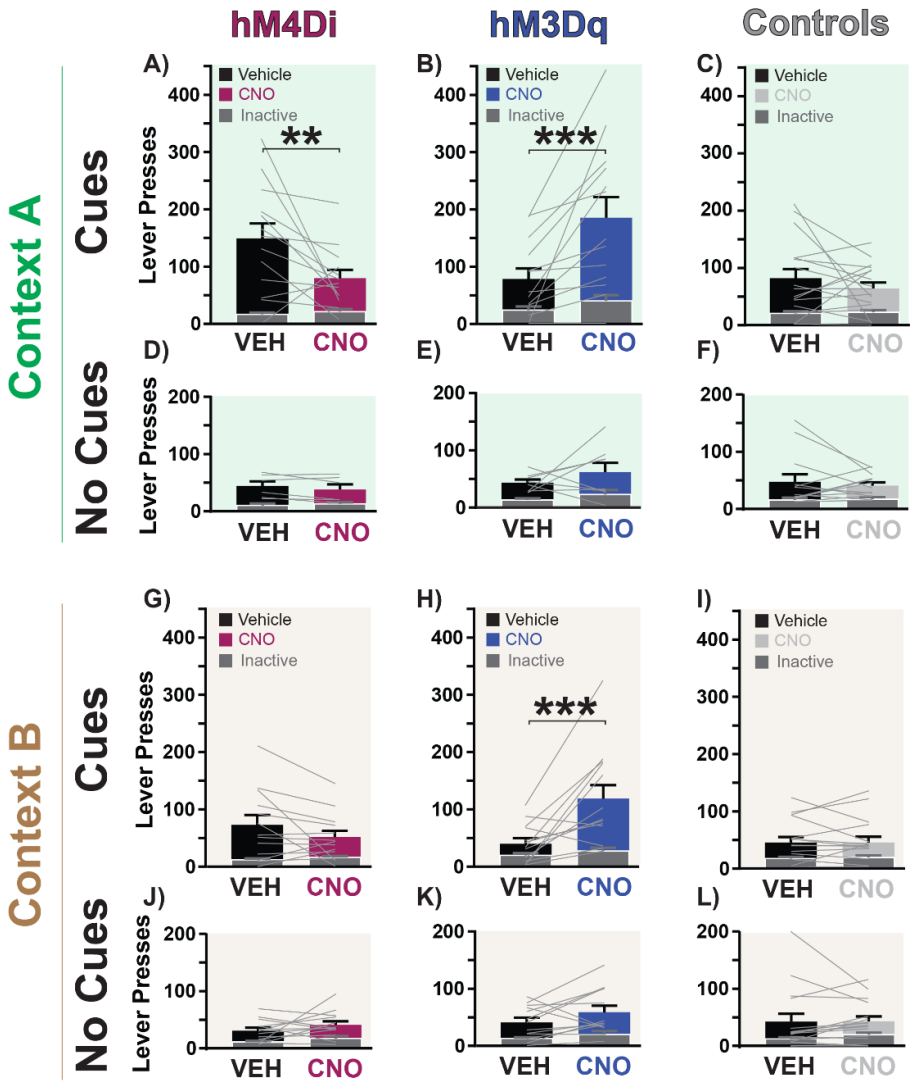

Figure 12. Following punishment, inhibiting or stimulating VP^{GABA} neurons bidirectionally controls remifentanil seeking. A-C) In Context A with cues, CNO treatment **A)** decreased opioid seeking in hM4Di rats (purple bar), **B)** increased seeking in hM3Dq rats (blue bar), and **C)** was without effect in control rats (light gray bar), relative to vehicle treatment (black bars). **D-F)** In Context A with no cues, CNO treatment was without effect on opioid seeking in **D)** hM4Di rats (purple bar), **E)** hM3Dq rats (blue bar), and **F)** control rats (light gray bar), relative to vehicle treatment day (black bars). **G-I)** In Context B with cues, CNO treatment **G)** was without effect on opioid seeking in hM4Di rats (purple bar), **H)** increased opioid seeking in hM3Dq rats (blue bar), and **F)** did not impact opioid seeking in control rats (light gray bar), relative to vehicle treatment day (black bars). **J-L)** In Context B with no cues, CNO treatment was without effect on opioid seeking in **J)** hM4Di rats (purple bar), **K)** hM3Dq rats (blue bar), and **L)** control rats (light gray bar), relative to vehicle treatment (black bars). Dark gray overlaid bars with white outline represent inactive lever presses, and light gray lines depict individual rats' active lever pressing on each session. Repeated measures two-way ANOVA, Sidak post hoc: $p^{**} < 0.01$, $p^{***} < 0.001$. Data presented as mean + SEM.

$p = 0.52$; treatment x lever interaction: $F_{(1, 10)} = 3.38$, $p = 0.096$), showing that inhibiting VP^{GABA}

neurons suppressed seeking in Context A only in the presence of discrete cues. Moreover, vehicle day reinstatement was statistically comparable across DREADD groups (DREADD main effect: $F_{(2,11)}$ = 2.31, p = 0.10; DREADD x cue x context interaction: $F_{(2,11)}$ = 0.23, p = 0.80). CNO treatment in hM4Di rats trended towards reducing opioid seeking in Context B with cues (**Fig 12G,** treatment x lever interaction: $F_{(1, 24)}$ = 3.98, p = 0.058), but no main effect of treatment, or treatment x lever interaction was detected in Context B without cues (**Fig 12J**, treatment: $F_{(1, 24)}$ = 2.79, p = 0.11; treatment x lever: $F_{(1, 24)}$ = 0.12, p = 0.73). A three-way RM ANOVA (treatment x context x cues) revealed no significant interaction for hM4Di rats ($F_{(1,5)}$ = 0.25, p = 0.64).

Stimulating VP^{GABA} neurons augments remifentanil reinstatement after punishment. In Group^{Punish} rats expressing hM3Dq DREADDs in VP^{GABA} neurons, CNO strongly increased

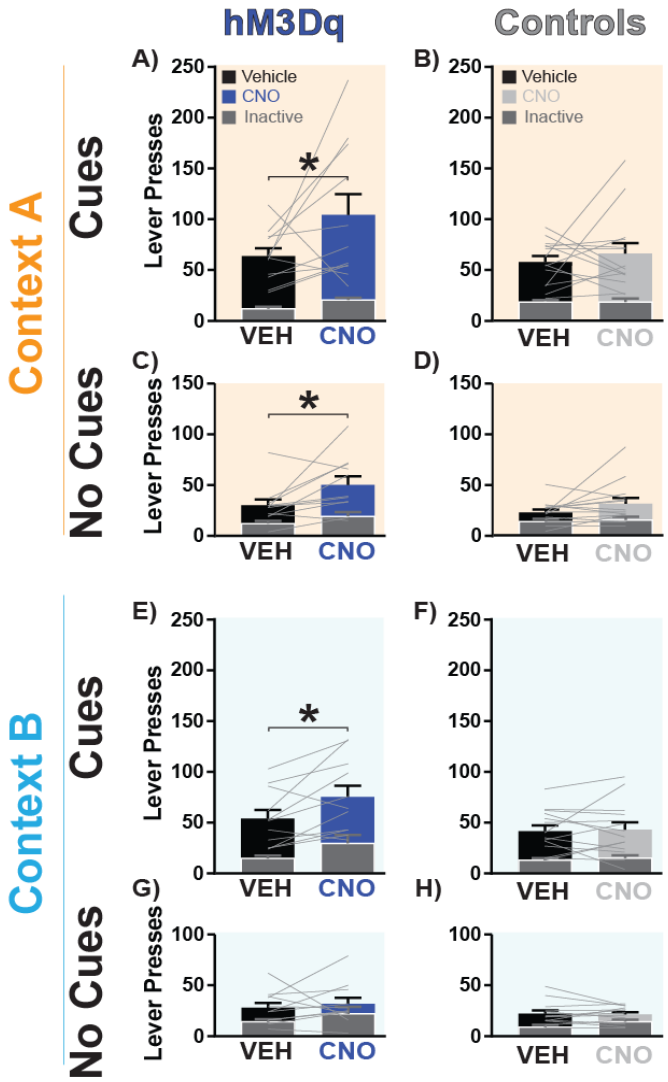

Figure 13. Following extinction, stimulating VP^{GABA} neurons augments reinstatement in a cue- and context-dependent manner. A-B) CNO treatment (blue bar) in hM3Dq rats augmented opioid seeking in Context A with cues relative to vehicle (black bar), but no effect was detected in controls (light gray bar versus black bar). **C-D)** CNO treatment (blue bar) in hM3Dq rats increased opioid seeking in Context A with no cues relative to vehicle, but no effect was seen in controls (light gray bar versus black bar). **E-F)** CNO (blue bar) in hM3Dq rats increased opioid seeking in Context B with cues, relative to vehicle treatment (black bar), but no effect was observed in controls (light gray bar versus black bar). **G-H)** CNO treatment in hM3Dq rats (blue bar) or controls (light gray bar) was without effect on opioid reinstatement in Context B with no cues, relative to vehicle treatment (black bars). Dark gray overlaid bars with white outline represent inactive lever presses, and light gray lines depict individual rats' active lever pressing. p^* < 0.05. Data presented as mean + SEM.

opioid seeking, and appeared to do so in a cue-dependent manner. Specifically, CNO augmented active lever pressing in *both* Context A with cues and Context B with cues (**Fig 12B**, Context A with cues treatment x lever interaction: $F_{(1, 24)} = 8.78$, $p = 0.0068$, active lever Sidak post hoc: $p = 0.0001$; **Fig 12H**, Context B with cues treatment x lever interaction: $F_{(1, 24)} = 9.79$, $p = 0.0046$, active lever Sidak post hoc: $p = 0.0001$). In contrast, CNO in hM3Dq rats failed to augment seeking in Context A in the absence of cues (**Fig 12E,** Context A with no cues treatment x lever interaction: $F_{(1, 14)} = 0.22$, $p = 0.64$; Context A with no cues treatment: $F_{(1, 14)} = 2.08$, $p = 0.17$). CNO in hM3Dq rats subtly increased pressing on both the active and inactive lever in Context B with no cues, as indicated by a main effect of treatment accompanied by a non-significant treatment x lever interaction (**Fig 12K**, Context B with no cues treatment: $F_{(1, 24)} = 4.77$, $p = 0.039$; Context B with no cues treatment x lever interaction: $F_{(1, 24)} = 0.92$, $p = 0.35$; active lever Sidak post hoc: $p = 0.071$; inactive lever: $p = 0.63$). A three-way RM ANOVA (treatment x context x cues) revealed no significant interaction in hM3Dq rats ($F_{(1,7)} = 0.0001$, $p = 0.98$).

Stimulating VP^{GABA} neurons augments remifentanil seeking after extinction. In Group^{Ext} rats with hM3Dq DREADDs, CNO treatment augmented seeking in the presence of cues, irrespective of whether rats were in Context A or B (**Fig 13A**, treatment main effect Context A with cues: $F_{(1, 20)} = 4.91$, $p = 0.038$, active lever Sidak post hoc: $p = 0.037$; **Fig 13E**, treatment main effect Context B with cues: $F_{(1, 20)} = 9.86$, $p = 0.0052$, active lever Sidak post hoc: $p = 0.033$). In the absence of cues, CNO augmented opioid reinstatement only in Context A, but not in Context B (**Fig 13C**, treatment main effect Context A with no cues: $F_{(1, 20)} = 8.84$, $p = 0.0075$, active lever Sidak post hoc: $p = 0.011$; **Fig 13G,** treatment main effect Context B with no cues: $F_{(1, 20)} = 2.10$, $p = 0.16$; treatment x lever interaction: $F_{(1, 20)} = 0.19$, $p = 0.67$). A three-way RM ANOVA (treatment x context x cues) revealed no significant interaction in hM3Dq rats ($F_{(1,10)} = 0.04$, $p = 0.84$). Overall, we find that stimulating VP^{GABA} neurons in Group^{Punish} or Group^{Ext} rats

augments seeking in either Context in the presence of cues, but only increases non-cued seeking in Context A in Group^{Ext} but not in Group^{Punish}.

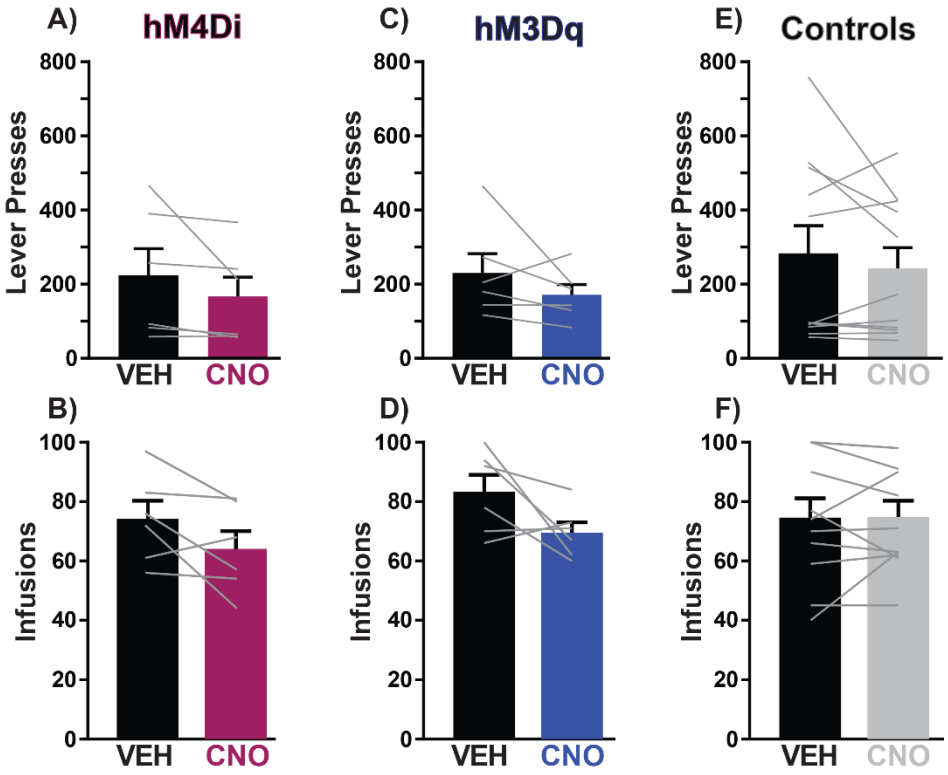

Figure 14. No impact of inhibiting or stimulating VP^{GABA} neurons on remifentanil self-administration. Relative to vehicle day performance in the same rats (black bars), CNO treatment failed to alter **A)** active lever presses or **B)** infusions obtained during unpunished opioid self-administration in hM4Di rats (purple bars). **C,D)** Analogous self-administration data is shown for hM3Dq rats (blue bars), and **E,F)** control rats (gray bars). Gray lines represent individual rats' behavioral output. Data presented as mean + SEM.

Neither inhibiting nor stimulating VP^{GABA} neuron alters opioid self-administration. Finally, we asked whether VP^{GABA} neuron manipulations influence unpunished opioid self-administration in a subset of Group^{Punish} rats, retrained to self-administer after reinstatement testing. Stable self-administration was unaffected by CNO treatment in hM4Di rats (**Fig 14A**, treatment: $F_{(1, 10)} = 2.14$, $p = 0.17$; treatment x lever interaction: $F_{(1, 10)} = 2.14$, $p = 0.17$) or hM3Dq rats (**Fig 14C**, treatment: $F_{(1, 10)} = 1.63$, $p = 0.23$; treatment x lever interaction: $F_{(1, 10)} = 1.63$, $p = 0.23$). The number of infusions obtained was similarly unaffected by VP^{GABA} neuron manipulations (**Fig 14B**, hM4Di: $t_5 = 1.89$, $p = 0.12$; **Fig 14D**, hM3Dq: $t_5 = 1.98$, $p = 0.10$).

No effect of CNO on behaviors in DREADD-free control rats. In Group^{Punish} control rats, CNO did not influence opioid reinstatement in Context A with cues (**Fig 12C**) or without them

(**Fig 12F**), or in Context B with (**Fig 12I**) or without cues (**Fig 12L**, treatment: *F*s < 0.86, *p*s > 0.35; treatment x lever interaction: *F*s < 1.28, *p*s > 0.26). Similarly, in Group^{Ext} control rats, CNO did not impact reinstatement after extinction in Context A with cues (**Fig 13B**) or with no cues (**Fig 13D**), or Context B with (**Fig 13F**) or with no cues (**Fig 13H**, treatment: *F*s < 3.56, *p*s > 0.06; treatment x lever interaction: *F*s < 2.61, *p*s > 0.11). CNO (versus vehicle) showed no main effect (Group^{Punish}: $F_{(1,11)} = 0.47$, $p = 0.51$; Group^{Ext}: $F_{(1,14)} = 1.98$, $p = 0.18$) or interactions with cue or context variables (three-way RM ANOVA (treatment x context x cues): Group^{Punish}: $F_{(1,11)} = .01$, $p = 0.92$; Group^{Ext}: $F_{(1,14)} = 0.002$, $p = 0.97$). Likewise, CNO was also without effect on remifentanil self-administration in controls (**Fig 14E**, treatment: $F_{(1, 20)} = 0.98$, $p = 0.34$; treatment x lever interaction: $F_{(1, 20)} = 1.07$, $p = 0.31$; **Fig 14F**, control infusions: $t_{10} = 0.082$, $p = 0.94$). Specificity of CNO effects were confirmed with two-way ANOVAs examining DREADD group x treatment effects on active lever pressing in CNO-impacted reinstatement conditions. For Group^{Punish} rats, on reinstatement tests for which CNO had an effect, we found specificity of CNO effects (DREADD x treatment interactions: *F*s > 12.63, *p*s < 0.0001). For Group^{Ext} rats, given that there were only hM4Di and control groups, DREADD x treatment interactions were non-significant (*F*s < 4.09, *p*s > 0.054).

Discussion

Using chemogenetic inhibition/stimulation and Fos expression analyses, we found that VP^{GABA} neurons play a key role in opioid relapse-like behavior. Following remifentanil self-administration and subsequent abstinence from drug taking, chemogenetically inhibiting VP^{GABA} neurons suppressed, and stimulation enhanced opioid reinstatement—especially when it was driven by discrete, response-contingent drug cues. VP^{GABA}'s role was apparent across multiple reinstatement models, and it was specific to reinstatement, in that the same chemogenetic manipulations did not affect remifentanil's primary reinforcing properties. We also validated hM3Dq DREADDs as being capable of Fos-activating GABA neurons in GAD1:Cre transgenic rats, and determined that VP^{GABA} neurons were equivalently stimulated by DREADDs in the

presence or absence of drug-associated cues. This is despite the fact that the presence of cues during such stimulation was generally required for increased drug-seeking behavior to occur. Finally, we found that endogenous neural activity (Fos) in rostral, but not caudal, VP cells correlated with reinstatement behavior. These experiments thus show a specific role for VP^{GABA} neurons in opioid relapse-like behaviors, regardless of the preclinical model employed—potentially positioning VP as a future target for intervention in this chronic, relapsing disorder.

In hopes of better modeling the circumstances of drug addiction, preclinical models have emerged in which drug taking is coupled with adverse consequences which cause rats to decide to quit using (Marchant et al., 2013a; Farrell et al., 2018; Marchant et al., 2019; Venniro et al., 2020)—similar to the self-imposed abstinence present in most humans attempting to control their drug intake. We and others have suggested that through such efforts to better model human addiction and relapse-like behaviors in rats we may gain new insights into the neural circuit dynamics most likely engaged in people with addiction. Here, we build on prior work to establish a model of remifentanil cue- and context-induced relapse after punishment-induced abstinence, adapting those previously used with other drugs of abuse (Marchant et al., 2013b; Krasnova et al., 2014; Pelloux et al., 2018b; Farrell et al., 2019; Fredriksson et al., 2020). Using the short-acting but strongly reinforcing opioid drug remifentanil, we built on the work of Panlilio and colleagues who previously established that footshock punishment suppresses remifentanil self-administration, and that remifentanil seeking can be subsequently reinstated (Panlilio et al., 2003, 2005). Here, we expand on these models by incorporating an explicit contextual element to the reinstatement tests (with or without discrete drug-paired cues), allowing us to interrogate the facilitatory and suppressive effects of these learned stimuli on drug seeking. We note that unlike extinction- or forced abstinence-based reinstatement models, voluntary abstinence models may mimic the conflicted motivational processes that often arise in people with addiction attempting to control their drug use due to mounting life consequences. We hope that

developing this approach in rats could ultimately lead to deeper understanding of neural circuits that are engaged when humans decide to try to quit using.

Discrete cues occurring in conjunction with drug use (e.g., paraphernalia), and diffuse contextual elements (e.g., location of prior drug use) serve as powerful triggers that can ultimately lead an abstinent person to relapse. The ability of discrete cues and contexts to elicit drug seeking appears to depend on overlapping yet distinct neural circuits (Crombag et al., 2008; Bossert et al., 2013; Farrell et al., 2018), some of which involve VP or its close neural connections (McFarland et al., 2003; Fuchs et al., 2008; Perry and McNally, 2013; Stefanik et al., 2013; Mahler et al., 2014; Prasad and McNally, 2016; Prasad et al., 2020; Kupchik and Prasad, 2021). Therefore, we examined VP^{GABA} involvement in reinstatement elicited by both discrete cues and contexts in our behavioral relapse models. After punishment-induced abstinence, inhibiting VP^{GABA} neurons *only* reduced remifentanil seeking in the "safe" Context A in the presence of cues—the condition in which reinstatement was highest. In contrast, we found that inhibiting VP^{GABA} neurons did not affect seeking in the punishment-associated Context B in the presence or absence of cues, potentially in part due to a floor effect resulting from low responding in this "dangerous" context. These results are reminiscent of our prior report with cocaine showing that chemogenetic inhibition of VP neurons suppressed cue-induced drug seeking in a safe Context A, but not in a dangerous Context B, using an analogous voluntary abstinence-based reinstatement model (Farrell et al., 2019). Here, we also examined effects of *stimulating* VP^{GABA} neurons on post-punishment opioid seeking, which we found to robustly augment cue-induced remifentanil seeking in *both* Context A and Context B. In the absence of cues, however, stimulating VP^{GABA} neurons exhibited no effect in either Context A or B. It appears, then, that response-contingent cues are required to reveal the motivation-enhancing effects observed with hM3Dq stimulation after punishment-induced abstinence. Overall, these data suggest cue- and context-dependent roles for VP^{GABA} in reinstatement following voluntary abstinence.

Though we found cue- and context-dependent effects of manipulating VP^{GABA} neurons on opioid seeking following punishment-induced abstinence, the way in which abstinence is achieved in preclinical models determines the neural circuits recruited during reinstatement (Fuchs et al., 2006; Farrell et al., 2018; Pelloux et al., 2018a; Marchant et al., 2019). Therefore, we asked whether stimulating VP^{GABA} neurons would have similar effects on cue or context-induced reinstatement using an analogous extinction-based abstinence reinstatement model. We found that VP^{GABA} neuron stimulation in extinguished rats similarly augmented cue-induced remifentanil seeking in both Context A and B. However, unlike in punishment-trained rats, VP^{GABA} neuron stimulation in extinguished rats augmented seeking in Context A in the absence of cues, not just in their presence. This could suggest that VP^{GABA} roles in context-induced reinstatement may differ based on the affective associations imbued in these contexts (i.e. fear of shock versus extinction-related disengagement), or contrast effects between the always safe Context A with the extinction- or punishment-paired Context B. Alternatively, differences between the models in the number of training days required for extinction- versus punishment-induced abstinence, or other methodological differences between the procedures could have contributed to this distinction. Future work ought also to explore how punishment learning in Context A (rather than a distinct Context B) might impact neural circuit recruitment and reinstatement. Regardless, these findings of a relatively pervasive, necessary and sufficient role for VP^{GABA} neurons in cue-induced reinstatement contrast with other limbic nodes like the BLA or dorsal striatum, since inactivating these nodes differentially affects reinstatement behavior depending on the way in which abstinence was achieved (Fuchs et al., 2006; Pelloux et al., 2018a). Overall, these results suggest that VP^{GABA} neurons are involved in cue-induced drug seeking across rat relapse models, suggesting they might also play an analogous role in human opioid relapse.

Prior work from us and others suggests nuanced roles for VP and its neuronal subpopulations in drug seeking, as well as motivated behavior more generally (Root et al.,

2013; Leung and Balleine, 2015; Root et al., 2015; Richard et al., 2016; Ottenheimer et al., 2020; Farrell et al., 2021). In particular, recent reports support a role for phenotypically-defined VP cellular subpopulations in relapse to drug seeking across drugs of abuse and relapse models (Mahler et al., 2014; Prasad and McNally, 2016; Heinsbroek et al., 2017; Farrell et al., 2019; Pardo-Garcia et al., 2019; Heinsbroek et al., 2020; Prasad and McNally, 2020; Pribiag et al., 2021). For example, VP DA D_3-receptor expressing populations and their outputs to lateral habenula (LHb) are critical for cue-induced cocaine seeking (Pribiag et al., 2021). VP^{GABA} and parvalbumin-expressing VP neurons are also recruited by alcohol-associated contextual cues, and chemogenetic inhibition of these subpopulations suppressed context-induced relapse to alcohol seeking (Prasad et al., 2020). Stimulation of a subset of enkephalin-expressing VP^{GABA} neurons enhanced cue-induced cocaine reinstatement, whereas stimulating VP glutamate neurons instead suppressed cocaine reinstatement (Heinsbroek et al., 2020). However, although broad stimulation of VP^{GABA} neurons induced reinstatement to cocaine seeking in extinguished mice, it failed to augment cue-induced reinstatement (Heinsbroek et al., 2020). These findings are collectively in accordance with the idea that VP glutamate neurons constrain reward seeking, and have opposite motivational roles to VP^{GABA} neurons, which are instead involved in appetitive processes (Faget et al., 2018; Tooley et al., 2018; Stephenson-Jones et al., 2020; Farrell et al., 2021). Our results further demonstrate the critical role of VP^{GABA} neurons in opioid seeking, especially when triggered by drug-paired cues.

Consistent with prior reports examining cocaine seeking, we identified that rostral, but not caudal, VP neural activity (Fos) was positively correlated with cue-induced drug seeking(Mahler et al., 2014), and that VP neural activity was elevated following reinstatement testing in both punishment-associated Context B or reward-associated Context A (Farrell et al., 2019). Our Fos results demonstrate that rostral, not caudal VP is activated when rats undergo cue-induced reinstatement of remifentanil seeking, and that rostral VP Fos scales with the intensity of drug seeking across individual animals. Several groups have also shown a

functional gradient along VP's rostrocaudal axis (Heimer et al., 1991; Johnson et al., 1993; Churchill and Kalivas, 1994; Panagis et al., 1995; Calder et al., 2007; Kupchik and Kalivas, 2013). For example, caudal VP contains a 'hedonic hotspot' in which locally applied orexin$_A$ or μ opioid receptor agonists enhance hedonic orofacial 'liking' reactions to sweet liquid rewards (Smith and Berridge, 2007; Ho and Berridge, 2013). Though our Fos analysis (**Fig 10**) was not restricted to VP^{GABA} cells, the majority of Fos-positive cells were likely GABAergic, since VP consists of mostly GABAergic neurons across its rostrocaudal axis (Root et al., 2015; Faget et al., 2018; Bernat et al., 2021). We also note that our DREADD manipulations were targeted in central VP, and therefore spanned both rostral and caudal VP zones. Future work should further dissect anatomical, cellular, and molecular profiles spanning rostrocaudal VP zones to determine the specific roles of neuronal populations within these subregions responsible for this apparent anterior-posterior functional gradient.

We show that Gq-DREADDs robustly stimulate Fos in VP^{GABA} neurons, as seen in other neural populations (Mahler et al., 2014; Nation et al., 2016; Yoshimura et al., 2017; Mahler et al., 2019; Haaranen et al., 2020; Sharma et al., 2020), and here we further asked whether the behavioral situation impacts hM3Dq-induced Fos, as it does for hM3Dq-induced behavior. Specifically, we reasoned that since hM3Dq-stimulated reinstatement was most robust in the presence of response-contingent cues, the presentation of these cues might further augment hM3Dq-simulated Fos levels, relative to rats exposed to no cues, or tested outside a drug-seeking context (homecage). However, the presence or absence of discrete, passively administered cues made no difference—Fos levels in mCherry-hM3Dq VP neurons following CNO administration were similar regardless of whether testing occurred in the presence of drug cues. This indicates that hM3Dq DREADD stimulation enhances activity of VP^{GABA} neurons regardless of behavioral situation, though the same stimulation only caused consistent increases in drug seeking the presence of cues. This likely implies that VP activation either results in drug seeking or does not depending on the cue-elicited activity state of the wider

motivation circuits within which VP interacts. Perhaps this is not surprising conceptually—enhanced activity of the VP^{GABA} projection neurons cannot inhibit cue-evoked activity in target regions (e.g., VTA) if cues are not present to cause activity capable of being inhibited. In theory, this could be a useful feature of manipulating such inhibitory circuits to treat psychiatric disorders, as the behavioral/cognitive effects of activating GABAergic projections may only become apparent in the presence of symptom-related circumstances related to abnormal neuronal hyperactivity in downstream regions.

These studies have some limitations that should be considered, and explicitly followed up in future studies. For example, both male and female rats were used in these studies, but in some cases unequal numbers of each sex were present, precluding our ability to examine sex differences in most cases. This said, in our prior work we detected no sex differences in effects of chemogenetic manipulations of VP neurons, or VP^{GABA} neurons (Farrell et al., 2019; Farrell et al., 2021), though sex-dependent VP effects are still likely (Lim et al., 2004; DiBenedictis et al., 2020; Lee et al., 2021) and worthy of additional study. CNO doses equivalent or higher than that used here (5 mg/kg) have no discriminable effects on reinstatement or self-administration behaviors in our hands (Mahler et al., 2014; Farrell et al., 2019; Mahler et al., 2019; Farrell et al., 2021). Likewise, no observable effects of CNO were seen in non-DREADD expressing control rats here—though off target effects of the compound have been reported and should always be controlled for (Gomez et al., 2017; Mahler and Aston-Jones, 2018). We did not test here effects of VP^{GABA} neuron inhibition on post-extinction reinstatement, only stimulation. Several prior reports have shown VP is essential for post-extinction reinstatement (McFarland and Kalivas, 2001; McFarland et al., 2004; Rogers et al., 2008b; Mahler et al., 2014; Prasad and McNally, 2016; Prasad et al., 2020), but the pattern of effects in our specific context/cue model are unknown. Though our prior results have shown that chemogenetic VP^{GABA} neuron manipulations do not affect locomotor activity per se (Farrell et al., 2019; Farrell et al., 2021), we did not explicitly control for such locomotor effects in the current study. Finally, it is important to

note that DREADD stimulation of neurons is unlikely to recapitulate natural firing patterns generated endogenously by VP circuits, and VP firing dynamics should be further studied using complementary methods.

Our results establish that VP^{GABA} neurons regulate reinstatement across preclinical opioid relapse models, adding to the growing evidence for a key role of VP within motivation circuits (Napier and Mitrovic, 1999; Floresco et al., 2003; Smith et al., 2009; Tachibana and Hikosaka, 2012; Root et al., 2015; Creed et al., 2016; Ottenheimer et al., 2018; Levi et al., 2019; Inbar et al., 2020; Kaplan et al., 2020). Though such evidence implies that targeting VP circuits might be a useful strategy for helping humans struggling to control their drug use, many questions remain. How does molecular heterogeneity within neurotransmitter-defined VP circuits influence motivated behavior? Is it possible to modulate the activity of VP to influence maladaptive drug seeking without impairing healthy desires? How is VP's efferent and afferent connectivity involved in different types of motivated behavior? Further investigating these questions may yield fruitful insights not only about VP's role in addiction, but also fundamental ways in which motivational systems interact with cognitive and memory systems more generally.

CHAPTER 3: Ventral pallidum GABA neurons mediate motivation underlying risky choice

Introduction

The previous chapters specifically investigated VP neuron populations in relapse-like behavior after abstinence, revealing that VP^{GABA} neurons are critical for motivating cocaine and opioid seeking behavior. Here, we explore the function of VP^{GABA} neurons in appetitive, aversive, and mixed motivational scenarios, revealing a fundamental role for VP^{GABA} neurons in motivation and decision making beyond drug seeking.

Executing appropriate action under conflicting motivations is fundamental for survival in a dynamic world. For example, balancing appetitive and aversive motivations is essential for most animals to eat without being eaten. In humans, this interplay of motivations is required for appropriate decision making, and inappropriately balancing reward and aversion likely contributes to a variety of psychiatric disorders including addiction. Indeed, compulsive drug use and relapse in addiction can be conceptualized as desire for drugs overcoming the perceived threat of consequences, leading to poor decisions. Yet most preclinical studies explore reward in the absence of threat, or threat without reward—conditions that rarely occur in the lives of opportunistic prey species like rodents. Understanding how functionally distinct cell populations within brain motivation circuits participate in appetitive, aversive, and also *mixed motivations* will provide novel insights into the neural substrates of both adaptive and maladaptive decision making.

The VP is at an anatomical interface of motivation and action (Heimer et al., 1982), and is ideally positioned to contribute to behavioral responses to both rewards and threats. Across species, VP neurons encode the motivational value of specific actions that result in reward, in a manner that reflects whether such actions are worth generating (Pessiglione et al., 2007; Tindell et al., 2009; Tachibana and Hikosaka, 2012; Richard et al., 2016; Fujimoto et al., 2019). VP also plays a causal role in reward, as pharmacological stimulation enhances spontaneous food intake (Stratford et al., 1999; Smith et al., 2009) and hedonic evaluations of tastes (Berridge and

Kringelbach, 2015), whereas perturbing VP disrupts conditioned motivation (McAlonan et al., 1993; Chang et al., 2015), and reward-related working memory (Floresco et al., 1999). Notably, VP also plays a crucial role in seeking of multiple classes of addictive drugs (Rogers et al., 2008a; Mahler et al., 2014; Farrell et al., 2019; Heinsbroek et al., 2019; Prasad and McNally, 2020).

However, it has become clear that VP not only contributes to reward, but also to aversive motivational processes. Pharmacological disinhibition of VP neurons generates spontaneous defensive behavior in rats (Smith and Berridge, 2005), and disrupts the ability of monkeys to avoid a cued aversive airpuff (Saga et al., 2016). Perhaps relevant to this are recent reports revealing that a glutamatergic subpopulation of VP neurons mediates aversive motivation and learning in mice, as they fire in response to aversive stimuli, promote avoidance and curtail reward seeking when optogenetically stimulated, and generally cause opposite effects when optogenetically inhibited (Faget et al., 2018; Tooley et al., 2018; Heinsbroek et al., 2019; Stephenson-Jones et al., 2020).

In contrast to VP glutamate neurons, VP^{GABA} neurons have instead been linked to reward seeking and approach responses in mice. For example, photostimulating VP^{GABA} neurons is reinforcing, and induces food intake (Zhu et al., 2017; Faget et al., 2018; Stephenson-Jones et al., 2020). VP^{GABA} neurons also selectively fire to reward cues, and their activity is required for operant reward seeking, but not avoidance responses (Stephenson-Jones et al., 2020). These results support the notion of extensive functional heterogeneity amongst VP cell populations (Smith and Berridge, 2005; Kupchik and Kalivas, 2013; Mahler et al., 2014; Root et al., 2015), and show that VP^{GABA} neurons play a distinct, though poorly characterized role in behavior.

Here we systematically characterize the behavioral functions of VP^{GABA} neurons, in transgenic GAD1:Cre rats. Using validated, specific, and reversable chemogenetic inhibition of VP^{GABA} neurons, we show they mediate both highly motivated pursuit of salient foods, and

avoidance of shocks. In contrast, inhibiting these cells does not affect shock-induced aversion, low-motivation food seeking, free food consumption, or locomotion. Notably, when rats made choices about food rewards under threat of shock, VP^{GABA} inhibition shifted choice bias towards a more risk averse strategy, increasing preference for small/safe rewards over large/risky ones. Together, these results show that VP^{GABA} neurons govern high-stakes motivational processes underlying risky decision making.

Methods

Subjects. Male (*n* = 46) and female (*n* = 35) Long-Evans hemizygous GAD1:Cre rats (Sharpe et al., 2017; Gibson et al., 2018; Wakabayashi et al., 2019) and their Cre-negative wildtype littermates (WT) were pair-housed in polycarbonate tub-style cages (48 × 20 × 27 cm) with bedding and nesting material. Rats were maintained on a reverse 12 hr light-dark cycle, with testing in the dark phase. Water was available *ad libitum* and food was restricted to ~90% of free-feeding weight during behavioral testing (~6-9 g/day/rat), unless otherwise noted. During food restriction, food was placed in the homecage after each behavioral testing session. All procedures were approved by the University of California Irvine Institutional Animal Care and Use Committee, and are in accordance with the NIH Guide for the Care and Use of Laboratory Animals.

Chemogenetic methods.

Surgery and viral vectors.

Rats were anesthetized with ketamine (56.5 mg/kg) and xylazine (8.7 mg/kg), and treated for pain with meloxicam (1.0 mg/kg). An adeno-associated vector containing double-floxed, inverted open reading frame (DIO) mCherry-tagged hM4Di designer receptors (Armbruster et al., 2007) (DREADDs; AAV2-hSyn-DIO-hM4D(Gi)-mCherry; titer: 1×10^{12} GC/mL; Addgene) was injected bilaterally into VP (relative to bregma: AP 0.0 mm, ML ±2.0 mm, DV -8.2 mm; ~300 nL/hemisphere) using a Picospritzer and glass micropipette. Injections occurred over 1 min, and the pipette was left in place for 5 min after injection to limit spread.

Both GAD1:Cre and WT rats were injected with the active hM4Di DREADD virus, and lack of hM4Di/mCherry expression was confirmed in each WT rat.

Drugs.

Clozapine-N-oxide (CNO) was obtained from NIDA, and subsequently stored at 4° C in powder aliquots stored in desiccant, and protected from light. CNO was dissolved in a vehicle containing 5% dimethyl sulfoxide (DMSO) in saline, and injected at 5 mg/kg intraperitoneally (IP), 30 min prior to tests. For microinjections, bicuculline methiodide (Sigma) was dissolved in artificial cerebrospinal fluid (Thermofisher), stored in aliquots at -20° C, and thawed just prior to use.

DREADD validation.

Localization of DREADD expression to VP.

Virus expression in GAD1:Cre rats was amplified with mCherry immunohistochemistry, and sections were co-stained for substance P, an anatomical marker of VP borders. First, behaviorally-tested rats were perfused with cold 0.9% saline and 4% paraformaldehyde after completion of experiments. Brains were cryoprotected in 20% sucrose, sectioned at 40 µm, and blocked in 3% normal donkey serum PBST. Tissue was incubated 16 hrs in rabbit anti-substance P (ImmunoStar; 1:5000) and mouse anti-mCherry antibodies (Clontech; 1:2000) in PBST-azide with 3% normal donkey serum. After washing, slices were incubated in the dark for 4 hrs in Alexafluor donkey anti-Rabbit 488 and donkey anti-Mouse 594 (Thermofisher), then washed, mounted, and coverslipped with Fluoromount (Thermofisher). mCherry expression was imaged at 10x, and the zone of expression in each hemisphere of each rat was mapped in relation to VP borders, and a rat brain atlas (Paxinos and Watson, 2006).

Localization of DREADDs Specifically to VP^{GABA} Neurons.

Experimentally-naïve GAD1:Cre rats (*n* = 4) injected in VP with AAV2-hSyn-DIO-mCherry were euthanized, and fresh brains were immediately extracted and frozen in isopentane before storage at −80 °C. Brains were serially cut (20 µm) on a cryostat, and placed

directly onto slides before returning to storage at −80 °C. Three different coronal sections of the VP near the center of mCherry expression were used per brain. In situ hybridizations were performed using the RNAscope Multiplex Fluorescent Assay (Advanced Cell Diagnostics). RNA hybridization probes included antisense probes against rat *Gad1* (316401-C1), rat *Slc17a6* (vglut2 gene; 317011-C3) and *mCherry* (431201-C2) (*n* = 2), or antisense probes against rat *Gad1* (316401-C1), rat *Slc32a1* (vgat gene; 424541-C3) and *mCherry* (431201-C2) (*n* = 2), both respectively labeled with alexa488, atto647, and atto550 fluorophores. DAPI was used to label nuclei and identify cells. Three images/hemisphere/section were taken at 63x (1.4 NA) magnification using a Zeiss AxioObserver Z1 widefield Epifluorescence microscope with a Zeiss ApoTome 2.0 for structured illumination and Zen Blue software for counting. Wide-field images were taken at 20x (0.75 NA) magnification. Cells that exhibited at least 4 puncta (RNA molecules) in addition to DAPI were counted as expressing the respective gene.

DREADD-dependent inhibition of VP^{GABA} neurons by CNO.

In order to verify the ability of CNO to inhibit VP neurons in a DREADD-dependent manner, we tested the ability of systemic CNO to inhibit exogenously-stimulated VP neural activity. Experimentally-naïve GAD1:Cre rats (*n* = 3) were injected unilaterally with the previously described AAV2 DIO-hM4Di-mCherry vector in ipsilateral VP, and contralaterally in VP with a matched AAV2 DIO-mCherry control vector (4.7 x 10^{12} GC/mL, AddGene). Three weeks later, bilateral intracranial cannulae were implanted 2 mm dorsal to the injection target, using previously described procedures (Mahler et al., 2013a; Mahler et al., 2014; Mahler et al., 2019), and rats recovered for 5 d. Rats were then injected systemically with CNO, in order to engage unilaterally expressed VP^{GABA} hM4Di receptors. 30 min later, rats were bilaterally injected in VP with 0.5 µL of bicuculline (0.01 µg/0.5 µL/50 s), inducing neural activity in the local VP area in both hemispheres. 90 min later, rats were perfused, and brains were processed for Fos and mCherry to determine whether bicuculine-induced Fos was suppressed by hM4Di activation (i.e. if there was less Fos expression in the hM4Di hemisphere than the mCherry

hemisphere). VP sections near the center of the microinjection sites were incubated overnight at room temperature in rabbit anti-Fos (1:5000; Millipore) and mouse anti-DSRed (targeting mCherry; 1:2000; Clontech), washed, incubated in Alexafluor donkey anti-Rabbit 488 and donkey anti-Mouse 594 in dark for 4 hrs at room temperature, then coverslipped as above. For each rat, 2-3 brain sections/hemisphere/rat with VP-localized microinjector tip damage were selected for manual quantification at 10x magnification by an observer blind to experimental manipulation. mCherry-only, and mCherry/Fos co-expressing cells within VP borders (Paxinos and Watson, 2006) were counted in both hemispheres. The percentage of mCherry cells co-expressing Fos in each sample was calculated, and per-hemisphere averages were computed for each rat for statistical analysis.

Behavioral testing methods.

Operant apparatus.

All operant testing was performed in Med Associates operant chambers in sound-attenuating boxes, equipped with two retractable levers with associated stimulus lights above them. Between the two levers was a food magazine connected to a food pellet dispenser. Two nose-poke ports were positioned on the opposite wall with a yellow light in one of the ports. Boxes were equipped with tone/white noise and footshock generators.

Habituation training.

We adapted a previously reported risky decision task and associated training protocol (Simon et al., 2009; Simon and Setlow, 2012; Orsini et al., 2015a). Mildly food deprived male (*n* = 23) and female rats (*n* = 22) were familiarized to highly palatable, banana-flavored, sucrose, fat, and protein-containing pellets in their homecage (Bio-Serv, Ct # F0024), then on day 1 of training, 38 pellets were delivered into the food magazine on a variable time 100 s schedule (140, 100, 60 s) during a single ~60 min session. Rats that failed to eat > 19 pellets were given a second day of magazine training.

Lever pressing training.

Next, rats were trained to lever press for the banana pellets in daily 30 min sessions. Each session began with illumination of the house light, and extension of a single lever plus illumination of the associated stimulus light (right or left, counterbalanced). One pellet and a brief auditory tone cue (0.5 s, 2.9 kHz) were delivered on a fixed ratio 1 (FR1) schedule, with a 10 s timeout period between pellet deliveries. Daily FR1 training continued until criterion was met (50 pellet/30 min session), followed by training on the alternate (left or right) lever, again until criterion.

Lever choice training.

The next training phase consisted of daily 1 hr sessions that taught rats to press levers within 10 s of their extension. Sessions began with illumination of the houselight, and every 40 s one lever (right or left) was extended for 10 s, along with the associated stimulus light. Lever presses yielded 1 food pellet, and the tone cue. If no press occurred during the 10 s extension window, the lever retracted and stimulus light extinguished, the trial was counted as an omission, and rats were required to wait until the next lever extension trial. Each session consisted of 35 left lever, and 35 right lever extensions with a 40 s intertrial interval, independent of the rats' pressing or omitting. Rats that met criterion (< 10 omissions) on two consecutive sessions were moved to the next phase of the task. In this phase procedures were the same, except that now pressing one lever (left or right, counterbalanced) delivered 1 pellet accompanied by the tone cue, and pressing the other lever delivered 2 pellets and 2 tone cues. Rats were trained for at least 3 d in this manner, until 2 consecutive days with < 10 omissions.

Risky decision task.

Rats were next trained on the risk task, in which the threat of shock was introduced. At session start, as above one lever yielded 1 pellet, and the other 2 throughout the session. However, now the 2-pellet option came with the chance of concurrently-delivered shock; the probability of which increased over the course of the session. Sessions consisted of 5 blocks with 20 trials each, for a total of 66 min. Blocks represent changes in footshock probability

associated with large/risky lever presses such that in the first 20-trial block there was no chance of shock, and in each subsequent block shock probability increased by 25% (Block 1: 0% probability, Block 2: 25%, Block 3: 50%, Block 4: 75%, Block 5: 100%). Each 20-trial block began with 8 'forced choice' trials in which a single lever was extended (4 large/risky and 4 small/safe lever extensions, random order) to establish the shock contingency for that block. Following the 8 forced choice trials, 12 'free choice' trials commenced in which both the large/risky and small/safe levers were extended simultaneously to allow choice of the preferred option (small/safe; large/risky). If no lever press occurred within 10 s, the lever(s) were retracted, stimulus light(s) extinguished, and the trial was considered an omission. Footshock intensity (mA) was titrated individually for each rat to ensure sufficient parametric space to observe either increases or decreases in risky choice, as reported previously (Orsini et al., 2017). Footshock intensity started at 0.15 mA for each rat upon beginning the risky decision task, and percent choice of the large/risky reward was monitored daily for fluctuations in decision making. Footshock intensity was increased or decreased each day by 0.05 mA, until stable decision-making behavior was achieved in all animals.

Stable pre-test baseline performance.

Rats generally achieved stability within 10-20 sessions, with near-exclusive choice of the "risky" 2 pellet option when chance of shock was zero, then a parametric shift to the "safe" 1 pellet option as shock probability increased across blocks (interaction of block X lever: $F_{(4, 132)}$ = 111.5, $p < 0.0001$). Rats were trained until performance was stable for 5 consecutive days (no difference in 5 d average performance pre-vehicle/CNO: $F_{(1, 229)} = 0.45$, n.s.; or interaction of block x treatment: $F_{(4, 229)} = 0.023$, n.s.), then were assigned to receive counterbalanced vehicle and CNO tests, between which behavior was re-stabilized over ~5 days of training. Over the course of these experiments, 6 rats made > 50% omissions during vehicle treatment sessions (range 50-72 omissions over 100 trials), making interpretation of their data problematic. Accordingly, their data were excluded from risky decision analyses.

Reward magnitude discrimination.

To characterize potential VP inhibition effects on mere preference for larger versus smaller rewards, a separate cohort of GAD1:Cre rats (*n* = 8) were trained identically to above, except that shock was never introduced. We then evaluated CNO effects (versus vehicle) on choice of the 2-pellet lever over the 1-pellet lever, in the absence of shock. Rats required ~5-10 training sessions before displaying stable preference for the larger reward, after which they received CNO and vehicle tests on separate days. After the first test, rats received ~3 days of training to re-stabilize performance, then were given their second counterbalanced treatment.

Spontaneous palatable food intake.

Ad libitum-fed rats (*n* = 18) were placed in polycarbonate cages (44.5 x 24 x 20 cm) with bedding and ~12 g of peanut butter M&M chocolates for 1 hr on 2 consecutive days, to habituate them to test conditions. The next day, rats were administered CNO or vehicle (counterbalanced, separate days) 30 min prior to a 1 hr intake test. 48 hrs later the procedure was repeated with the other drug treatment. Food intake (g) was measured.

High effort instrumental responding for palatable food.

To assess the involvement of the VP in food seeking under higher effort requirements, mildly food-deprived rats (*n* = 39) were trained to nosepoke on a progressive ratio schedule of reinforcement. Sessions began with illumination of the both the houselight and a light within the active nosepoke port. When the required schedule was achieved, 3 banana pellets + 3 concurrently-delivered 0.5 s white noise pulses were delivered. The number of nosepokes required for reward increased each time the prior requirement was achieved (FR 1, 6, 15, 20, 25, 32, 40, 50, 62, 77, 95, 118, 145, 178, 219, 268, 328, 402, 492, 603 (Smith and Aston-Jones, 2012)). Inactive port entries were inconsequential, but recorded. Sessions lasted a maximum of 2 hrs, or less if the rat failed to reach the next ratio within 20 min of achieving the prior one. Training continued until rats achieved stable performance for 2 consecutive sessions (< 25%

change in active nosepokes). Pressing was re-stabilized between counterbalanced vehicle/CNO tests.

Low effort instrumental responding for palatable food or conventional chow.

Mildly-food deprived rats or *ad libitum* fed rats (*n* = 16) were trained to nosepoke for palatable 45 mg banana pellets on an FR1 schedule of reinforcement during daily 1 hr sessions. Separate animals (*n* = 8) were trained to respond for 45 mg chow pellets (Bio-Serv, Ct # F0165) instead using the same procedures. Sessions began with illumination of the houselight and active nosepoke port light. Active nosepokes resulted in delivery of a pellet into the food cup, while inactive nosepokes were without consequence. Rats were trained until achieving stability (< 25% change in active nosepokes) for 2 consecutive sessions (2-7 sessions), then tested with counterbalanced vehicle/CNO, with 1+ days of re-stabilization between tests.

Operant shock avoidance/escape task.

Procedures were adapted from a previously described shock avoidance/escape task (Oleson et al., 2012). Rats (*n* = 18 trained) that had previously performed the risky decision task, progressive ratio task, and palatable food FR1 task were tested, and footshock intensity (mA) was the same as that used for the rat during the previously-trained risk task (0.15-45 mA). Each 30 min session began with illumination of the houselight, and every 20 s an active and inactive lever were extended. Initial training taught rats to press a lever to turn off a repeated foot shock. During this initial 'escape only' training, lever extension was met with a concurrent footshock that repeated (0.1 s footshock every 2 s) until the active lever was pressed, at which time footshock ceased, both active and inactive levers were retracted, and a 20 s white noise safety signal was played. Then the next trial began with re-extension of both levers, a sequence that was repeated until the end of the 30 min session. Training proceeded for at least 2 d, until consistent escape behavior was observed.

Next, rats were trained to avoid, as well as to escape shocks in 30 min sessions. In this phase, levers were again extended at the start of each trial, but now this occurred 2 s prior to

initiation of shocks. If the active lever was pressed in this 2 s period (an avoid response), no shock occurred, levers retracted, and the safety signal was played for 20 s. If no press occurred before 2 s elapsed, repeating footshock commenced as above, until an active lever press occurred (escape response), at which time levers were retracted and the safety signal was played for 20 s. Inactive lever presses were inconsequential but recorded. All rats with > 5 avoidance lever presses on the vehicle test day were included for analyses (n = 18). Rats were administered counterbalanced vehicle and CNO tests 30 min prior to avoidance/escape sessions, with ~3 d between tests to re-stabilize behavior. Data were analyzed by assessing 1) the change in the ratio of avoidance presses to escape presses from pre-test baseline (i.e. change from baseline avoidance %), 2) the ratio of avoidance presses to escape presses on vehicle and CNO tests (i.e. raw avoidance %), 3) latency to avoid footshock, and 4) latency to escape repeated footshock.

Motor responses to shock.

To query the role of VP^{GABA} in affective responses to shock itself, rats (n = 16) were tested for overt motor reactions to shocks of ascending intensity in a chamber in which they had not been previously tested. The houselight was illuminated and 2 min elapsed. This waiting period ended with one 0.30 mA footshock to limit ongoing exploration. Following this shock, rats were administered 5 consecutive 1 s, 0.05 mA shocks, each separated by 10 s. After these 5 shocks, the procedure was repeated with blocks of increasingly intense shocks, increasing by 0.05 mA with each block. Motor reactivity was evaluated during testing, according to previously published criteria (Bonnet and Peterson, 1975). Briefly, motor reactivity was separated into 4 categories: 0: no movement, 1: flinch of a paw or a startle response, 2: elevation of one or two paws, 3: rapid movement of three or all paws. When 3 out of 5 shocks at a particular intensity elicited level 3+ motor reactivity, the session was terminated. CNO/vehicle tests were counterbalanced, and administered 48 hrs apart.

Ultrasonic vocalization responses to shock.

To further query affective shock responses, rats (*n* = 16) were administered 2 shock-induced ultrasonic vocalization tests after counterbalanced vehicle or CNO, held 48 hrs apart. Recordings again occurred in a chamber in which they had not been previously tested. Sessions began with illumination of the houselight, and following a 2 min baseline period, rats received 5 unsignaled footshocks (1 s, 0.75 mA), each separated by 1 min. Recordings were made with condenser ultrasound microphones (frequency range: 10–200 kHz; CM16/CMPA, Avisoft Bioacoustics, Berlin, Germany) that were centered atop the operant chamber and pointed directly toward the center of the chamber (~18 cm above the floor). USV recordings were made on an UltraSoundGate 416H data acquisition device (Avisoft Bioacoustics; sampling rate 250 kHz; 16-bit resolution), as reported previously (Mahler et al., 2013b). Spectrograms were visualized using Avisoft software, and ultrasonic vocalizations (USVs) were manually quantified by an observer blind to experimental conditions. Aversion-related 22 kHz USVs were operationalized as 18-30 kHz with a duration greater than 10 ms, and positive affect-related high frequency USVs were operationalized as those > 30 kHz frequency, with a duration greater than 10 ms.

General locomotor activity.

General locomotor activity was assessed in a locomotor testing chamber (43 × 43 × 30.5 cm) with corncob bedding. Following two daily 2 hr habituation sessions, infrared beams captured horizontal distance traveled and number of vertical rears following vehicle/CNO injections (counterbalanced tests, 48 hrs apart).

Data analysis. Graphpad Prism and SPSS were used for all statistical analyses. CNO and vehicle tests were counterbalanced for each experiment. An independent samples *t*-test was used to compare %Fos in ipsilateral mCherry+ VP neurons versus %Fos in contralateral hM4Di-mCherry neurons following bicuculline microinjection and systemic CNO injection. Male and female footshock intensities required on the risky decision task were compared with an independent samples *t*-test. For the risky decision task, reward magnitude discrimination, and

motor shock reactivity tasks, effects of drug and block were analyzed with separate two-way ANOVAs in GAD1:Cre and WT rats, along with Sidak posthoc tests. Win-stay and lose-shift behavior was characterized on choice trials, and analyzed with separate paired sample *t*-tests for GAD1:Cre and WT rats. Win-stay was operationalized as the number of risky choices after a non-shocked risky choice, divided by the total number of non-shocked risky choices, whereas lose-shift was the number of safe choices followed by a shocked risky choice, divided by the total number of shocked risky choices. In addition, we performed two-way ANOVAs with treatment (vehicle and CNO) and genotype (WT and GAD1:Cre) as factors for relevant comparisons, along with a third factor (bin) for risk task data. Pearson's correlation was used to determine whether footshock intensity employed in the risky decision task correlated with pressing for the large/risky over the small/safe option. Separate one-way ANOVAs were conducted to ask whether latency to press the small/safe or large/risky options increased across the session when tested with vehicle treatment. Latency data for the risky decision task excluded all trials in which omissions occurred. For avoidance/escape task, FR1, and progressive ratio tasks, effects of CNO versus vehicle in GAD1:Cre and WT rats were analyzed with paired sample t-tests. Due to the high variability in USV production among rats, all USV data were analyzed as percent of vehicle test day, and compared to 100% with one-sample *t*-test. Sample sizes were chosen based on those used in prior experiments (Simon and Setlow, 2012; Orsini et al., 2017; Farrell et al., 2019). Two-tailed tests with a significance threshold of $p < 0.05$ were used for all analyses.

Results

Selective, functional hM4Di expression in VP^{GABA} neurons. GAD1:Cre rats exhibited hM4Di-mCherry expression ($n = 53$) that was largely localized within substance P-defined VP borders (**Fig 15A-B**). Specifically, at the center of expression, mean $\pm$ SEM = 68.9% ± 1.2 of total viral expression area was localized within VP, and in behaviorally tested rats 68.8% ± 1.3 of VP area contained mCherry expression. At least 55% of DREADD expressing cells were localized within

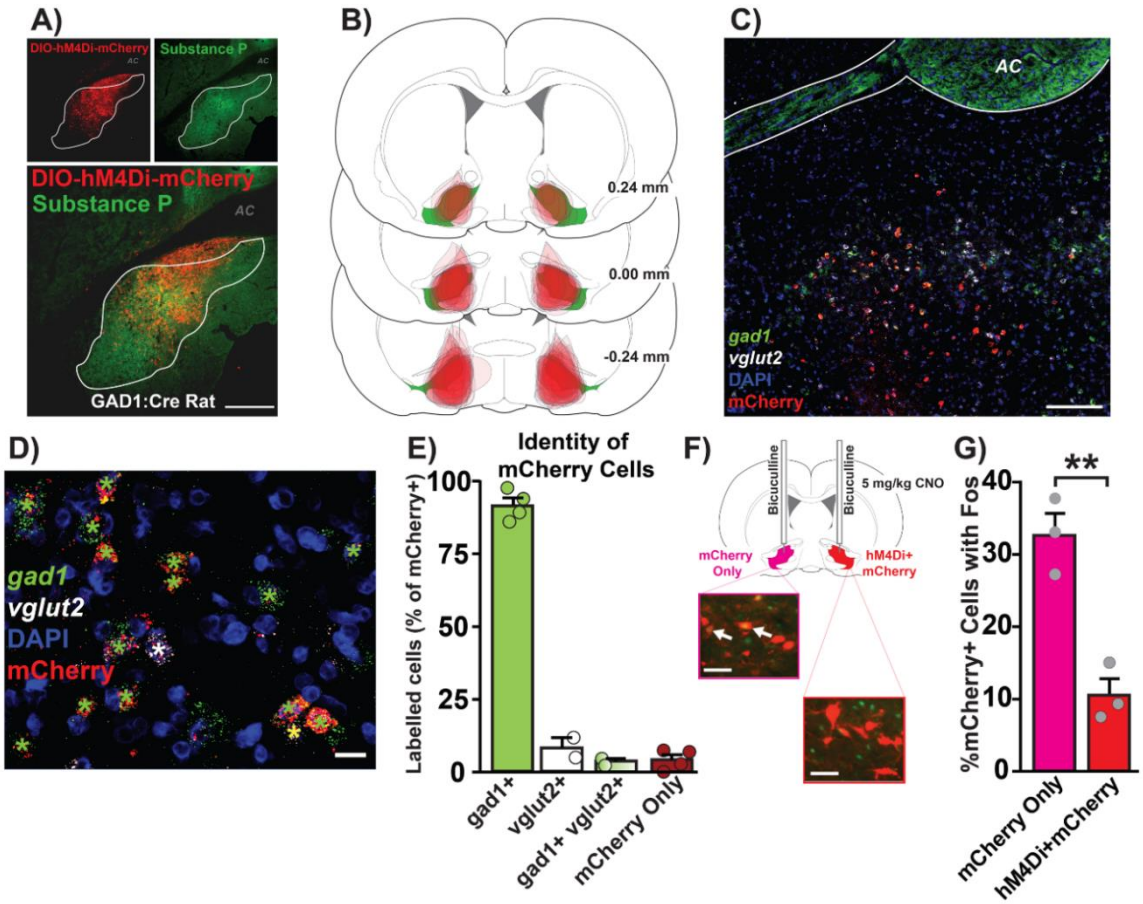

Figure 15. Anatomical, cellular, and functional characterization of hM4Di DREADDs in VP^{GABA} neurons. A) Localization of DIO-hM4Di-mCherry in substance P-defined VP borders. Top left panel: DIO-hM4Di-mCherry in VP. Top right panel: substance P demarcates VP from surrounding basal forebrain. Bottom: Merged DIO-hM4Di-mCherry and substance P image. AC = anterior commissure. Scale bar = 400 µm. **B)** Mapping of viral expression for each individual rat expressing hM4Di DREADDs. Numbers represent rostral/caudal coordinates relative to bregma. Green = substance P-defined VP. Red = DIO-hM4Di-mCherry expression. **C)** RNAscope fluorescent in situ hybridization for gad1, vglut2 and mcherry mRNA, with DAPI co-stain. Scale bar = 200 µm. **D)** Higher magnification of mRNA signal; Scale bar = 20 µm. Green star: mCherry+gad1; white star: mCherry+vglut2; yellow star: mCherry+gad1+vglut2. **E)** Identity of mCherry cells in VP. mCherry co-localized largely with gad1 mRNA (green bar), with few mCherry+ neurons expressing vglut2 mRNA. A small population of mCherry+ neurons expressed both gad1 and vglut2 (green+white gradient), and some cells lacked observable gad1 or vglut2 mRNA and only expressed mCherry (red). **F)** Schematic illustrating bilateral bicuculline (0.01 µg/0.5 µL) microinjection and systemic CNO (5 mg/kg) in rats with ipsilateral mCherry and contralateral hM4Di+mCherry in VP^{GABA} neurons (left image, Fos = green, red = mCherry; right image, Fos = green, red = hM4Di+mCherry). White arrows indicate colocalization of Fos in mCherry+ neurons. Scale bars = 40 µm. **G)** CNO reduced %mCherry+ cells colocalized with Fos in hM4Di+mCherry neurons, compared with contralateral mCherry only neurons. $^{**}p < 0.01$, independent sample *t*-test. Each graph depicts mean + SEM, with dots representing individual rats.

VP borders of included rats, though most animals also had at least some expression in adjacent

GABAergic structures. At least some extra-VP expression was observed in lateral preoptic area of 20.8% of rats, bed nucleus of the stria terminalis (30.2%), horizontal limb of the diagonal band of Broca (66%), and globus pallidus (15.1% of rats). Verifying specificity of expression, we used RNAscope to show that mCherry mRNA was largely colocalized with GABA-specific markers *gad1* and *vgat* mRNA in VP (mCherry+gad1+: m = 91.28 ± 2.6; mCherry+vgat+: m = 91.58 ± 2.75) (data not shown). The vast majority of these neurons were triple labeled for *mCherry*, *gad1*, and *vgat* (mCherry+gad1+vgat+: m = 87.92 ± 2.58), indicating robust expression in GABAergic VP neurons. Little mCherry expression was detected in vglut2+ neurons (mCherry+vglut2+: m = 8.42 ± 3.42), and of these mCherry+vglut2+ cells, 40.6% also localized with *gad1* (mCherry+vglut2+gad1+: m = 3.42 ± 1.08) (**Fig 15C-E**), possibly indicating co-expression of GABA and glutamate in some pallidal neurons (Meye et al., 2016; Faget et al., 2018; Farrell et al., 2019).

To verify that hM4Di DREADDs measurably inhibit neural activity in VP^{GABA} neurons, we administered CNO systemically to GAD1:Cre rats (n = 3) with unilateral VP GAD1-dependent expression of hM4Di+mCherry, and contralateral VP GAD1-dependent mCherry only. We then pharmacologically disinhibited VP neurons bilaterally, using microinjections of the $GABA_A$ antagonist, bicuculine (0.01 µg/0.5 µL), which robustly induces VP Fos (Smith and Berridge, 2005; Turner et al., 2008). As expected, fewer mCherry + Fos VP neurons were found in the hM4Di-expressing hemisphere than the mCherry hemisphere (**Fig 15F**; t_2 = 18.12, p = 0.003), despite the fact that cannulae localizations were equivalent in each hemisphere. These results demonstrate that CNO, via actions at hM4Di, is capable of suppressing Fos in pharmacologically disinhibited VP^{GABA} cells, presumably by recruiting endogenous $G_{i/o}$ signaling (Pleil et al., 2015; Roth, 2016).

Inhibiting VP^{GABA} neurons reduces risky choices. Rats (n = 45) performed the risk task as expected, shifting their choices from the large reward when chance of shock was low, to the smaller but unpunished reward as the probability of shock increased (**Fig 16A**; GAD1:Cre rats

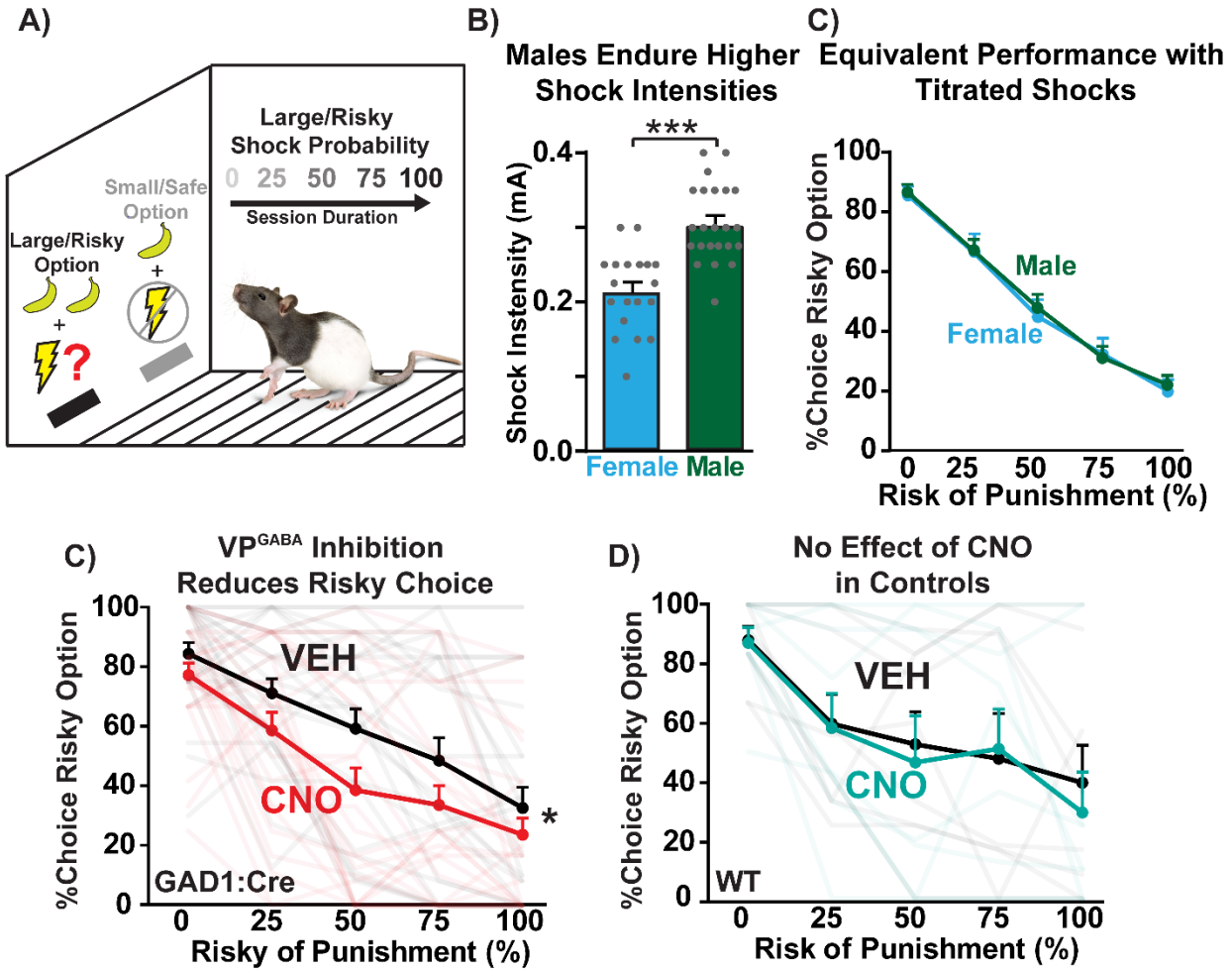

Figure 16. Inhibiting VP^{GABA} neurons reduces risky choice. A) Schematic of risky decision task modified from (Simon et al., 2009). Sessions consisted of forced choice trials (1 available option; small/safe or large/risky) and free choice trials (2 available options; small/safe and large/risky), with ascending footshock probability associated with selection of the large/risky reward option. **B)** Male rats required a higher shock intensity than females for appropriate performance of the risky decision task, as previously reported (Orsini et al., 2016). **C)** Equivalent average performance of male and female rats on the risky decision task with shock titration. **D)** GAD1:Cre rats administered CNO (red line) exhibit a decrease in %choice of the risky option relative to vehicle-treated rats (black line). **E)** No effect of CNO (teal line) in WT rats compared with vehicle treatment (black line). ***$p < 0.0001$, Independent sample *t*-test; *$p < 0.05$, treatment main effect. Semi-transparent lines represent data from individual rats tested with CNO (red/teal) or vehicle (black). Each graph depicts mean + SEM.

main effect of block: $F_{(4, 96)} = 40.68$, $p < 0.0001$; rats: $F_{(4, 32)} = 13.4$, $p < 0.0001$). Male rats required higher average shock intensities than female rats (**Fig 16B**, $t_{40} = 5.6$, $p < 0.0001$), as reported previously (Orsini et al., 2016). However, after this individualized shock titration, males

and females performed equivalently on the task; similarly shifting their choice from the large/risky to the small/safe reward option as shock probability increased (block: $F_{(4, 179)} = 76.5$, $p < 0.0001$). Importantly, no sex differences were detected for percent choice of the risky option (**Fig 16C**, sex: $F_{(1, 179)} = 0.19$, n.s.; block x sex interaction: $F_{(4, 179)} = 0.07$, n.s.). Shock intensity required for stable behavior in each GAD1:Cre rat did not predict the subsequent magnitude of VP^{GABA} neuron inhibition effects; i.e. shock intensity did not correlate with CNO effects (CNO day - vehicle day) on large/risky lever pressing ($r = 0.14$, n.s.) nor on small/safe pressing ($r = -0.05$, n.s.). In GAD1:Cre rats ($n = 30$), CNO reduced choice of the large, risky reward option (**Fig 16D**, treatment: $F_{(1, 24)} = 4.62$, $p = 0.042$). Though no significant overall treatment x block

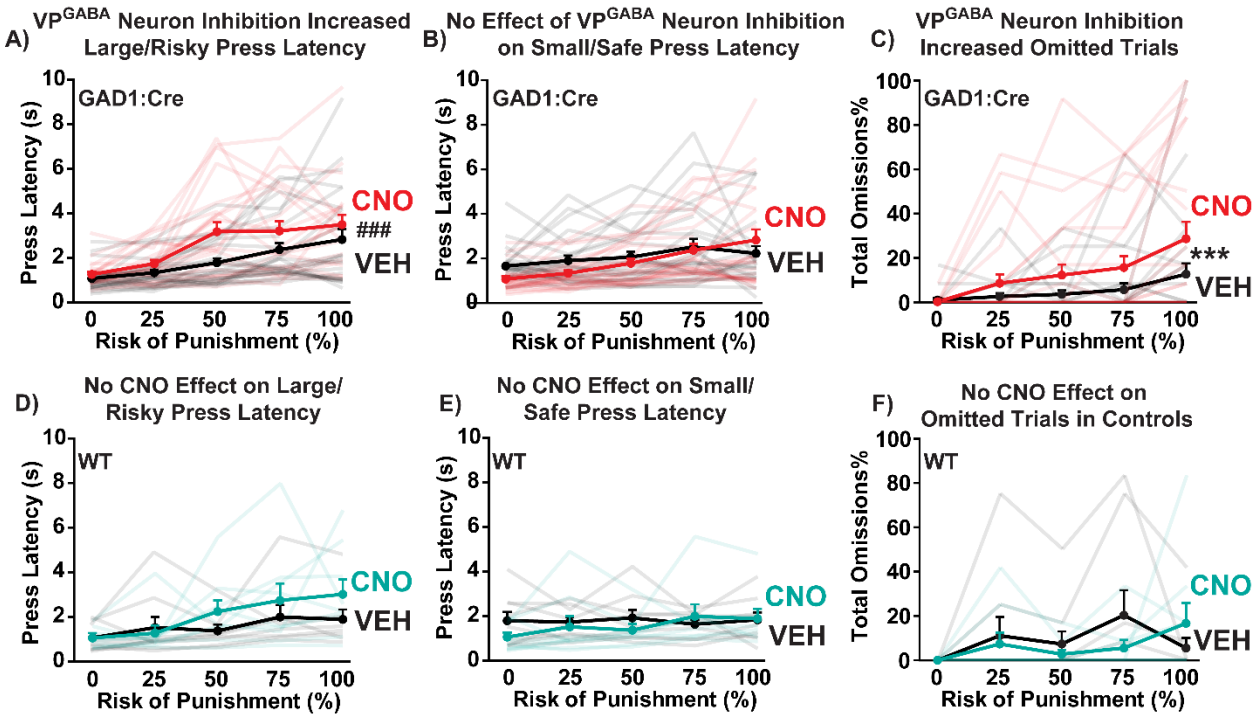

Figure 17. VP^{GABA} neuron inhibition increases latency to select the large/risky option, and trial omissions. A-C) In GAD1:Cre rats, CNO (red lines) increased the latency to press the large/risky reward lever, relative to vehicle day in the same rats (black lines; ###$p <$ 0.001, treatment main effect). **B)** In contrast, CNO in GAD1:Cre rats did not affect latency to press the small/safe reward lever. **C)** CNO in GAD1:Cre rats increased the percentage of trials omitted on high-risk blocks (***$p < 0.001$, treatment x block interaction). **D-F)** In WT rats without VP DREADDs, CNO (teal lines) did not alter **D)** omissions, **E)** latency to press the large/risky reward lever, **F)** or latency to press the small/safe reward option, relative to vehicle day (black lines). Semi-transparent lines represent data from individual rats tested with CNO (red/teal) or vehicle (black). Each graph depicts mean + SEM.

interaction was detected, block-specific comparisons revealed that suppression of choice of the large reward was statistically different during the 50% (Sidak: $p = 0.0014$) and 75% (Sidak: $p = 0.038$) blocks, but not at the 0, 25, or 100% shock probability blocks (all n.s.). To further probe effects of VP^{GABA} inhibition on the ability of positive or negative experiences to adjust ongoing behavior, we performed a win-stay/lose-shift analysis (Onge et al., 2011). CNO, relative to vehicle, did not alter the proportion of trials in which either win-stay (Vehicle: m $\pm$ SEM = 0.70 ± 0.055; CNO: m = 0.69 ± 0.036; $t_{18} = 0.18$, n.s.) or lose-shift occurred (Vehicle: m = 0.42 ± 0.062; CNO: m = 0.49 ± 0.076; $t_{18} = 0.71$, n.s.), indicating that the effects of VP^{GABA} inhibition on choice were not driven by altered sensitivity to outcomes of recent choices. As expected, latency to press the large/risky reward option increased as the footshock probability increased (one-way ANOVA for vehicle day data: $F_{(4, 118)} = 7.21$, $p < 0.0001$), which did not occur for latency to press the small/safe reward option ($F_{(4, 119)} = 1.44$ n.s.). CNO selectively increased the latency to press the large/risky reward option (**Fig 17A**, treatment: $F_{(1, 231)} = 13.5$, $p = 0.0003$), especially when the uncertainty of footshock was maximum; during the 50% footshock block (Sidak posthoc: $p = 0.0053$). In contrast, CNO failed to impact latency to press the small/safe reward option (**Fig 17B**, $F_{(1, 237)} = 1.29$, n.s.). CNO also increased the total number of omitted trials, especially in the blocks with the highest probability of shock (**Fig 17C**, treatment x block interaction: $F_{(4, 96)} = 11.91$, $p < 0.0001$; Sidak posthoc: 50% block: $p = 0.0006$; 75%: $p < 0.0001$; 100%: $p < 0.0001$). In addition, due to decreased pressing of the large/risky option and increased omissions, CNO-treated GAD1:Cre rats obtained fewer rewards overall than on vehicle day (treatment: $F_{(1, 24)} = 6.95$, $p = 0.015$, data not shown).

VP^{GABA} inhibition effects are specific to risky choices: No effect on reward magnitude discrimination.

Reward magnitude discrimination.

A separate group of GAD1:Cre rats ($n = 8$) were trained as described above, but in the absence of shock, to confirm their ability to discriminate reward magnitude after VP^{GABA} neuron

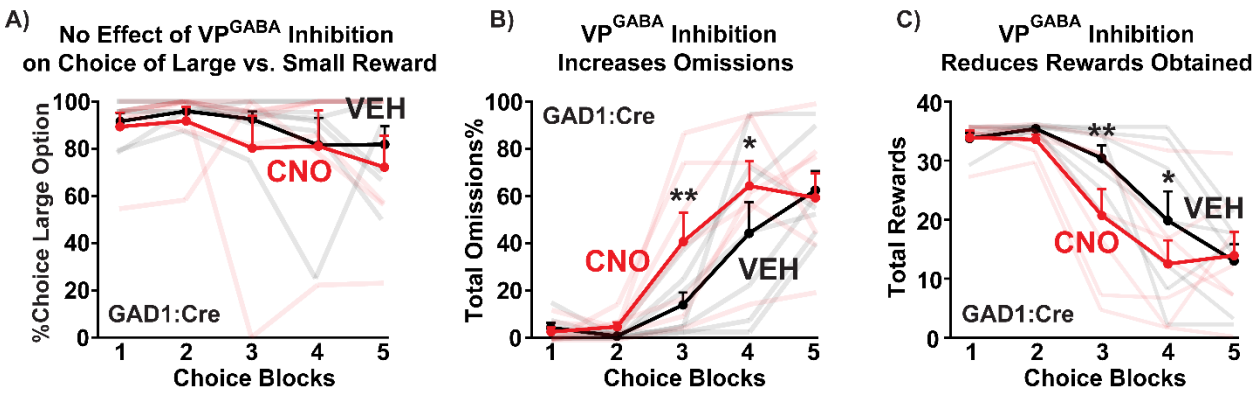

Figure 18. Inhibiting VP^{GABA} neurons spares the ability to choose between large and small rewards, while decreasing motivation. A) In the absence of shock punishment, CNO-treated GAD1:Cre rats (red line) showed no change in percentage choice of the large (2 pellets) versus small (1 pellet) reward option, compared with vehicle treatment (black line). **B)** GAD1:Cre rats omitted more trials during CNO tests (red line) compared with vehicle treatment (black line). **C)** CNO treatment in GAD1:Cre rats (red line) reduced rewards obtained relative to vehicle (black line). Semi-transparent lines represent data from individual rats tested with CNO (red/teal) or vehicle (black). Each graph depicts mean + SEM. *p < 0.05, **p < 0.01, Sidak posthoc tests.

inhibition. As expected, rats nearly exclusively chose the large reward over the small one during training, and after vehicle treatment (vehicle day: large versus small reward: t_7 = 11.11, p < 0.0001). After CNO, GAD1:Cre rats showed a nearly identical preference as on their vehicle test day (**Fig 18A,** treatment: $F_{(1, 56)}$ = 1.08, n.s.), showing that VP^{GABA} inhibition does not affect rats' preference for a large reward over a small one. This said, as in the task where the larger reward was associated with a probabilistic shock, CNO increased omitted trials (**Fig 18B,** treatment x block interaction: $F_{(4, 24)}$ = 4.0, p = 0.013), and decreased total rewards obtained (**Fig 18C,** treatment x block interaction $F_{(4, 24)}$ = 3.73, p = 0.017), consistent with an overall reduction in motivation. Posthoc tests revealed that CNO increased omissions only in the 3rd block (Sidak posthoc: p < 0.01) and 4th block (p < 0.05), and similarly only decreased rewards obtained in the 3rd (Sidak posthoc: p < 0.01) and 4th (p < 0.05) blocks. Emergence of satiety in later blocks likely accounts for why the 5th block of trials converged for both omissions and rewards obtained, as a significant main effect of block was observed for both omissions ($F_{(4, 24)}$ = 21.4, p < 0.001) and rewards obtained ($F_{(4, 24)}$ = 19.4, p < 0.001). However, CNO did not impact choice latency

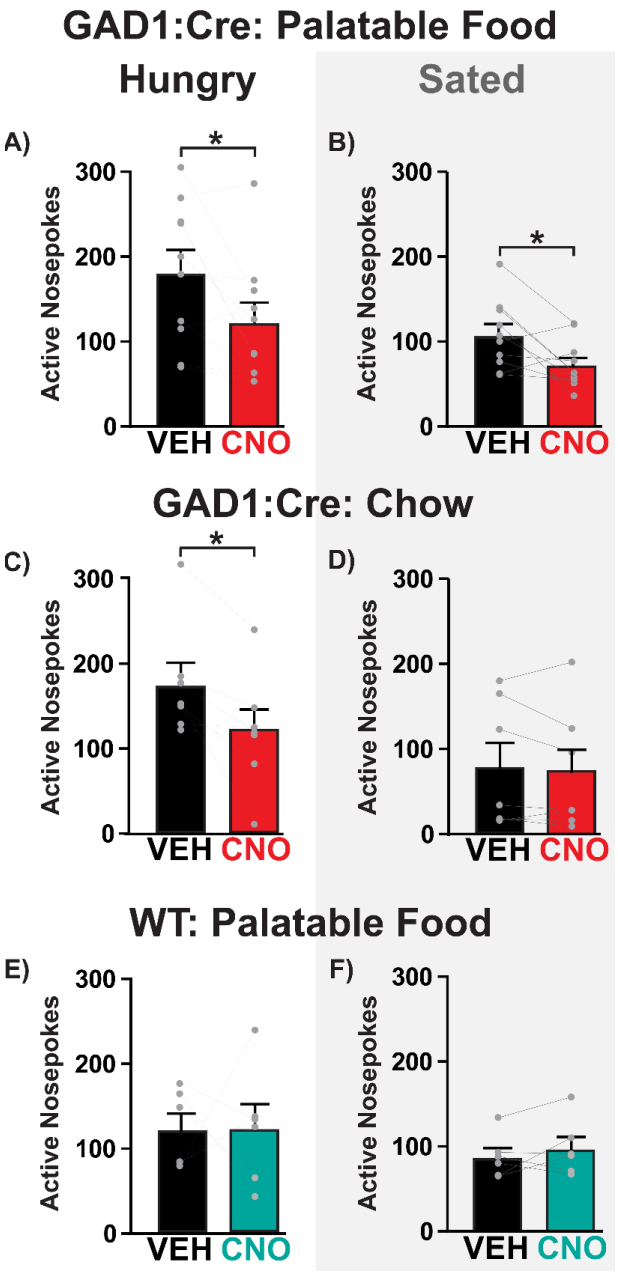

Figure 19. Inhibiting VP^{GABA} neurons reduces responding for palatable food and chow in hungry rats, but only reduces responding for palatable food (not chow) in sated rats. A-B) In GAD1:Cre rats, CNO (red bars) reduced FR1 active nosepokes for palatable food in **A**) hungry and **B**) sated rats, relative to vehicle treatments (black bars). **C-D)** CNO in GAD1:Cre rats (red bars) reduced FR1 active nosepokes for chow relative to vehicle (black bars) in **C**) hungry , but not **D**) sated rats. **E-F**) No effect of CNO on active nosepokes in WT controls (teal bars) relative to vehicle treatment (black bars) under **E**) hungry or **F**) sated conditions. *$p < 0.05$, paired sample *t*-test. Each graph depicts mean + SEM, and dots represent individual rats.

relative to vehicle (treatment: $F_{(1, 59)} = 0.86$, n.s.), unlike in the shock version of the task where CNO selectively increased latency to press the large/risky lever. The lack of effect on choice latencies induced by VP^{GABA} neuron inhibition in this experiment suggest that the increased decision times observed on the risky decision task were not attributable to a generalized psychomotor slowing, but rather to increased deliberation time in weighing the costs and benefits of the risky choice.

Inhibiting VP^{GABA} neurons suppresses instrumental responding for high value foods, without impairing general locomotion.

Similar suppression of palatable food responding during hunger and satiety.

We examined effects of inhibiting VP^{GABA} neurons on low effort (FR1) operant responding for highly palatable banana pellets. When GAD1:Cre rats (n = 10) were tested under

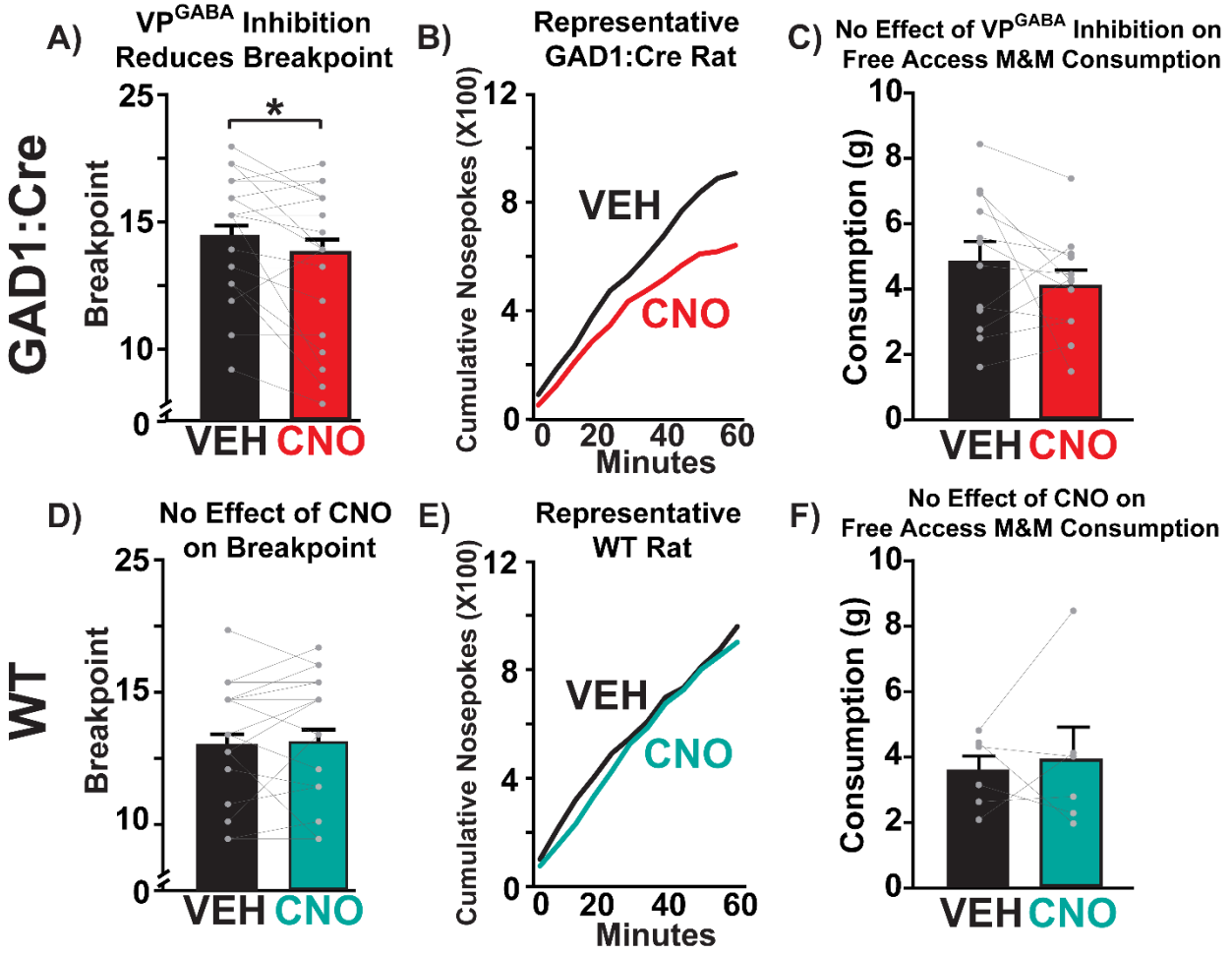

Figure 20. Inhibiting VP^{GABA} neurons reduces progressive ratio motivation for palatable food, without impairing free access palatable chocolate intake. A) In GAD1:Cre rats, CNO (red bar) reduces breakpoint relative to vehicle (black bar). **B)** Cumulative nosepokes for a representative GAD1:Cre rat during vehicle (black line) and CNO (red line) progressive ratio tests are shown. **C)** CNO in GAD1:Cre rats (red bar) fails to alter 1 hr free access M&M consumption, relative to vehicle test (black bar). **D)** In WT controls, CNO (teal bar) does not affect breakpoint compared with vehicle day (black bar). **E)** Cumulative nosepokes for representative WT rat during vehicle (black line) and CNO (teal line) progressive ratio tests are shown. **F)** CNO in WT rats (teal bar) fails to alter 1 hr free access M&M consumption, relative to vehicle test (black bar). *$p < 0.05$, paired sample *t*-test. Each graph depicts mean + SEM, and dots represent individual rats.

mild food restriction, CNO reduced active port responding (**Fig 19A**: $t_9 = 2.58$, $p = 0.03$), without affecting inactive port responding ($t_9 = 0.79$, n.s.). Effects of VP^{GABA} neuron inhibition were similar when rats were tested in the same manner while maintained on *ad libitum* chow 23 hrs/day (**Fig 19B**, active port responses: $t_9 = 2.65$, $p = 0.027$, inactive: $t_9 = 0.97$, n.s.), indicating

that VP^{GABA} neurons are required for low effort instrumental pursuit of a highly salient, palatable reward regardless of physiological need state.

Suppression of responding for less-palatable chow only during hunger.

We next examined effects of inhibiting VP^{GABA} neurons on low effort (FR1) operant responding for standard chow pellets under hunger and satiety conditions (n = 8). Inhibiting VP^{GABA} neurons reduced active port responding for chow when rats were hungry (**Fig 19C**, t_6 = 3.12, p = 0.021), but not when they were fed ad libitum (**Fig 19D**, t_6 = 0.89, n.s.), as shown by the significant interaction between hunger state and vehicle/CNO treatment ($F_{(1, 6)}$ = 6.31, p = 0.046). However, we note that responding for chow during satiety was quite low in some animals, raising the possibility of a floor effect.

Robust suppression of high-effort palatable food seeking.

When GAD1:Cre rats (n = 22) were trained on a progressive ratio to stably respond for palatable banana pellets, CNO suppressed breakpoint (**Fig 20A-B**, t_{21} = 2.4, p = 0.026), and trended toward suppressing active port responses (vehicle: m = 1050 ± 136.7, CNO: m = 847.5 ± 122.4; t_{21} = 2.0, p = 0.059). The low number of inactive port responses was unaffected (vehicle: m = 15.8 ± 2.9, CNO: m = 18.3 ± 4.0; t_{21} = 0.53, n.s.).

Non-operant spontaneous intake of palatable food is unaffected.

To determine effects of VP^{GABA} neuron inhibition on spontaneous intake of a highly palatable sweet and fatty food meal (n = 12), we examined 2 hr intake of peanut butter M&M™ candies, placed directly on the floor of a familiar testing chamber. CNO failed to affect intake (g) in GAD1:Cre rats (**Fig 20C**, t_{11} = 1.24, n.s.).

Locomotor activity.

Effects of VP^{GABA} inhibition with CNO treatment failed to alter either horizontal locomotion or rearing behavior in GAD1:Cre rats (n = 12) (Distance travelled: vehicle m = 12026 ± 1006 cm, CNO m = 13185 ± 1601 cm, t_{11} = 0.71, n.s.; Rearing: vehicle m = 183.6 ± 17.1 rears, CNO m = 188 ± 22.7 rears, t_{11} = 0.20, n.s.).

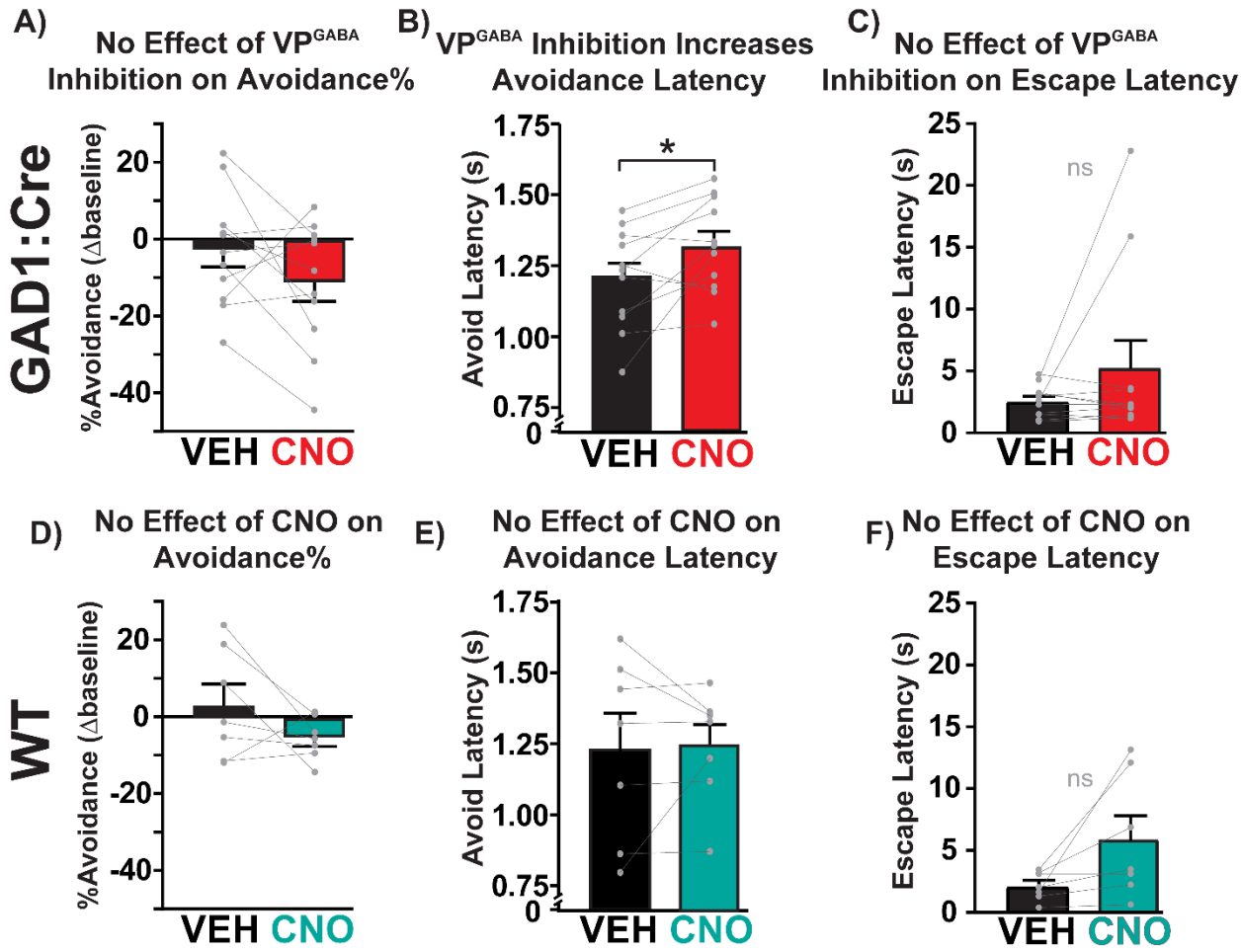

Figure 21. Inhibiting VP^{GABA} neurons increases avoidance latency, without affecting avoidance propensity or escape latency. A) CNO did not affect avoidance% in GAD1:Cre rats (red bar) relative to vehicle treatment (black bar) (change in avoidance% on vehicle/CNO test from the day preceding each treatment). **B)** CNO increased latency to lever press to avoid being shocked in GAD1:Cre rats (red bar) compared with vehicle treatment (black bar). **C)** No effect of CNO on escape latency in GAD1:Cre rats. **D-F)** CNO in WT controls (teal bars) failed to impact **D)** avoidance%, **E)** avoidance latency, or **F)** escape latency relative to vehicle treatments (black bars). *$p < 0.05$, paired sample *t*-test. Each graph depicts mean + SEM, and dots represent individual rats.

Inhibiting VP^{GABA} neurons decreases motivation to avoid footshock without impacting motor or affective reactions to shock.

Latency to avoid footshock increases after VP^{GABA} neuron inhibition.

VP^{GABA} neuron inhibition suppressed operant risky decision making and food seeking, so we next sought to determine whether this manipulation also affects negatively reinforced operant responding (n = 11). CNO did not affect the overall propensity of rats to avoid shocks

rather than to escape them (**Fig 21A**, change from baseline avoidance%: t_{10} = 1.50, n.s.; Vehicle: m = 38.82 ± 5.71; CNO: m = 28.96 ± 5.07; raw %avoidance: t_{10} = 2.2, p = 0.053), suggesting that their general strategy was not altered by this manipulation. However, CNO selectively increased latency to press to avoid shock in GAD1:Cre rats (**Fig 21B**, t_{10} = 2.60, p = 0.027), consistent with reduced motivation to avoid the impending, signaled shock. Escape latency was not similarly impacted by CNO (**Fig 21C**, t_{10} = 1.36, n.s.), indicating that rats were still fully capable of pressing to terminate an ongoing shock.

No effects on motor or affective responses to shock.

As expected, shock-induced motor reactivity scores parametrically increased with footshock intensity (**Fig 22A,** GAD1:Cre block: $F_{(6, 112)}$ = 100.9, p < 0.0001). Motor reactivity scores were not affected by CNO in GAD1:Cre rats (n = 11) (treatment: $F_{(1, 112)}$ = 0.27, n.s.), nor was the maximum shock intensity endured altered (vehicle m = 0.27 ± 0.017 mA; CNO m = 0.29 ± 0.014 mA, t_{10} = 0.94, n.s.).

No effect on shock-induced negative affective vocalizations.

We also examined aversion-related 22 kHz ultrasonic vocalizations emitted in response to repeated, moderate intensity shocks (0.75 mA/1 s, delivered every min for 5 min). These

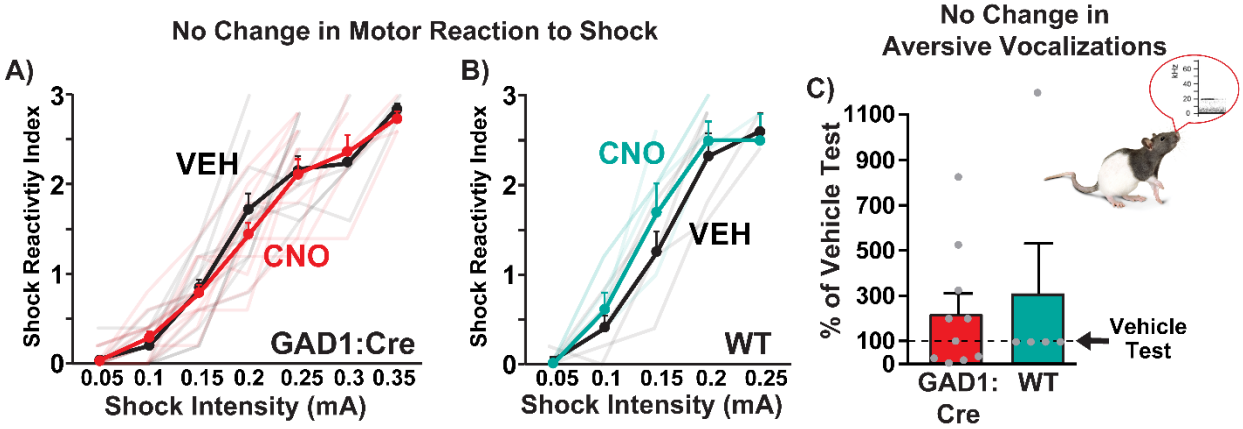

Figure 22. Motor and affective reactions to footshock unaffected by inhibiting VP^{GABA} neurons. A) CNO in GAD1:Cre (red line) or in **B)** WT rats (teal line) did not impact shock reactivity index associated with ascending intensity footshocks, relative to vehicle rats (black lines). **C)** CNO in GAD1:Cre rats (red bar) or WT controls (teal bar) failed to alter aversion-related ultrasonic vocalizations during high intensity footshock (0.75 mA) sessions (percent of vehicle test day). Each graph depicts mean + SEM, and dots represent individual rats.

USVs were in the frequency range of well-characterized aversion-related USVs (Knutson et al., 2002; Portfors, 2007; Mahler et al., 2013b), with a mean frequency of m = 23.5 ± 1.1 kHz, and a mean duration of m = 1306.4 ± 142.1 ms. CNO failed to alter the number of 22 kHz vocalizations emitted in GAD1:Cre rats (*n* = 10) (**Fig 22C**, % of vehicle day USVs, compared to 100% with one sample *t*-test: t_9 = 1.5, n.s.). We also observed some vocalizations > 30 kHz, linked to positive affect (Knutson et al., 2002; Portfors, 2007; Brudzynski, 2013). These vocalizations, however, occurred largely during the 2 min pre-footshock baseline (high frequency USVs/min on vehicle test for GAD1:Cre and WT: m = 46.4 ± 14.8) compared to the subsequent 5 min intermittent footshock period (m = 9.6 ± 5.8; pre-footshock vs. footshock period: t_{14}=3.16, p = 0.0069). Production of these high frequency vocalizations was also unaffected by CNO treatment (% of vehicle day USVs, compared to 100% with one sample *t*-test: t_9 = 1.74, n.s.).

Minimal DREADD-independent effects of CNO. Across all nine behavioral tasks implemented here, we saw few non-specific effects of CNO in WT rats lacking DREADD expression. In the risky decision task, administering CNO to WT rats did not affect risky choice (**Fig 16E**, treatment x block ANOVA, no main effect of treatment: $F_{(1, 8)}$ = 0.055, n.s.), though an overall ANOVA did not reveal a significant three-way interaction of treatment, genotype, and block ($F_{(4, 154)}$ = 0.47, n.s.), or a genotype x treatment interaction ($F_{(1,32)}$ = 0.61, n.s.), likely due to the relatively low WT rat group size. In WT rats, CNO had no effect on total omissions (**Fig 17F**, treatment: $F_{(1, 8)}$ = 0.60, n.s.), total rewards obtained (treatment: $F_{(1, 8)}$ = 0.044, n.s.), or latency to press for either large/risky (**Fig 17D**, treatment: $F_{(1, 77)}$ = 2.68, n.s.) or small/safe rewards (**Fig 17E,** treatment: $F_{(1, 77)}$ = 0.91, n.s.), though no significant genotype x treatment x block interactions were detected for these variables (p > 0.05).

CNO also failed to alter FR1 responding for palatable pellets in either food-deprived (**Fig 19E**, active vehicle versus CNO: t_5 = 0.036, n.s.; inactive: t_5 = 1.04, n.s.) or sated WT rats (**Fig 19F**; active: t_5 = 1.01, n.s.; inactive: t_5 = 1.04, n.s.), and a significant genotype x treatment

interaction further demonstrate this DREADD-specific effect in sated rats (genotype x treatment interaction; active lever: $F_{(1, 14)} = 5.70$, $p = 0.032$), though not significantly so for food-deprived ones (genotype x treatment interaction; active lever: $F_{(1, 14)} = 1.89$, n.s.). Progressive ratio responding for palatable pellets was also unaffected by CNO in WT rats (**Fig 20D-E**, breakpoint: $t_{16} = 0.63$, n.s.; active nosepokes: $t_{16} = 0.54$, n.s.; inactive nosepokes: $t_{16} = 0.59$, n.s.), as was spontaneous M&M consumption (**Fig 20F**, $t_5 = 0.41$, n.s.). A significant genotype x treatment interaction was found for breakpoint on the progressive ratio task (genotype x treatment interaction breakpoint: $F_{(1, 37)} = 4.49$, $p = 0.041$), but this was not significant for spontaneous M&M consumption (genotype x treatment interaction: $F_{(1, 16)} = 1.11$, n.s.). Likewise, CNO in WT rats did not impact general locomotion (vehicle m = 13621 ± 2580 cm, CNO m = 16768 ± 3039 cm, $t_5 = 1.02$, n.s.) or rearing (vehicle m = 197.8 ± 29.7 rears, CNO m = 174 ± 26.7 rears, $t_5 = 0.56$, n.s.), and the genotype x treatment interactions were also non-significant (locomotion: $F_{(1, 16)} = 0.40$, n.s.; rearing: $F_{(1, 16)} = 0.42$, n.s.).

Shock-related behaviors were also largely unaffected in WTs by CNO, including motor reactions to shock (**Fig 22B**, treatment: $F_{(1, 33)} = 0.85$, n.s.), maximum shock intensity tolerated (vehicle: m = 0.22 ± 0.012; CNO: m = 0.21 ± 0.019; $t_4 = 1.0$, n.s.), avoidance propensity (**Fig 21D**, change from baseline avoidance%: vehicle day raw percentage: m = 42.08 ± 10.73, CNO day raw percentage: m = 28.96 ± 9.07, t_6=1.54, n.s.), or avoidance latency (**Fig 21E**, $t_6 = 0.064$, n.s.), though raw avoidance% was modestly decreased by CNO in WT rats ($t_6 = 2.9$, $p = 0.027$). No significant genotype x treatment interaction was found for either avoidance propensity ($F_{(1, 16)} = 0.0002$, n.s.) or avoidance latency ($F_{(1, 16)} = 1.79$, n.s.). Both 22 kHz (aversion-related) and > 30 kHz (positive affect-related) USVs were unchanged by CNO in WT rats (**Fig 22C**, % of vehicle day USVs, compared to 100% with one sample *t*-test, 22kHz: $t_4 = 1.0$, n.s.; > 30 kHz: $t_4 = 0.96$, n.s.). CNO in WT rats trended towards increasing latency to escape (**Fig 21F**, $t_6 = 2.2$, $p = 0.07$), though no genotype x treatment interaction was found ($F_{(1, 16)} = 0.14$, n.s.).

Discussion

Here we show that VP^{GABA} neurons play a fundamental role in high-stakes motivation, and thereby affect risky decision-making strategies. Engaging $G_{i/o}$ signaling in VP^{GABA} neurons with DREADDs interfered with both operant pursuit of desirable foods, as well as operant response to cancel an impending shock. In contrast, VP^{GABA} neurons play no apparent role in pursuit of less valuable food, in spontaneous food consumption, or in affective responses to shock itself. This selective VP^{GABA} neuron involvement in motivated operant responding may therefore extend beyond the pursuit of rewards, into avoidance of harm. Accordingly, when both opportunity and risk are present (as is usually the case in the natural world), VP^{GABA} inhibition biased decision making toward a more conservative, risk-averse strategy. Collectively, these results show that VP^{GABA} neurons crucially influence high-stakes decision making, and thus likely contribute to both the normal desires of life, and to darker pursuits in those with disorders of impaired judgement like addiction.

VP^{GABA} neuron inhibition promotes conservative decision making by suppressing motivation.

In a risky decision making task, chemogenetically inhibiting VP^{GABA} neurons promoted selection of a small but safe option over a large but risky one, without impairing the ability to discriminate between rewards of different magnitudes. VP^{GABA} inhibition also increased trial omissions and decreased the number of rewards obtained in the presence or absence of shock—consistent with decreased motivation for food. Similar increases in latency and omissions have been shown following optogenetic inhibition of all VP neurons in operant assays of sucrose seeking (Richard et al., 2016). Yet VP^{GABA} inhibition effects were not merely motivational in nature—food seeking was not indiscriminately suppressed. Instead, VP^{GABA} inhibited rats shifted more readily to a small but safe reward option, avoiding the large but risky one, even when the risk of shock was relatively low. Moreover, when rats did select the large/risky choice, VP^{GABA} inhibition caused them to deliberate longer—an effect which was not present on trials when the small/safe option was chosen. In contrast, when VP^{GABA} neuron inhibition occurred in a low stakes (no shock) version of the task, no such effects on choice

latency were seen. In other words, inhibiting VP^{GABA} neurons seemed to selectively promote a more conservative, risk-averse decision-making strategy by suppressing appetitive motivation.

Of course, VP does not act alone to influence risky choice, but rather within wider mesocorticolimbic circuits that integrate motivational states with encountered opportunities and threats, in pursuit of generating maximally adaptive behavior under motivational conflict. Indeed, numerous brain regions contribute to risky decision making in rats, including prefrontal cortices, BLA, LHb, VTA, and NAc (Floresco et al., 2008; Orsini et al., 2015b). Notably, lateral orbitofrontal cortex lesions have similar effects on latency and propensity to make risky choices as VP^{GABA} neuron inhibition did here (Orsini et al., 2015a), implying functional, if not direct anatomical interactions between these structures (Simmons et al., 2014). Interestingly, activating D2 DA receptors in VP's largest afferent input, the GABAergic NAc, similarly promotes risk-averse behavior in adolescent rats (Mitchell et al., 2014). Though infusion of a D2 agonist in NAc would likely disinhibit (excite) VP neurons (Gallo et al., 2018), paradoxically we find here that *inhibiting* VP^{GABA} neurons with DREADDs causes a similarly risk-averse phenotype. Reconciling these findings is an important future direction, and could involve experience-related plasticity in D1 (i.e. "direct pathway") versus D2 (i.e. "indirect pathway") inputs from NAc (Kupchik et al., 2015; Creed et al., 2016; Heinsbroek et al., 2017; O'Neal et al., 2019), differences between adolescent and adult decision making processes (Spear, 2000), currently-unknown specificity of NAc inputs to VP cell subpopulations (e.g., glutamate versus GABA), or potentially non-NAc inputs to VP that may influence reward-seeking decisions (Richard et al., 2016; Ottenheimer et al., 2018).

Role for VP^{GABA} neurons in seeking high value food, without affecting food consumption.

Having found that VP^{GABA} neuron perturbation stifled risky choice, we next sought to determine how inhibiting these neurons impacts "pure" tests of food seeking and intake, in the absence of potential harm. VP's role in food ingestion and hedonics has been known for decades (Morgane, 1961; Stratford et al., 1999; Castro et al., 2015), though how VP neuronal

subtypes participate in this was unclear. Here, we show that chemogenetically inhibiting VP^{GABA} neurons suppresses operant pursuit of high-value foods like palatable pellets under both low and high effort conditions. In contrast, pursuit of less palatable chow was affected by VP^{GABA} inhibition only when this food was valued because rats were hungry. These results suggest that VP^{GABA} neurons selectively promote seeking of high-value rewards, regardless of whether value is instantiated by the inherent palatability of the food, by the presence of hunger, or by the necessity to pay a cost such as effortful responding, or potential for shock.

Interestingly, whereas inhibiting VP^{GABA} neurons decreased operant pursuit of valuable food rewards, it did not impair spontaneous consumption of palatable chocolate, suggesting that these neurons mediate instrumental *seeking* of high value rewards, but not necessarily *consumption* of the reward, once obtained. Neurobiological dissociation between seeking and consumption has been previously shown within ventral striatal networks (Berridge and Robinson, 2003). For example, intra-NAc DA antagonism diminishes operant reward seeking, but leaves reward consumption unimpaired (Kelley et al., 2005; Salamone and Correa, 2012). Similarly, inhibiting VP impairs conditioned food or salt seeking, without impacting unconditioned consumption of these rewards (Farrar et al., 2008; Chang et al., 2017). Our results extend these findings, showing that VP^{GABA} neurons in particular are required for pursuit, but not consumption of food. This said, VP stimulation with opioid agonist or GABA antagonist drugs robustly increases chow consumption, and opioid drugs also enhance hedonic reactivity to sweet tastes (Smith and Berridge, 2005, 2007). In addition, VP lesions suppress all food intake, and lesioned animals will starve without forced feeding (Cromwell and Berridge, 1993). Given these findings, the present results could suggest lack of VP^{GABA} neuron involvement in these consummatory effects, or they could be a product of mechanistic differences between DREADDs and lesions, or other unknown factors.

VP^{GABA} neurons and appetitive versus aversive motivation.

A recent surge of studies suggest that VP^{GABA} neurons promote appetitive behavior and reward, whereas intermingled VP glutamate neurons instead mediate behavioral withdrawal and aversion. For example, VP^{GABA} neurons fire in response to water rewards and their predictors in mice, especially when those rewards are particularly valuable due to thirst (Stephenson-Jones et al., 2020). Optogenetic activation of mouse VP^{GABA} neurons elicits food intake and operant water seeking (Zhu et al., 2017; Stephenson-Jones et al., 2020) and is reinforcing (Zhu et al., 2017; Faget et al., 2018), while optogenetic stimulation of VP glutamate neurons elicits aversive responses and promotes operant avoidance (Faget et al., 2018; Tooley et al., 2018; Levi et al., 2019; Stephenson-Jones et al., 2020)—though a recent report suggests that VP glutamate neurons may mediate salience irrespective of valence (Wang et al., 2020). None of these prior mouse studies indicated a role for VP^{GABA} neurons in aversive motivation, but they did not examine more complex types of aversive responding.

To address the function of VP^{GABA} neurons further, we examined the contribution of VP^{GABA} neurons to shock-induced affective responses, and to instrumental responding to avoid or escape shocks. Inhibiting VP^{GABA} neurons failed to impact shock-induced motor reactions or ultrasonic vocalizations, suggesting that these cells do not mediate aversion *per se*. However, when rats were trained to press a lever either to avoid an impending shock or to escape an ongoing one, DREADD inhibition revealed a hidden role for VP^{GABA} neurons in aversive motivation. Specifically, the latency to press a lever in order to cancel an impending shock was increased by VP^{GABA} inhibition, while latency to press to escape an ongoing shock was unaffected. Together, these data show that VP^{GABA} inhibition affected neither affective reactions to shock itself, nor the ability of an ongoing shock to induce escape responses. Instead, VP^{GABA}-inhibited rats simply appeared to less urgently avoid impending punishment (though the proportion of trials escaped versus avoided was not altered). This increase in avoidance latency represents a departure from the common notion that VP^{GABA} neurons are solely implicated in appetitive behavior. Rather, these neurons seem instead to facilitate high-stakes instrumental

behavior of many types. This said, we note that when rats pressed to avoid footshock, they also received a 20 s signal indicating freedom from impending threat. It is therefore possible that DREADD inhibition did not impact aversive motivation itself, but instead reduced the conditioned reinforcing properties of this safety signal (Fernando et al., 2014). Dissociating avoidance of harm from pursuit of safety is famously difficult (LeDoux et al., 2017; Sangha et al., 2020), so further work is needed to disambiguate this newly-discovered role for VP^{GABA} neurons in aversive motivation.

Specificity of effects.

We found very little evidence of non-selective effects of CNO in WT rats without DREADDs. In the absence of DREADDs, CNO can have off-target behavioral effects in some experiments (MacLaren et al., 2016; Gomez et al., 2017; Manvich et al., 2018). Yet across the numerous behaviors tested here, we identified only a trend towards an increase in escape latency in WT rats—indicating predominantly DREADD-specific effects of CNO (Mahler and Aston-Jones, 2018). In addition, although VP is sometimes considered a motor structure (Mogenson et al., 1980; Heimer et al., 1982), it is unlikely that VP^{GABA} DREADD effects were due to nonspecific motoric inhibition. Neither horizontal locomotion nor rearing behavior were affected by engaging VP^{GABA} DREADDs, and behavioral effects were specific to highly-motivated instrumental contexts—other behaviors like spontaneous chocolate intake, and pressing for chow in a sated state were unaffected.

VP DREADD expression was mostly localized within strictly-defined VP borders here, though in most rats at least some expression encroached upon nearby subcortical structures containing GABAergic neurons with important behavioral roles (Koob, 2004; Silberman et al., 2009; Jennings et al., 2013; Barker et al., 2017; Saga et al., 2017; Gordon-Fennell et al., 2020), so we cannot definitively exclude overlapping roles for these neurons in behavioral effects.

Similar to our prior findings (Farrell et al., 2019), we saw no evidence of sex-dependent behavioral effects of chemogenetic VP manipulation, though we also cannot exclude this possibility since studies were not powered to fully explore this variable.

We note that a portion of VP^{GABA} neurons also express other peptides such as parvalbumin and enkephalin, and such co-expression may have functional implications. For example, VP parvalbumin neurons, which consist of both GABAergic and glutamatergic neurons, are necessary for both alcohol seeking and depression-like behavior (Knowland et al., 2017; Prasad et al., 2020). Moreover, VP^{GABA} neurons that co-express enkephalin drive cue-induced cocaine seeking (Heinsbroek et al., 2019). A significant portion of these VP subpopulations also express GABA markers, though others are glutamatergic. Since VP glutamate and GABA neurons have dissociable roles in behavior (Faget et al., 2018; Tooley et al., 2018; Stephenson-Jones et al., 2020), further work is needed to parse the relative functional roles played by VP cells expressing GABA, glutamate, various co-expressed proteins, and combinations thereof.

Conclusion.

These results demonstrate an essential role for VP^{GABA} neurons in high-stakes motivated behavior—be it to pursue valued rewards, to avoid impending harm, or to make important decisions when motivations are mixed. We show for the first time that VP^{GABA} neurons' role in motivation impacts decision making, since inhibiting these cells yields a conservative, risk-averse decision-making strategy rather than a simple decrease in all reward seeking. If successfully harnessed therapeutically, we speculate that suppressing VP^{GABA} neuron activity might be useful for treating addiction, or other disorders of maladaptive, risky decision making.

General Discussion

The overall results of this dissertation show a key role for VP^{GABA} circuits in guiding appetitive motivated behavior when weighing costs and benefits of choices. Our results are generally consistent with the notion that VP^{GABA} neural activity is related to whether a goal is worth pursuing. Indeed, inhibiting largely VP^{GABA} neurons reduces reinstatement for cocaine and remifentanil, and, consistently, decreases effortful exertion for food reward as well as the amount of risk worth tolerating to pursue a large/risky food reward. In contrast, stimulating VP^{GABA} neurons instead strongly augments a rat's willingness to pursue remifentanil, even in a 'dangerous' context in which it had received footshock for taking drug. These results collectively highlight that VP^{GABA} neurons are critical for sustaining motivated effort to pursue rewards, and perhaps in weighing costs and benefits associated with particular decisions. Such a function positions VP to control the deployment of cognitive resources to overcome obstacles, pursue goals in the face of adversity, and weigh whether a goal is worth pursing in the first place. These features are at the heart of what drives us forward in the world.

But many important open questions remain. I dedicate the rest of my dissertation to addressing some of these important questions and use my own work to contextualize these issues. The main topics of focus are as follows: 1) how we as a field might improve preclinical relapse models, 2) discuss emerging ideas about VP circuit function in motivated behavior, and 3) examine how better understanding neural circuits through chemogenetic (and other) approaches may improve treatment options for psychiatric disorders in the future.

Improving relapse models in rodents. Self-administration-based reinstatement models have remained the go-to behavioral model for dissecting the neural circuits of relapse-like behavior. This approach teaches rats to perform an operant response (e.g., lever press) for intravenous infusion of a drug, often accompanied by a light and tone cue as outlined above (Farrell et al., 2019; Farrell et al., 2022). After stable responding is achieved, rats are subjected to extinction training in which operant responses no longer deliver the drug or cues associated with drug use.

After extinction training, rats undergo reinstatement sessions in which they are exposed to drug-associated cues or contexts, stressors, priming doses of the drug itself, or a combination thereof. Quantifying the levels of operant seeking in the absence of the drug itself operationalizes ‘relapse’.

Cues, stressors, or priming doses precipitate relapse in humans, and, analogously, precipitate reinstatement in preclinical models. However, extinction (as occurs in preclinical models) rarely occurs in humans during the transition to abstinence. This stark difference between the way in which abstinence occurs in preclinical models and the human condition might constrain the translatability of preclinical models. For this reason, we and other have developed reinstatement models that better capture motivational conflict that arises when a person decides to quit using drugs (Marchant et al., 2013a; Farrell et al., 2018; Reiner et al., 2019; Venniro et al., 2020; Fredriksson et al., 2021). In such models, abstinence is initiated by mutually exclusive choice between drug and an alternative reinforcer such as food or access to a social partner. Or, as in our model, by exposure to negative consequences (e.g., footshock) contingent on drug infusion. Such punishment-based models attempt to capture how potential negative consequences sculpt decision making processes in the context of addiction, and we and others have argued that such models might be better suited for developing novel therapeutics (Farrell et al., 2018).

Our model builds on prior work investigating the ability of aversive consequences to constrain drug seeking. Prior work has employed electrified floors in front of drug-associated operant manipulanda (Cooper et al., 2007), footshock-associated conditioned stimuli (Vanderschuren and Everitt, 2004), footshock itself (Deroche-Gamonet et al., 2004; Marchant et al., 2013b; Pelloux et al., 2018b; Farrell et al., 2019; Farrell et al., 2022), or bitter adulterants in the case of liquid drug rewards (Wolffgramm, 1991; Siciliano et al., 2019). Such models can probe individual differences in punishment-resistance, which represents the willingness of an animal to undergo realized or potential negative consequences to continue drug use. Persistent

drug use despite adverse consequences is, indeed, a hallmark of the human condition (American Psychiatric, 2013), and is interesting to consider what behavioral or neurobiological differences might contribute to the punishment-resistant phenotype. Punishment-resistant rats can be identified behaviorally based on individual differences in the degree of pre-cocaine voluntary exploration of a novel environment (Belin et al., 2011), impulsivity in the 5-choice serial reaction time task (Economidou et al., 2009), or the pattern of cocaine intake during initial self-administration training (Belin et al., 2009).

Behavioral metrics like those mentioned above (e.g., impulsivity, exploration) can predict which rodents will become punishment resistant. What neurobiological features may underlie such addiction-like drug seeking? Seminal work demonstrated that punishment-resistant rats (who sought cocaine despite footshock), relative to punishment-sensitive rats, exhibited decreased *ex vivo* intrinsic excitability of medial prefrontal cortex (mPFC) pyramidal neurons (Chen et al., 2013). Acutely reversing this hypoactive mPFC state *in vivo* via optogenetics reversed the behavioral phenotype—turning punishment-resistant rats into punishment-sensitive rats. Consistently, mPFC activity in mice during their first alcohol exposure predicted which animals would develop punishment-resistant drinking behavior (Siciliano et al., 2019). These and other neurobiological findings (Goldstein and Volkow, 2011; Kasanetz et al., 2013; Hu et al., 2019) concerning mPFC's role in addiction-like behavior have informed non-invasive neurostimulation-based approaches targeting mPFC for treatment of addiction (Diana et al., 2017). Exploring other neural circuits that might be preferentially engaged in animals exhibiting addiction-like behavior might result in more circuit targets for intervention in people with addiction.

Along these lines, my work showed that in rats that were relatively punishment resistant (ie, tended to seek cocaine despite contingent footshock), displayed the most pronounced decrease in seeking upon chemogenetic inhibition of VP neurons (Farrell et al., 2019). Moreover, chemogenetically stimulating VP^{GABA} neurons robustly augmented remifentanil

seeking even in the ‘dangerous’ context, in which rats had previously received footshock for taking drug (Farrell et al., 2022). These results are consistent with the idea that VP^{GABA} neurons are important for driving addiction-like behavior despite adverse consequences—a hallmark of addiction in humans. Such punishment-based models might, therefore, facilitate understanding the neural circuits that promote *pathological* drug seeking despite potential adverse consequences, including VP^{GABA} neurons. Future work ought to parse the contribution of VP^{GABA} neurons and their connected circuits in generating compulsive, punishment-resistant drug seeking.

Despite much evidence implicating various neural circuits in reinstatement in rats, we are far from understanding how these circuits function in human addiction and relapse. Conventional reinstatement models capture some of the overt characteristics of the addiction/relapse cycle, including voluntary drug use, cessation of drug taking, and resumption of drug use precipitated by similar stimuli to those eliciting relapse in humans. However, many details differ between the situations experienced by experimental animals in these studies and those experienced by recovering addicted individuals, potentially hindering our ability to map circuit/behavior relationships across species (Epstein et al., 2006, Torregrossa and Taylor, 2013). For this reason, as mentioned, we and others have implemented models that capture how negative consequences impact drug intake, putatively better mirroring the human condition. However, multiple questions remain about whether these newer models bring the field closer to treatment development.

Development of models that incorporate negative consequences coincident with drug taking have improved the face validity of the reinstatement model. Indeed, humans often quit using drugs of abuse due to mounting negative consequences and footshock is intended to mirror negative consequences that humans may experience because of drug use. However, in humans, consequences are typically not contingent on drug use, but instead might arise far in the future (e.g., financial ruin, future health risks). Whether the nature of contingent footshock in

rats engages comparable neural circuits to those engaged in humans considering these far future consequences remains to be seen. Future work might incorporate delayed negative consequences (e.g., delayed footshock) to assess whether future consequences associated with drug use might impact addiction-relevant neural circuits. Indeed, such disregard of future negative consequences and myopia on current drug seeking and use in humans is a critical component of the addiction process.

VP circuit function and motivated behavior: Where we are and where we're going. Much work in recent years has begun illuminating the circuit and computational principles by which VP operates to support adaptive behavior. Indeed, technological developments in systems, molecular, and computational neuroscience have allowed unprecedented access to the functional diversity of VP cell types in across motivated behaviors. Here I will contextualize my findings concerning VP^{GABA} neurons' role in motivated behavior with recent developments in understanding of VP circuitry and cell types across species, with an emphasis on how the idea of cell types provides an important lens through which we understand neural circuits.

VP was once considered a key neural node involved in translating motivational information into motor output (Mogenson et al., 1980). However, VP now is generally considered a motivational hub, and not a simply relay node to downstream motor effectors. One key aspect of VP circuitry that informs understanding its function is that of cell types. While in this dissertation I largely focus on neurotransmitter-defined VP^{GABA} neurons, the neurotransmitter released from a particular cell is only one way in which we can distinguish cell types. Much recent work has even illuminated the capacity of neurons to release multiple distinct types of neurotransmitter/neuromodulators (Seal and Edwards, 2006; Hnasko and Edwards, 2012; Tritsch et al., 2016), including in VP (Faget et al., 2018). Electrophysiological properties, connectivity with up- or downstream brain regions, transcriptomic profile, expression of particular proteins, morphological characteristics, and location within VP borders all constitute complementary ways to parse neural networks in order to better understand their function.

Indeed, VP's function appears to depend upon projection targets (Mahler et al., 2014; Faget et al., 2018; Pribiag et al., 2021), protein expression (Knowland et al., 2017; Prasad et al., 2019; Heinsbroek et al., 2020), rostrocaudal or mediolateral anatomical location (Smith and Berridge, 2007; Mahler et al., 2014), or a combination thereof (Root et al., 2015).

While each of these facets of VP function is relevant for understanding its function, the neurotransmitter released from VP in downstream targets appears particularly relevant. While histological experiments demonstrated the existence of GABAergic, glutamatergic, and cholinergic cells in VP, only recently have systems neuroscience been able to selectively target these cell types to understand their function. VP^{GABA} neurons constitute ~70-80% of cells in VP with a minority expressing glutamatergic (~15%) and cholinergic (~10%) markers. We and others have demonstrated that a minority of GABAergic cells also express glutamatergic markers, highlighting that individual cells may have the capacity to co-release both excitatory and inhibitory neurotransmitters (Faget et al., 2018; Farrell et al., 2019; Farrell et al., 2021). While such co-release is an exciting motif found in diverse neural circuits, the importance of this minority population in VP and surrounding basal forebrain regions remains largely unclear. Nonetheless, a surge of recent studies has revealed largely opposing role for VPGABA and glutamate neurons, with the former promoting appetitive motivation and the latter supporting aversive motivation (Faget et al., 2018; Tooley et al., 2018; Heinsbroek et al., 2020; Stephenson-Jones et al., 2020). Interestingly, VP^{GABA} and glutamatergic neurons display similar projection profiles, sending projections to multiple downstream nodes including subthalamic nucleus, VTA, LHb, MD, lateral hypothalamus, and substantia nigra pars reticulata among other regions. Such similar projection patterns lead to the idea that these cells might compete locally or in downstream targets in a push-pull manner, though much work must be done to understand such network connectivity and related functional implications.

Our results are largely in accordance with the notion that VP^{GABA} neural activity encodes and promotes appetitive motivation. In our hands, pan-neuronal inhibition of VP neurons (which

targeted largely GABAergic cells) strongly decreased cocaine seeking following punishment-induced abstinence in a model of cocaine relapse. Specifically, we found that chemogenetically inhibiting VP neurons suppressed cue- and context-induced reinstatement in the 'safe' context in which rats had never received footshock (Farrell et al., 2019), especially in those rats that are relatively punishment resistant (ie, continue taking cocaine despite footshock). While our DREADD manipulations here were not GABA-neuron specific, *in situ* hybridization revealed that hM4Di-expressing neurons were largely GABAergic, consistent with the predominant population of GABAergic cells in VP. These results demonstrate that inhibiting largely VP^{GABA} neurons can potently suppress appetitive cocaine-seeking behavior after punishment-induced abstinence—building upon prior work showing that VP circuits are key for drug-seeking after explicit extinction training (McFarland and Kalivas, 2001; McFarland et al., 2004; Mahler et al., 2014; Prasad et al., 2019; Prasad and McNally, 2020).

My subsequent work employed GAD1:Cre transgenic rats in combination with Cre-dependent excitatory (hM3Dq) and inhibitory (hM4Di) DREADDs to selectively target VP^{GABA} neurons. While a large body of work has accumulated investigating VP's role in cocaine seeking, its role in seeking of opioid drugs is less well understood. VP is embedded within neural circuits in which opioid signaling plays a critical role in hedonic impact of rewards and appetitive motivation, yet the function of VP^{GABA} neurons in opioid seeking was unexplored. Using a similar punishment-induced abstinence model as employed previously (Farrell et al., 2019), we found that chemogenetically inhibiting VP^{GABA} neurons suppressed seeking of the potent μ opioid receptor agonist, remifentanil, after punishment-induced abstinence (Farrell et al., 2022). On the other hand, stimulating VP^{GABA} neurons strongly potentiated remifentanil seeking, even in the context that was previously coupled with footshock—a key finding given that a hallmark of drug addiction is seeking drug despite potential adverse consequences (American Psychiatric, 2013). Stimulating VP^{GABA} neurons similarly increased remifentanil reinstatement following extinction training, suggesting that VP^{GABA} neuron stimulation can

enhance motivation for drug irrespective of whether rats underwent voluntary, punishment-induced abstinence or extinction. Effects of VP^{GABA} neuron stimulation and inhibition were specific to opioid *seeking* rather than opioid *taking*, since neither manipulation impacted remifentanil self-administration. These findings are consistent with the notion that VP^{GABA} neurons promote appetitive motivation for desirable rewards, and further expand upon our understanding by implying a role for VP^{GABA} neurons in promoting motivation despite potential adverse consequences.

While chemogenetically stimulating VP^{GABA} neurons robustly enhances remifentanil reinstatement, how might endogenous VP circuit function impact addiction-like behavior? To address this, we further asked whether VP neurons were activated in response to cocaine- (Farrell et al., 2019) or remifentanil-associated cues (Farrell et al., 2022). Specifically, we were interested in examining neural activity in distinct mediolateral and rostrocaudal VP subregions, which exhibit distinct input and output connectivity and are differentially involved in reward-associated behaviors (Smith et al., 2009; Root et al., 2010; Root et al., 2013; Mahler et al., 2014). For our cocaine experiments, we found that VP neurons, irrespective of their rostrocaudal or mediolateral location, were robustly recruited by cocaine-associated cues and contexts, as measured by Fos immunohistochemistry. This VP neuronal recruitment extended to the punishment-associated context, in which rats had previously received footshock punishment for taking cocaine. Similarly, we observed broad activation of VP neurons across rostrocaudal VP in both in both footshock- and non-fooshock-associated contexts. Notably, however, opioid reinstatement was positively correlated only with Fos in rostral, but not caudal, VP. These results collectively mirror prior findings from our group and others (Mahler et al., 2014), yet a key open question is whether animals that exhibit an addiction-like phenotype exhibit greater VP activation in response to drugs of abuse or their predictors. Inhibiting VP neurons suppressed cocaine seeking to the greatest extent in punishment-resistant rats—however, this leaves open the critical question of whether endogenous VP dynamics are

coupled with addiction-like behavior. More work ought to be conducted to understand the extent to which VP circuits are selectively recruited in compulsively drug-seeking animals, and, ultimately, people with addiction.

We were further interested in pursuing the idea that VP^{GABA} neurons are important for the decision-making process when appetitive and aversive motivational tendencies compete for behavioral control. To do so, we implemented a model based on prior work from Barry Setlow's group (Simon et al., 2009; Orsini et al., 2015b), in which rats select between a large/risky and small/safe food reward option. This task pits reward seeking and harm avoidance tendencies against each other. We uncovered that inhibiting VP^{GABA} neurons suppressed seeking of the large/risky option. Even when rats selected the large/risky option, they did so with a longer latency than their counterparts with intact VP^{GABA} neuron function. These results support the idea that VP^{GABA} neurons are critical for overcoming potential adverse consequences in decision-making scenarios.

Our results further suggest that VP^{GABA} neuron inhibition decreases motivation in general. Indeed, inhibiting VP^{GABA} neurons decreased participation in the risky decision task, as demonstrated by an increase in the number of trial omissions. Moreover, in the absence of potential footshock punishment, we showed that inhibiting VP^{GABA} neurons suppressed high-effort progressive ratio responding as well as low-effort FR1 responding for palatable food. Interestingly, the satiety state of the rat was a critical determinant of VP^{GABA} neuron effects since we observed that inhibiting VP^{GABA} neurons only suppressed operant chow seeking when rats were hungry, but not when they were sated. Such effects on appetitive food motivation are in accordance with much prior literature pinpointing VP as a key region associated with incentive motivation (Smith and Berridge, 2007; Smith et al., 2011; Tachibana and Hikosaka, 2012; Richard et al., 2016; Richard et al., 2018). However, inhibiting VP^{GABA} neurons failed to impact food consumption since this manipulation failed to influence free palatable chocolate intake when it was freely available. Therefore, collectively it appears that chemogenetic VP^{GABA}

neurons inhibition results in food and drug *seeking*, rather than food or drug *consumption* (Farrell et al., 2021; Farrell et al., 2022). Such results are generally at odds with the notion that VP is a critical element of feeding behavior in general, though many of the experiments supporting this idea performed non-GABA neuron specific pharmacological or lesion manipulations (Smith et al., 2009; Castro et al., 2015). One hint that may reconcile the seeking/consumption dissociation is the fact that VP^{GABA} neurons project to distinct downstream targets. Indeed, recent work has demonstrated that suppression of ventral pallidostriatal ('arkypallidal') are permissive of consumption, and potentially suppresses ongoing seeking (Vachez et al., 2021). Further dissection of these projection-specific VP^{GABA} neuron subpopulations will be necessary to deepen our understanding of seeking versus consummation in ventral basal ganglia networks.

Inhibiting VP^{GABA} neurons suppressed risky decision making in the presence of potential adverse consequences and appetitive motivation in the absence of such consequences—does inhibiting VP^{GABA} neurons also impact aversive motivation or the perception of harm? Two affective readouts of sensitivity to footshock revealed that inhibiting VP^{GABA} neurons failed to influence either motor reactivity to shock or footshock-evoked ultrasonic vocalizations, suggesting that VP^{GABA} neurons might not be critical elements of aversive reactions to harm. However, we uncovered hints that VP^{GABA} neuron inhibition does impact aversive *motivation*, rather than aversive affective responses. Though inhibiting VP^{GABA} neurons failed to impact the percentage of avoidance responses emitted during a footshock avoidance/escape model, we did find that rats took longer to lever press to avoid footshock. Longer latency/decreased task participation is a hallmark of inhibiting VP in appetitive tasks, but this, to our knowledge, is the first demonstration of slowed response times in an aversive motivation task resulting from VP^{GABA} perturbations. Thus, this provides a hint that VP^{GABA} neurons might be involved in both avoidance and reward seeking more generally, though future work ought to explore VP's role

more specifically in aversive tasks that tap into dissociable psychological processes (e.g., fear conditioning, active avoidance, inhibitory avoidance).

My work collectively shows that VP itself is not selectively recruited when potential negative consequences are present. For example, I showed that VP neural activity (measured by Fos) is increased during remifentanil reinstatement irrespective of whether reinstatement testing occurred in the 'safe' Context A or the punishment-associated Context B. If it were the case that VP neurons were selectively recruited to overcome potential consequences, we likely would have seen greater Fos in the punishment-associated context. Consistently, inhibiting VP^{GABA} neurons not only decreased choice of a large/risky option, but also generally decreased appetitive motivation in the absence of potential harm. Thus, it appears that VP^{GABA} neurons are critical for appetitive motivation for food or drugs of abuse more generally, rather than playing a specific role in reward seeking despite adverse consequences.

Activity of VP^{GABA} neurons are likely necessary for overcoming obstacles, potential consequences, or effort requirements. Such incentive motivational properties of VP, and its GABAergic neurons therein, scale with the incentive value of reward-associated cues depending on the internal state of the animal. If the incentive value is high, either due to close reward proximity or an internal need state (e.g., hunger, craving), then an animal ought to be willing to overcome potential negative consequences or other obstacles and engage in reward seeking actions. If, however, incentive value is low, potential negative consequences will instead constrain reward seeking, limiting the exertion of effort or willingness to overcome potential harm. Indeed, my work illustrates that VP^{GABA} neurons are a primary contributor to incentive motivation, building on the shoulders of much work examining VP's role in reward and motivation (Smith et al., 2009).

Understanding neural circuits to improve psychiatric treatment: Chemogenetics as tool or potential treatment? Two main goals of behavioral neuroscience are: 1) to understand how the brain generates behavior and 2) intervening in brain operation to treat neuropsychiatric

disorders. Ideally, there exists bidirectional information flow between these two goals such that understanding yields new treatments, and, potentially, that treatments can inform understanding. For example, understanding the basic functional organization of basal ganglia circuits prompted the idea that electrically stimulating subthalamic nucleus might effectively treat Parkinson's disease (Benabid et al., 2009). On the other hand, serendipitous discoveries like the utility of chlorpromazine for the treatment of psychotic disorders revealed something about the neurochemical basis of schizophrenia (Ban, 2007). Similarly, the efficacy of selective serotonin reuptake inhibitors for treatment of depression demonstrated that depression might in part result from serotonergic dysfunction (Vaswani et al., 2003). These examples highlight this bidirectional relationship in the goals of behavioral neuroscience—treatments can inform understanding the nervous system and understanding the nervous system can inform treatments.

The technology of chemogenetics (and optogenetics) exists at the crossroads of understanding the nervous system and functioning as a potential therapeutic. Chemogenetics represents an approach that uses engineered receptor proteins designed to initiate signal transduction based on binding to an otherwise inert ligand (Sternson and Roth, 2014; English and Roth, 2015; Roth, 2016). Application of chemogenetic technology, largely using DREADDs (Armbruster et al., 2007), has yielded unprecedented insights into the function of cell- and pathway-specific neural circuits in preclinical models of addiction (and behavioral neuroscience more generally) (Smith et al., 2016). The work presented throughout this dissertation is illustrative of such advances. However, a question that naturally arises from this work and the work of others is whether chemogenetic technology could be itself therapeutically applied, rather than serve merely as a preclinical tool.

Psychiatric disorders arise from a complex interaction among multiple levels of analysis including the social, psychological, and neurobiological, and such disorders are generally treated via psychotherapy, medication, or a combination thereof. Although effective for treating

psychiatric disorder in some, psychiatric medication is by no means a panacea and is often coupled with negative side effects. One reason for the relative ineffectiveness of pharmacotherapies is that such approaches are neurobiologically blunt tools. Psychiatric drugs are often promiscuous, interacting with multiple targets distributed throughout the CNS and the periphery. Even with the advent of exquisitely selective pharmacological compounds (Roth et al., 2017), it seems unlikely that psychiatric disorders would result from dysfunction in a particular neurotransmitter system, receptor, or protein target.

The question then is in what sense is a chemogenetic approach might be better than traditional pharmacotherapeutics. An inherent limitation of pharmacological approaches is that they bathe the entire brain with medication, despite the profound heterogeneity of neural circuitry. Ubiquitous receptor expression throughout the brain (e.g., serotonin, DA receptors) suggests that such pharmacological approaches target circuits for their therapeutic benefits, but spill over into other circuits that may produce unwanted side effects. Chemogenetics, and other circuit-targeted approaches, affords a potential solution to this problem by delivering therapeutic stimulation only to relevant neural circuits and cell types, thus potentially limiting off-target side effects. Chemogenetic approaches also afford the ability to target select cell- and pathway-specific cell types, unlike neurostimulation approaches like deep brain stimulation that activate neuronal cell bodies *and* fibers of passage irrespective of cell type (though DBS protocols are being developed to preferentially target specific cell types (Spix et al., 2021)). Indeed, chemogenetic approaches might be considered anatomically-defined cell- and pathway-specific medication, which allows us to incorporate the latest understanding derived from circuit neuroscience in an effort to better treat psychiatric disorders. Beyond gleaning insight about neural circuit function from chemogenetic approaches, much work must be done in the bioengineering space to develop non-invasive chemogenetic delivery methods to target select neural circuits (Szablowski et al., 2018; Challis et al., 2019).

However, the unprecedented advances derived from cell-type and pathway-specific chemogenetic manipulations afforded by modern systems neuroscience tools belies our lack of understanding the computations that neural circuits perform that lead to behavior. For example, much is known about VP and its surrounding brain regions. We have relatively good understanding about its cell types, transcriptomic profile, intrinsic and extrinsic connectivity, electrophysiological profile, and how its stimulation or inhibition impacts behavior. Moreover, this dissertation expanded upon our understanding of VP^{GABA} neurons, and their role in addiction-like and decision-making behavior. However, despite this seemingly deep understanding, relatively straightforward questions remain almost completely opaque. Some of these questions include: How are VP^{GABA} neurons intrinsically/extrinsically wired to support motivation? How might VP handle different types of motivational states? How does the convergence of D1- and D2-MSNs in VP impact computation? What information is relayed to downstream targets via distinct VP cell types? Clearly, much work must be done to better understand VP circuit computations and its contributions to motivated behavior—an goal likely best served by a combination of computational modeling, careful behavioral dissection, and theory-driven circuit monitoring and manipulation.

Conclusion. This dissertation supports the idea that VP^{GABA} neurons are involved in orchestrating adaptive behavior in the context of addiction. I showed that VP^{GABA} neurons are critical in seeking of psychostimulants and opioids across relapse models, and that activity in mediolateral and rostrocaudal VP zones are associated with drug seeking. Moreover, VP^{GABA} neurons are critical for driving appetitive motivation for natural rewards as well as guiding decision making when reward pursuit and harm avoidance compete for control of behavior. Overall, these results support the notion that VP^{GABA} neurons are a critical element involved in generating appetitive motivation to overcome obstacles, potential harm, and effort requirements. While such a capacity is critical to drive us forward in the world, such motivational systems may break down in the case of psychiatric disorders like addiction. Further understanding these

systems will pave the way for developing novel neuroscience-based therapeutics for the treatment of psychiatric disorders in years to come.

References

Ahmed SH, Lenoir M, Guillem K (2013) Neurobiology of addiction versus drug use driven by lack of choice. Current opinion in neurobiology 23:581-587.

Alexander GE, DeLong MR, Strick PL (1986) Parallel organization of functionally segregated circuits linking basal ganglia and cortex. Annual review of neuroscience 9:357-381.

Alheid GF, Heimer L (1988) New perspectives in basal forebrain organization of special relevance for neuropsychiatric disorders: the striatopallidal, amygdaloid, and corticopetal components of substantia innominata. Neuroscience 27:1-39.

Ambroggi F, Ishikawa A, Fields HL, Nicola SM (2008) Basolateral amygdala neurons facilitate reward-seeking behavior by exciting nucleus accumbens neurons. Neuron 59:648-661.

American Psychiatric A (2013) Diagnostic and statistical manual of mental disorders (DSM-5®): American Psychiatric Pub.

Anthony JC, Warner LA, Kessler RC (1994) Comparative epidemiology of dependence on tobacco, alcohol, controlled substances, and inhalants: basic findings from the National Comorbidity Survey. Experimental and clinical psychopharmacology 2:244.

Armbruster BN, Li X, Pausch MH, Herlitze S, Roth BL (2007) Evolving the lock to fit the key to create a family of G protein-coupled receptors potently activated by an inert ligand. Proceedings of the National Academy of Sciences 104:5163-5168.

Austin MC, Kalivas PW (1990) Enkephalinergic and GABAergic modulation of motor activity in the ventral pallidum. Journal of Pharmacology and Experimental Therapeutics 252:1370-1377.

Badiani A, Belin D, Epstein D, Calu D, Shaham Y (2011) Opiate versus psychostimulant addiction: the differences do matter. Nature Reviews Neuroscience 12:685.

Ban TA (2007) Fifty years chlorpromazine: a historical perspective. Neuropsychiatric disease and treatment 3:495.

Barker DJ, Miranda-Barrientos J, Zhang S, Root DH, Wang H-L, Liu B, Calipari ES, Morales M (2017) Lateral preoptic control of the lateral habenula through convergent glutamate and GABA transmission. Cell reports 21:1757-1769.

Beaver JD, Lawrence AD, Van Ditzhuijzen J, Davis MH, Woods A, Calder AJ (2006) Individual differences in reward drive predict neural responses to images of food. Journal of Neuroscience 26:5160-5166.

Belin D, Balado E, Piazza PV, Deroche-Gamonet V (2009) Pattern of intake and drug craving predict the development of cocaine addiction-like behavior in rats. Biological psychiatry 65:863-868.

Belin D, Belin-Rauscent A, Everitt BJ, Dalley JW (2016) In search of predictive endophenotypes in addiction: insights from preclinical research. Genes, Brain and Behavior 15:74-88.

Belin D, Berson N, Balado E, Piazza PV, Deroche-Gamonet V (2011) High-novelty-preference rats are predisposed to compulsive cocaine self-administration. Neuropsychopharmacology 36:569-579.

Benabid AL, Chabardes S, Mitrofanis J, Pollak P (2009) Deep brain stimulation of the subthalamic nucleus for the treatment of Parkinson's disease. The Lancet Neurology 8:67-81.

Bernat N, Campbell R, Nam H, Basu M, Odesser T, Elyasaf G, Engeln M, Chandra R, Golden S, Ament S (2021) Distinct properties in ventral pallidum projection neuron subtypes.

Berridge KC, Robinson TE (2003) Parsing reward. Trends in neurosciences 26:507-513.

Berridge KC, Kringelbach ML (2015) Pleasure systems in the brain. Neuron 86:646-664.

Blanchard DC, Griebel G, Pobbe R, Blanchard RJ (2011) Risk assessment as an evolved threat detection and analysis process. Neuroscience & Biobehavioral Reviews 35:991-998.

Blanchard RJ, Blanchard DC, Weiss SM, Meyer S (1990) The effects of ethanol and diazepam on reactions to predatory odors. Pharmacology Biochemistry and Behavior 35:775-780.

Blanco-Gandía MC, Rodríguez-Arias M (2018) Pharmacological treatments for opiate and alcohol addiction: A historical perspective of the last 50 years. European journal of pharmacology 836:89-101.
Bock R, Shin JH, Kaplan AR, Dobi A, Markey E, Kramer PF, Gremel CM, Christensen CH, Adrover MF, Alvarez VA (2013) Strengthening the accumbal indirect pathway promotes resilience to compulsive cocaine use. Nature neuroscience 16:632.
Bonnet KA, Peterson KE (1975) A modification of the jump-flinch technique for measuring pain sensitivity in rats. Pharmacology Biochemistry and Behavior 3:47-55.
Bossert JM, Marchant NJ, Calu DJ, Shaham Y (2013) The reinstatement model of drug relapse: recent neurobiological findings, emerging research topics, and translational research. Psychopharmacology 229:453-476.
Bossert JM, Ghitza UE, Lu L, Epstein DH, Shaham Y (2005) Neurobiology of relapse to heroin and cocaine seeking: an update and clinical implications. European journal of pharmacology 526:36-50.
Bossert JM, Stern AL, Theberge FRM, Marchant NJ, Wang H-L, Morales M, Shaham Y (2012) Role of projections from ventral medial prefrontal cortex to nucleus accumbens shell in context-induced reinstatement of heroin seeking. Journal of Neuroscience 32:4982-4991.
Bourdy R, Barrot M (2012) A new control center for dopaminergic systems: pulling the VTA by the tail. Trends in neurosciences 35:681-690.
Bouton ME (2019) Extinction of instrumental (operant) learning: interference, varieties of context, and mechanisms of contextual control. Psychopharmacology 236:7-19.
Brudzynski SM (2013) Ethotransmission: communication of emotional states through ultrasonic vocalization in rats. Current opinion in neurobiology 23:310-317.
Burkle H, Dunbar S, Van Aken H (1996) Remifentanil: a novel, short-acting, mu-opioid. Anesthesia & Analgesia 83:646-651.
Caillé S, Parsons LH (2004) Intravenous heroin self-administration decreases GABA efflux in the ventral pallidum: an in vivo microdialysis study in rats. European Journal of Neuroscience 20:593-596.
Caillé S, Parsons LH (2006) Cannabinoid modulation of opiate reinforcement through the ventral striatopallidal pathway. Neuropsychopharmacology 31:804.
Calder AJ, Beaver JD, Davis MH, Van Ditzhuijzen J, Keane J, Lawrence AD (2007) Disgust sensitivity predicts the insula and pallidal response to pictures of disgusting foods. European Journal of Neuroscience 25:3422-3428.
Carelli RM, Ijames SG, Crumling AJ (2000) Evidence that separate neural circuits in the nucleus accumbens encode cocaine versus “natural”(water and food) reward. Journal of Neuroscience 20:4255-4266.
Carlsen J, Záborszky L, Heimer L (1985) Cholinergic projections from the basal forebrain to the basolateral amygdaloid complex: a combined retrograde fluorescent and immunohistochemical study. Journal of Comparative Neurology 234:155-167.
Castro DC, Cole SL, Berridge KC (2015) Lateral hypothalamus, nucleus accumbens, and ventral pallidum roles in eating and hunger: interactions between homeostatic and reward circuitry. Frontiers in systems neuroscience 9:90.
Challis RC, Ravindra Kumar S, Chan KY, Challis C, Beadle K, Jang MJ, Kim HM, Rajendran PS, Tompkins JD, Shivkumar K (2019) Systemic AAV vectors for widespread and targeted gene delivery in rodents. Nature protocols 14:379-414.
Chang SE, Todd TP, Smith KS (2018) Paradoxical accentuation of motivation following accumbens-pallidum disconnection. Neurobiology of learning and memory 149:39-45.
Chang SE, Todd TP, Bucci DJ, Smith KS (2015) Chemogenetic manipulation of ventral pallidal neurons impairs acquisition of sign-tracking in rats. European Journal of Neuroscience 42:3105-3116.

Chang SE, Smedley EB, Stansfield KJ, Stott JJ, Smith KS (2017) Optogenetic inhibition of ventral pallidum neurons impairs context-driven salt seeking. Journal of Neuroscience 37:5670-5680.
Chen BT, Yau H-J, Hatch C, Kusumoto-Yoshida I, Cho SL, Hopf FW, Bonci A (2013) Rescuing cocaine-induced prefrontal cortex hypoactivity prevents compulsive cocaine seeking. Nature 496:359.
Christoph GR, Leonzio RJ, Wilcox KS (1986) Stimulation of the lateral habenula inhibits dopamine-containing neurons in the substantia nigra and ventral tegmental area of the rat. Journal of Neuroscience 6:613-619.
Churchill L, Kalivas PW (1994) A topographically organized gamma-aminobutyric acid projection from the ventral pallidum to the nucleus accumbens in the rat. Journal of Comparative Neurology 345:579-595.
Cooper A, Barnea-Ygael N, Levy D, Shaham Y, Zangen A (2007) A conflict rat model of cue-induced relapse to cocaine seeking. Psychopharmacology 194:117-125.
Creed M, Ntamati NR, Chandra R, Lobo MK, Lüscher C (2016) Convergence of reinforcing and anhedonic cocaine effects in the ventral pallidum. Neuron 92:214-226.
Crombag HS, Bossert JM, Koya E, Shaham Y (2008) Context-induced relapse to drug seeking: a review. Philosophical Transactions of the Royal Society B: Biological Sciences 363:3233-3243.
Cromwell HC, Berridge KC (1993) Where does damage lead to enhanced food aversion: the ventral pallidum/substantia innominata or lateral hypothalamus? Brain research 624:1-10.
Cullinan WE (1992) Projections from the nucleus accumbens to cholinergic neurons of the ventral pallidum: a correlated light and electron microscopic double-immunolabeling study in rat. Brain research 570:92-101.
Day JJ, Wheeler RA, Roitman MF, Carelli RM (2006) Nucleus accumbens neurons encode Pavlovian approach behaviors: evidence from an autoshaping paradigm. European Journal of Neuroscience 23:1341-1351.
De Olmos JS, Heimer L (1999) The concepts of the ventral striatopallidal system and extended amygdala. Annals of the New York Academy of Sciences 877:1-32.
De Wit H, Stewart J (1981) Reinstatement of cocaine-reinforced responding in the rat. Psychopharmacology 75:134-143.
Deroche-Gamonet V, Belin D, Piazza PV (2004) Evidence for addiction-like behavior in the rat. Science 305:1014-1017.
Di Chiara G, Bassareo V (2007) Reward system and addiction: what dopamine does and doesn't do. Current opinion in pharmacology 7:69-76.
Diana M, Raij T, Melis M, Nummenmaa A, Leggio L, Bonci A (2017) Rehabilitating the addicted brain with transcranial magnetic stimulation. Nature Reviews Neuroscience 18:685-693.
DiBenedictis BT, Cheung HK, Nussbaum ER, Veenema AH (2020) Involvement of ventral pallidal vasopressin in the sex-specific regulation of sociosexual motivation in rats. Psychoneuroendocrinology 111:104462.
Economidou D, Pelloux Y, Robbins TW, Dalley JW, Everitt BJ (2009) High impulsivity predicts relapse to cocaine-seeking after punishment-induced abstinence. Biological psychiatry 65:851-856.
Egan TD (1995) Remifentanil pharmacokinetics and pharmacodynamics. Clinical pharmacokinetics 29:80-94.
English JG, Roth BL (2015) Chemogenetics—a transformational and translational platform. JAMA neurology 72:1361-1366.
Epstein DH, Preston KL, Stewart J, Shaham Y (2006) Toward a model of drug relapse: an assessment of the validity of the reinstatement procedure. Psychopharmacology 189:1-16.
Ersche KD, Barnes A, Jones PS, Morein-Zamir S, Robbins TW, Bullmore ET (2011) Abnormal structure of frontostriatal brain systems is associated with aspects of impulsivity and compulsivity in cocaine dependence. Brain 134:2013-2024.

Everitt BJ, Belin D, Economidou D, Pelloux Y, Dalley JW, Robbins TW (2008) Neural mechanisms underlying the vulnerability to develop compulsive drug-seeking habits and addiction. Philosophical Transactions of the Royal Society of London B: Biological Sciences 363:3125-3135.
Faget L, Osakada F, Duan J, Ressler R, Johnson AB, Proudfoot JA, Yoo JH, Callaway EM, Hnasko TS (2016) Afferent inputs to neurotransmitter-defined cell types in the ventral tegmental area. Cell reports 15:2796-2808.
Faget L, Zell V, Souter E, McPherson A, Ressler R, Gutierrez-Reed N, Yoo JH, Dulcis D, Hnasko TS (2018) Opponent control of behavioral reinforcement by inhibitory and excitatory projections from the ventral pallidum. Nature communications 9:849.
Farrar AM, Font L, Pereira M, Mingote S, Bunce JG, Chrobak JJ, Salamone JD (2008) Forebrain circuitry involved in effort-related choice: Injections of the GABAA agonist muscimol into ventral pallidum alter response allocation in food-seeking behavior. Neuroscience 152:321-330.
Farrell MR, Schoch H, Mahler SV (2018) Modeling cocaine relapse in rodents: Behavioral considerations and circuit mechanisms. Prog Neuropsychopharmacol Biol Psychiatry 87:33-47.
Farrell MR, Ye Q, Xie Y, Esteban JSD, Mahler SV (2022) Ventral pallidum GABA neurons bidirectionally control opioid relapse across rat behavioral models. bioRxiv.
Farrell MR, Esteban JSD, Faget L, Floresco SB, Hnasko TS, Mahler SV (2021) Ventral Pallidum GABA Neurons Mediate Motivation Underlying Risky Choice. Journal of Neuroscience 41:4500-4513.
Farrell MR, Ruiz CM, Castillo E, Faget L, Khanbijian C, Liu S, Schoch H, Rojas G, Huerta MY, Hnasko TS (2019) Ventral pallidum is essential for cocaine relapse after voluntary abstinence in rats. Neuropsychopharmacology:1-13.
Fernando ABP, Urcelay GP, Mar AC, Dickinson A, Robbins TW (2014) Safety signals as instrumental reinforcers during free-operant avoidance. Learning & Memory 21:488-497.
Ferster CB, Skinner BF (1957) Schedules of reinforcement.
Floresco SB (2015) The nucleus accumbens: an interface between cognition, emotion, and action. Annual review of psychology 66:25-52.
Floresco SB, Braaksma DN, Phillips AG (1999) Involvement of the ventral pallidum in working memory tasks with or without a delay. Annals of the New York Academy of Sciences 877:711-716.
Floresco SB, Onge JRS, Ghods-Sharifi S, Winstanley CA (2008) Cortico-limbic-striatal circuits subserving different forms of cost-benefit decision making. Cognitive, Affective, & Behavioral Neuroscience 8:375-389.
Floresco SB, West AR, Ash B, Moore H, Grace AA (2003) Afferent modulation of dopamine neuron firing differentially regulates tonic and phasic dopamine transmission. Nature neuroscience 6:968.
Fredriksson I, Applebey SV, Minier-Toribio A, Shekara A, Bossert JM, Shaham Y (2020) Effect of the dopamine stabilizer (-)-OSU6162 on potentiated incubation of opioid craving after electric barrier-induced voluntary abstinence. Neuropsychopharmacology 45:770-779.
Fredriksson I, Venniro M, Reiner DJ, Chow JJ, Bossert JM, Shaham Y (2021) Animal models of drug relapse and craving after voluntary abstinence: a review. Pharmacological Reviews 73:1050-1083.
Fuchs RA, See RE (2002) Basolateral amygdala inactivation abolishes conditioned stimulus-and heroin-induced reinstatement of extinguished heroin-seeking behavior in rats. Psychopharmacology 160:425-433.
Fuchs RA, Branham RK, See RE (2006) Different neural substrates mediate cocaine seeking after abstinence versus extinction training: a critical role for the dorsolateral caudate–putamen. Journal of Neuroscience 26:3584-3588.
Fuchs RA, Ramirez DR, Bell GH (2008) Nucleus accumbens shell and core involvement in drug context-induced reinstatement of cocaine seeking in rats. Psychopharmacology 200:545-556.

Fuchs RA, Evans KA, Ledford CC, Parker MP, Case JM, Mehta RH, See RE (2005) The role of the dorsomedial prefrontal cortex, basolateral amygdala, and dorsal hippocampus in contextual reinstatement of cocaine seeking in rats. Neuropsychopharmacology 30:296.

Fujimoto A, Hori Y, Nagai Y, Kikuchi E, Oyama K, Suhara T, Minamimoto T (2019) Signaling incentive and drive in the primate ventral pallidum for motivational control of goal-directed action. Journal of Neuroscience 39:1793-1804.

Gallo EF, Meszaros J, Sherman JD, Chohan MO, Teboul E, Choi CS, Moore H, Javitch JA, Kellendonk C (2018) Accumbens dopamine D2 receptors increase motivation by decreasing inhibitory transmission to the ventral pallidum. Nature communications 9:1086.

Geisler S, Derst C, Veh RW, Zahm DS (2007) Glutamatergic afferents of the ventral tegmental area in the rat. Journal of Neuroscience 27:5730-5743.

Geisler S, Marinelli M, DeGarmo B, Becker ML, Freiman AJ, Beales M, Meredith GE, Zahm DS (2008) Prominent activation of brainstem and pallidal afferents of the ventral tegmental area by cocaine. Neuropsychopharmacology 33:2688.

Gerfen CR, Surmeier DJ (2011) Modulation of striatal projection systems by dopamine. Annual review of neuroscience 34:441-466.

Gibson GD, Prasad AA, Jean-Richard-dit-Bressel P, Yau JOY, Millan EZ, Liu Y, Campbell EJ, Lim J, Marchant NJ, Power JM (2018) Distinct accumbens shell output pathways promote versus prevent relapse to alcohol seeking. Neuron 98:512-520.

Golden SA, Jin M, Shaham Y (2019) Animal models of (or for) aggression reward, addiction, and relapse: behavior and circuits. Journal of neuroscience:0151-0119.

Goldstein RZ, Volkow ND (2011) Dysfunction of the prefrontal cortex in addiction: neuroimaging findings and clinical implications. Nature reviews neuroscience 12:652-669.

Gomez JL, Bonaventura J, Lesniak W, Mathews WB, Sysa-Shah P, Rodriguez LA, Ellis RJ, Richie CT, Harvey BK, Dannals RF (2017) Chemogenetics revealed: DREADD occupancy and activation via converted clozapine. Science 357:503-507.

Gordon-Fennell AG, Will RG, Ramachandra V, Gordon-Fennell L, Dominguez JM, Zahm DS, Marinelli M (2020) The lateral preoptic area: a novel regulator of reward seeking and neuronal activity in the ventral tegmental area. Frontiers in neuroscience 13:1433.

Grimm JW, Hope BT, Wise RA, Shaham Y (2001) Incubation of cocaine craving after withdrawal. Nature 412:141-142.

Gritti I, Mainville L, Mancia M, Jones BE (1997) GABAergic and other noncholinergic basal forebrain neurons, together with cholinergic neurons, project to the mesocortex and isocortex in the rat. Journal of Comparative Neurology 383:163-177.

Groenewegen HJ, Berendse HW, Haber SN (1993) Organization of the output of the ventral striatopallidal system in the rat: ventral pallidal efferents. Neuroscience 57:113-142.

Haaranen M, Scuppa G, Tambalo S, Järvi V, Bertozzi SM, Armirotti A, Sommer WH, Bifone A, Hyytiä P (2020) Anterior insula stimulation suppresses appetitive behavior while inducing forebrain activation in alcohol-preferring rats. Translational psychiatry 10:1-11.

Haber SN, Nauta WJH (1983) Ramifications of the globus pallidus in the rat as indicated by patterns of immunohistochemistry. Neuroscience 9:245-260.

Haber SN, Watson SJ (1985) The comparative distribution of enkephalin, dynorphin and substance P in the human globus pallidus and basal forebrain. Neuroscience 14:1011-1024.

Haber SN, Groenewegen HJ, Grove EA, Nauta WJH (1985) Efferent connections of the ventral pallidum: evidence of a dual striato pallidofugal pathway. Journal of Comparative Neurology 235:322-335.

Hedegaard H, Miniño A, Spencer M, Warner M Drug Overdose Deaths in the United States, 1999–2020. NCHS Data Brief.

Heimer L, Switzer RD, Van Hoesen GW (1982) Ventral striatum and ventral pallidum: Components of the motor system? Trends in Neurosciences 5:83-87.
Heimer L, Zahm DS, Churchill L, Kalivas PW, Wohltmann C (1991) Specificity in the projection patterns of accumbal core and shell in the rat. Neuroscience 41:89-125.
Heimer L, Harlan RE, Alheid GF, Garcia MM, De Olmos J (1997) Substantia innominata: a notion which impedes clinical–anatomical correlations in neuropsychiatric disorders. Neuroscience 76:957-1006.
Heinsbroek J, Bobadilla A-C, Dereschewitz E, Assali A, Chalhoub RM, Cowan CW, Kalivas PW (2019) Opposing Regulation of Cocaine Seeking by Glutamate and Enkephalin Neurons in the Ventral Pallidum. CELL-REPORTS-D-19-03631.
Heinsbroek JA, Neuhofer DN, Griffin WC, Siegel GS, Bobadilla A-C, Kupchik YM, Kalivas PW (2017) Loss of plasticity in the D2-accumbens pallidal pathway promotes cocaine seeking. Journal of Neuroscience 37:757-767.
Heinsbroek JA, Bobadilla A-C, Dereschewitz E, Assali A, Chalhoub RM, Cowan CW, Kalivas PW (2020) Opposing regulation of cocaine seeking by glutamate and GABA neurons in the ventral pallidum. Cell reports 30:2018-2027.
Hikosaka O (2010) The habenula: from stress evasion to value-based decision-making. Nature reviews neuroscience 11:503.
Hjelmstad GO, Xia Y, Margolis EB, Fields HL (2013) Opioid modulation of ventral pallidal afferents to ventral tegmental area neurons. Journal of Neuroscience 33:6454-6459.
Hnasko TS, Edwards RH (2012) Neurotransmitter co-release: mechanism and physiological role. Annual review of physiology 74:225.
Ho C-Y, Berridge KC (2013) An orexin hotspot in ventral pallidum amplifies hedonic 'liking'for sweetness. Neuropsychopharmacology 38:1655.
Hong S, Jhou TC, Smith M, Saleem KS, Hikosaka O (2011) Negative reward signals from the lateral habenula to dopamine neurons are mediated by rostromedial tegmental nucleus in primates. Journal of Neuroscience 31:11457-11471.
Hu Y, Salmeron BJ, Krasnova IN, Gu H, Lu H, Bonci A, Cadet JL, Stein EA, Yang Y (2019) Compulsive drug use is associated with imbalance of orbitofrontal-and prelimbic-striatal circuits in punishment-resistant individuals. Proceedings of the National Academy of Sciences 116:9066-9071.
Hubner CB, Koob GF (1990) The ventral pallidum plays a role in mediating cocaine and heroin self-administration in the rat. Brain research 508:20-29.
Hunt HF, Brady JV (1955) Some effects of punishment and intercurrent" anxiety" on a simple operant. Journal of Comparative and Physiological Psychology 48:305.
Hunt WA, Barnett LW, Branch LG (1971) Relapse rates in addiction programs. Journal of clinical psychology 27:455-456.
Huys QJM, Maia TV, Frank MJ (2016) Computational psychiatry as a bridge from neuroscience to clinical applications. Nature neuroscience 19:404-413.
Inbar K, Levi LA, Bernat N, Odesser T, Inbar D, Kupchik YM (2020) Cocaine dysregulates dynorphin modulation of inhibitory neurotransmission in the ventral pallidum in a cell-type-specific manner. Journal of Neuroscience 40:1321-1331.
Itoga CA, Berridge KC, Aldridge JW (2016) Ventral pallidal coding of a learned taste aversion. Behavioural brain research 300:175-183.
Jennings JH, Sparta DR, Stamatakis AM, Ung RL, Pleil KE, Kash TL, Stuber GD (2013) Distinct extended amygdala circuits for divergent motivational states. Nature 496:224-228.
Jhou TC, Fields HL, Baxter MG, Saper CB, Holland PC (2009a) The rostromedial tegmental nucleus (RMTg), a GABAergic afferent to midbrain dopamine neurons, encodes aversive stimuli and inhibits motor responses. Neuron 61:786-800.

Jhou TC, Geisler S, Marinelli M, Degarmo BA, Zahm DS (2009b) The mesopontine rostromedial tegmental nucleus: a structure targeted by the lateral habenula that projects to the ventral tegmental area of Tsai and substantia nigra compacta. Journal of Comparative Neurology 513:566-596.
Ji H, Shepard PD (2007) Lateral habenula stimulation inhibits rat midbrain dopamine neurons through a GABAA receptor-mediated mechanism. Journal of Neuroscience 27:6923-6930.
Johnson PI, Stellar JR, Paul AD (1993) Regional reward differences within the ventral pallidum are revealed by microinjections of a mu opiate receptor agonist. Neuropharmacology 32:1305-1314.
Johnson SW, North RA (1992) Opioids excite dopamine neurons by hyperpolarization of local interneurons. Journal of neuroscience 12:483-488.
Kalivas PW, Volkow ND (2005) The neural basis of addiction: a pathology of motivation and choice. American Journal of Psychiatry 162:1403-1413.
Kaplan A, Mizrahi-Kliger AD, Israel Z, Adler A, Bergman H (2020) Dissociable roles of ventral pallidum neurons in the basal ganglia reinforcement learning network. Nature Neuroscience 23:556-564.
Kasanetz F, Lafourcade M, Deroche-Gamonet V, Revest JM, Berson N, Balado E, Fiancette JF, Renault P, Piazza PV, Manzoni OJ (2013) Prefrontal synaptic markers of cocaine addiction-like behavior in rats. Molecular psychiatry 18:729-737.
Kaufling J, Veinante P, Pawlowski SA, Freund-Mercier MJ, Barrot M (2009) Afferents to the GABAergic tail of the ventral tegmental area in the rat. Journal of Comparative Neurology 513:597-621.
Keiflin R, Janak PH (2015) Dopamine prediction errors in reward learning and addiction: from theory to neural circuitry. Neuron 88:247-263.
Kelley AE, Baldo BA, Pratt WE, Will MJ (2005) Corticostriatal-hypothalamic circuitry and food motivation: integration of energy, action and reward. Physiology & behavior 86:773-795.
Knowland D, Lilascharoen V, Pacia CP, Shin S, Wang EH-J, Lim BK (2017) Distinct ventral pallidal neural populations mediate separate symptoms of depression. Cell 170:284-297.
Knutson B, Burgdorf J, Panksepp J (2002) Ultrasonic vocalizations as indices of affective states in rats. Psychological bulletin 128:961.
Kohtz AS, Aston-Jones G (2017) Cocaine seeking during initial abstinence is driven by noradrenergic and serotonergic signaling in hippocampus in a sex-dependent manner. Neuropsychopharmacology 42:408.
Koob GF (2004) A role for GABA mechanisms in the motivational effects of alcohol. Biochemical pharmacology 68:1515-1525.
Koob GF, Volkow ND (2010) Neurocircuitry of addiction. Neuropsychopharmacology 35:217-238.
Krasnova IN, Marchant NJ, Ladenheim B, McCoy MT, Panlilio LV, Bossert JM, Shaham Y, Cadet JL (2014) Incubation of methamphetamine and palatable food craving after punishment-induced abstinence. Neuropsychopharmacology 39:2008.
Kravitz AV, Freeze BS, Parker PRL, Kay K, Thwin MT, Deisseroth K, Kreitzer AC (2010) Regulation of parkinsonian motor behaviours by optogenetic control of basal ganglia circuitry. Nature 466:622.
Kruyer A, Chioma VC, Kalivas PW (2020) The opioid-addicted tetrapartite synapse. Biological psychiatry 87:34-43.
Kruzich PJ, See RE (2001) Differential contributions of the basolateral and central amygdala in the acquisition and expression of conditioned relapse to cocaine-seeking behavior. Journal of Neuroscience 21:RC155-RC155.
Kupchik Y, Prasad AA (2021) Ventral pallidum cellular and pathway specificity in drug seeking. Neuroscience & Biobehavioral Reviews.
Kupchik YM, Kalivas PW (2013) The rostral subcommissural ventral pallidum is a mix of ventral pallidal neurons and neurons from adjacent areas: an electrophysiological study. Brain Structure and Function 218:1487-1500.

Kupchik YM, Brown RM, Heinsbroek JA, Lobo MK, Schwartz DJ, Kalivas PW (2015) Coding the direct/indirect pathways by D1 and D2 receptors is not valid for accumbens projections. Nature neuroscience 18:1230.
Lammel S, Lim BK, Ran C, Huang KW, Betley MJ, Tye KM, Deisseroth K, Malenka RC (2012) Input-specific control of reward and aversion in the ventral tegmental area. Nature 491:212.
LeDoux JE, Moscarello J, Sears R, Campese V (2017) The birth, death and resurrection of avoidance: a reconceptualization of a troubled paradigm. Molecular psychiatry 22:24-36.
Lee D (2013) Decision making: from neuroscience to psychiatry. Neuron 78:233-248.
Lee JDA, Reppucci CJ, Bowden SM, Huez EDM, Bredewold R, Veenema AH (2021) Structural and functional sex differences in the ventral pallidal vasopressin system are associated with the sex-specific regulation of juvenile social play behavior in rats. bioRxiv.
Leone P, Pocock D, Wise RA (1991) Morphine-dopamine interaction: ventral tegmental morphine increases nucleus accumbens dopamine release. Pharmacology Biochemistry and Behavior 39:469-472.
Leung BK, Balleine BW (2013) The ventral striato-pallidal pathway mediates the effect of predictive learning on choice between goal-directed actions. Journal of Neuroscience 33:13848-13860.
Leung BK, Balleine BW (2015) Ventral pallidal projections to mediodorsal thalamus and ventral tegmental area play distinct roles in outcome-specific Pavlovian-instrumental transfer. Journal of Neuroscience 35:4953-4964.
Levi LA, Inbar K, Nachshon N, Bernat N, Gatterer A, Inbar D, Kupchik YM (2019) Projection-specific potentiation of ventral pallidal glutamatergic outputs after abstinence from cocaine. Journal of Neuroscience.
Li Q, Li W, Wang H, Wang Y, Zhang Y, Zhu J, Zheng Y, Zhang D, Wang L, Li Y (2015) Predicting subsequent relapse by drug-related cue-induced brain activation in heroin addiction: an event-related functional magnetic resonance imaging study. Addiction biology 20:968-978.
Lim MM, Murphy AZ, Young LJ (2004) Ventral striatopallidal oxytocin and vasopressin V1a receptors in the monogamous prairie vole (Microtus ochrogaster). Journal of Comparative Neurology 468:555-570.
Lobo MK, Covington HE, Chaudhury D, Friedman AK, Sun H, Damez-Werno D, Dietz DM, Zaman S, Koo JW, Kennedy PJ (2010) Cell type–specific loss of BDNF signaling mimics optogenetic control of cocaine reward. Science 330:385-390.
Lüscher C (2016) The emergence of a circuit model for addiction. Annual review of neuroscience 39.
Lüscher C, Robbins TW, Everitt BJ (2020) The transition to compulsion in addiction. Nature Reviews Neuroscience:1-17.
MacLaren DAA, Browne RW, Shaw JK, Radhakrishnan SK, Khare P, España RA, Clark SD (2016) Clozapine N-oxide administration produces behavioral effects in Long–Evans rats: implications for designing DREADD experiments. eneuro 3.
Mahler SV, Aston-Jones GS (2012) Fos activation of selective afferents to ventral tegmental area during cue-induced reinstatement of cocaine seeking in rats. Journal of Neuroscience 32:13309-13325.
Mahler SV, Aston-Jones G (2018) CNO Evil? Considerations for the use of DREADDs in behavioral neuroscience. Neuropsychopharmacology 43:934.
Mahler SV, Smith RJ, Aston-Jones G (2013a) Interactions between VTA orexin and glutamate in cue-induced reinstatement of cocaine seeking in rats. Psychopharmacology 226:687-698.
Mahler SV, Moorman DE, Feltenstein MW, Cox BM, Ogburn KB, Bachar M, McGonigal JT, Ghee SM, See RE (2013b) A rodent “self-report” measure of methamphetamine craving? Rat ultrasonic vocalizations during methamphetamine self-administration, extinction, and reinstatement. Behavioural brain research 236:78-89.

Mahler SV, Vazey EM, Beckley JT, Keistler CR, McGlinchey EM, Kaufling J, Wilson SP, Deisseroth K, Woodward JJ, Aston-Jones G (2014) Designer receptors show role for ventral pallidum input to ventral tegmental area in cocaine seeking. Nature neuroscience 17:577.
Mahler SV, Brodnik ZD, Cox BM, Buchta WC, Bentzley BS, Quintanilla J, Cope ZA, Lin EC, Riedy MD, Scofield MD (2019) Chemogenetic Manipulations of Ventral Tegmental Area Dopamine Neurons Reveal Multifaceted Roles in Cocaine Abuse. Journal of Neuroscience 39:503-518.
Mantsch JR, Baker DA, Funk D, Lê AD, Shaham Y (2016) Stress-induced reinstatement of drug seeking: 20 years of progress. Neuropsychopharmacology 41:335.
Manvich DF, Webster KA, Foster SL, Farrell MS, Ritchie JC, Porter JH, Weinshenker D (2018) The DREADD agonist clozapine N-oxide (CNO) is reverse-metabolized to clozapine and produces clozapine-like interoceptive stimulus effects in rats and mice. Scientific reports 8:3840.
Marchant NJ, Li X, Shaham Y (2013a) Recent developments in animal models of drug relapse. Current opinion in neurobiology 23:675-683.
Marchant NJ, Khuc TN, Pickens CL, Bonci A, Shaham Y (2013b) Context-induced relapse to alcohol seeking after punishment in a rat model. Biological psychiatry 73:256-262.
Marchant NJ, Campbell EJ, Pelloux Y, Bossert JM, Shaham Y (2018) Context-induced relapse after extinction versus punishment: similarities and differences. Psychopharmacology:1-10.
Marchant NJ, Campbell EJ, Pelloux Y, Bossert JM, Shaham Y (2019) Context-induced relapse after extinction versus punishment: similarities and differences. Psychopharmacology 236:439-448.
Marchant NJ, Rabei R, Kaganovsky K, Caprioli D, Bossert JM, Bonci A, Shaham Y (2014) A critical role of lateral hypothalamus in context-induced relapse to alcohol seeking after punishment-imposed abstinence. Journal of Neuroscience 34:7447-7457.
Marchant NJ, Campbell EJ, Whitaker LR, Harvey BK, Kaganovsky K, Adhikary S, Hope BT, Heins RC, Prisinzano TE, Vardy E (2016) Role of ventral subiculum in context-induced relapse to alcohol seeking after punishment-imposed abstinence. Journal of Neuroscience 36:3281-3294.
McAlonan GM, Robbins TW, Everitt BJ (1993) Effects of medial dorsal thalamic and ventral pallidal lesions on the acquisition of a conditioned place preference: further evidence for the involvement of the ventral striatopallidal system in reward-related processes. Neuroscience 52:605-620.
McFarland K, Kalivas PW (2001) The circuitry mediating cocaine-induced reinstatement of drug-seeking behavior. Journal of Neuroscience 21:8655-8663.
McFarland K, Lapish CC, Kalivas PW (2003) Prefrontal glutamate release into the core of the nucleus accumbens mediates cocaine-induced reinstatement of drug-seeking behavior. Journal of neuroscience 23:3531-3537.
McFarland K, Davidge SB, Lapish CC, Kalivas PW (2004) Limbic and motor circuitry underlying footshock-induced reinstatement of cocaine-seeking behavior. Journal of Neuroscience 24:1551-1560.
McGovern DJ, Root DH (2019) Ventral pallidum: a promising target for addiction intervention. Neuropsychopharmacology 44:2151-2152.
McReynolds JR, Christianson JP, Blacktop JM, Mantsch JR (2018) What does the Fos say? Using Fos-based approaches to understand the contribution of stress to substance use disorders. Neurobiology of stress 9:271-285.
Meye FJ, Soiza-Reilly M, Smit T, Diana MA, Schwarz MK, Mameli M (2016) Shifted pallidal co-release of GABA and glutamate in habenula drives cocaine withdrawal and relapse. Nature neuroscience 19:1019-1024.
Mitchell MR, Weiss VG, Beas BS, Morgan D, Bizon JL, Setlow B (2014) Adolescent risk taking, cocaine self-administration, and striatal dopamine signaling. Neuropsychopharmacology 39:955.
Mogenson GJ, Jones DL, Yim CY (1980) From motivation to action: functional interface between the limbic system and the motor system. Progress in neurobiology 14:69-97.

Mohammadkhani A, Fragale JE, Pantazis CB, Bowrey HE, James MH, Aston-Jones G (2019) Orexin-1 receptor signaling in ventral pallidum regulates motivation for the opioid remifentanil. Journal of Neuroscience 39:9831-9840.
Morgane PJ (1961) Alterations in feeding and drinking behavior of rats with lesions in globi pallidi. American Journal of Physiology-Legacy Content 201:420-428.
Napier TC, Mitrovic I (1999) Opioid modulation of ventral pallidal inputs. Annals of the New York Academy of Sciences 877:176-201.
Nation HL, Nicoleau M, Kinsman BJ, Browning KN, Stocker SD (2016) DREADD-induced activation of subfornical organ neurons stimulates thirst and salt appetite. Journal of neurophysiology 115:3123-3129.
National Research C (2010) Guide for the care and use of laboratory animals: National Academies Press.
O'Brien CP, Childress AR, McLellan AT, Ehrman R (1992) Classical Conditioning in Drug-Dependent Humans a. Annals of the New York Academy of Sciences 654:400-415.
O'Brien CP, Childress AR, Ehrman R, Robbins SJ (1998) Conditioning factors in drug abuse: can they explain compulsion? Journal of psychopharmacology 12:15-22.
Oleson EB, Gentry RN, Chioma VC, Cheer JF (2012) Subsecond dopamine release in the nucleus accumbens predicts conditioned punishment and its successful avoidance. Journal of Neuroscience 32:14804-14808.
Omelchenko N, Bell R, Sesack SR (2009) Lateral habenula projections to dopamine and GABA neurons in the rat ventral tegmental area. European Journal of Neuroscience 30:1239-1250.
Onge JRS, Abhari H, Floresco SB (2011) Dissociable contributions by prefrontal D1 and D2 receptors to risk-based decision making. Journal of Neuroscience 31:8625-8633.
Orsini CA, Trotta RT, Bizon JL, Setlow B (2015a) Dissociable roles for the basolateral amygdala and orbitofrontal cortex in decision-making under risk of punishment. Journal of Neuroscience 35:1368-1379.
Orsini CA, Moorman DE, Young JW, Setlow B, Floresco SB (2015b) Neural mechanisms regulating different forms of risk-related decision-making: Insights from animal models. Neuroscience & Biobehavioral Reviews 58:147-167.
Orsini CA, Willis ML, Gilbert RJ, Bizon JL, Setlow B (2016) Sex differences in a rat model of risky decision making. Behavioral neuroscience 130:50.
Orsini CA, Hernandez CM, Singhal S, Kelly KB, Frazier CJ, Bizon JL, Setlow B (2017) Optogenetic inhibition reveals distinct roles for basolateral amygdala activity at discrete time points during risky decision making. Journal of Neuroscience 37:11537-11548.
Ottenheimer D, Richard JM, Janak PH (2018) Ventral pallidum encodes relative reward value earlier and more robustly than nucleus accumbens. Nature communications 9:4350.
Ottenheimer DJ, Bari BA, Sutlief E, Fraser KM, Kim TH, Richard JM, Cohen JY, Janak PH (2020) A quantitative reward prediction error signal in the ventral pallidum. Nature neuroscience 23:1267-1276.
O'Neal TJ, Nooney MN, Thien K, Ferguson SM (2019) Chemogenetic modulation of accumbens direct or indirect pathways bidirectionally alters reinstatement of heroin-seeking in high-but not low-risk rats. Neuropsychopharmacology:1-12.
Panagis G, Miliaressis E, Anagnostakis Y, Spyraki C (1995) Ventral pallidum self-stimulation: a moveable electrode mapping study. Behavioural brain research 68:165-172.
Panlilio LV, Thorndike EB, Schindler CW (2003) Reinstatement of punishment-suppressed opioid self-administration in rats: an alternative model of relapse to drug abuse. Psychopharmacology 168:229-235.
Panlilio LV, Thorndike EB, Schindler CW (2005) Lorazepam reinstates punishment-suppressed remifentanil self-administration in rats. Psychopharmacology 179:374-382.

Pardo-Garcia TR, Garcia-Keller C, Penaloza T, Richie CT, Pickel J, Hope BT, Harvey BK, Kalivas PW, Heinsbroek JA (2019) Ventral pallidum is the primary target for accumbens D1 projections driving cocaine seeking. Journal of Neuroscience 39:2041-2051.
Parent A, Hazrati L-N (1995) Functional anatomy of the basal ganglia. I. The cortico-basal ganglia-thalamo-cortical loop. Brain research reviews 20:91-127.
Paxinos G, Watson C (2006) The rat brain in stereotaxic coordinates: hard cover edition: Elsevier.
Pelloux Y, Everitt BJ, Dickinson A (2007) Compulsive drug seeking by rats under punishment: effects of drug taking history. Psychopharmacology 194:127-137.
Pelloux Y, Minier-Toribio A, Hoots JK, Bossert JM, Shaham Y (2018a) Opposite effects of basolateral amygdala inactivation on context-induced relapse to cocaine seeking after extinction versus punishment. Journal of Neuroscience 38:51-59.
Pelloux Y, Hoots JK, Cifani C, Adhikary S, Martin J, Minier-Toribio A, Bossert JM, Shaham Y (2018b) Context-induced relapse to cocaine seeking after punishment-imposed abstinence is associated with activation of cortical and subcortical brain regions. Addiction biology 23:699-712.
Perrotti LI, Bolaños CA, Choi KH, Russo SJ, Edwards S, Ulery PG, Wallace DL, Self DW, Nestler EJ, Barrot M (2005) ΔFosB accumulates in a GABAergic cell population in the posterior tail of the ventral tegmental area after psychostimulant treatment. European Journal of Neuroscience 21:2817-2824.
Perry CJ, McNally GP (2013) A role for the ventral pallidum in context-induced and primed reinstatement of alcohol seeking. European Journal of Neuroscience 38:2762-2773.
Pessiglione M, Schmidt L, Draganski B, Kalisch R, Lau H, Dolan RJ, Frith CD (2007) How the brain translates money into force: a neuroimaging study of subliminal motivation. Science 316:904-906.
Pickens CL, Airavaara M, Theberge F, Fanous S, Hope BT, Shaham Y (2011) Neurobiology of the incubation of drug craving. Trends in neurosciences 34:411-420.
Pierce RC, Kumaresan V (2006) The mesolimbic dopamine system: the final common pathway for the reinforcing effect of drugs of abuse? Neuroscience & biobehavioral reviews 30:215-238.
Pleil KE, Rinker JA, Lowery-Gionta EG, Mazzone CM, McCall NM, Kendra AM, Olson DP, Lowell BB, Grant KA, Thiele TE (2015) NPY signaling inhibits extended amygdala CRF neurons to suppress binge alcohol drinking. Nature neuroscience 18:545-552.
Portfors CV (2007) Types and functions of ultrasonic vocalizations in laboratory rats and mice. Journal of the American Association for Laboratory Animal Science 46:28-34.
Prasad AA, McNally GP (2016) Ventral pallidum output pathways in context-induced reinstatement of alcohol seeking. Journal of Neuroscience 36:11716-11726.
Prasad AA, McNally GP (2019) Ventral Pallidum and Alcohol Addiction. In: Neuroscience of Alcohol, pp 163-170: Elsevier.
Prasad AA, McNally GP (2020) The ventral pallidum and relapse to alcohol seeking. British Journal of Pharmacology.
Prasad AA, Xie C, Chaichim C, Killcross S, Power JM, McNally GP (2019) Complementary roles for ventral pallidum cell types and their projections in relapse. bioRxiv:533554.
Prasad AA, Xie C, Chaichim C, Nguyen JH, McClusky HE, Killcross S, Power JM, McNally GP (2020) Complementary roles for ventral pallidum cell types and their projections in relapse. Journal of Neuroscience 40:880-893.
Pribiag H, Shin S, Wang EH-J, Sun F, Datta P, Okamoto A, Guss H, Jain A, Wang X-Y, De Freitas B (2021) Ventral pallidum DRD3 potentiates a pallido-habenular circuit driving accumbal dopamine release and cocaine seeking. Neuron.
Redish AD (2004) Addiction as a computational process gone awry. Science 306:1944-1947.
Redish AD, Gordon JA (2016) Computational psychiatry: New perspectives on mental illness: MIT Press.

Redish AD, Jensen S, Johnson A (2008) Addiction as vulnerabilities in the decision process. Behavioral and brain sciences 31:461-487.
Reil JC (1809) Untersuchungen über den Bau des grossen Gehirns im Menschen. Arch Physiol 9:136-208.
Reiner DJ, Fredriksson I, Lofaro OM, Bossert JM, Shaham Y (2019) Relapse to opioid seeking in rat models: behavior, pharmacology and circuits. Neuropsychopharmacology 44:465-477.
Richard JM, Ambroggi F, Janak PH, Fields HL (2016) Ventral pallidum neurons encode incentive value and promote cue-elicited instrumental actions. Neuron 90:1165-1173.
Richard JM, Stout N, Acs D, Janak PH (2018) Ventral pallidal encoding of reward-seeking behavior depends on the underlying associative structure. Elife 7:e33107.
Ritz MC, Lamb RJ, Goldberg SR, Kuhar MJ (1987) Cocaine receptors on dopamine transporters are related to self-administration of cocaine. Science 237:1219-1223.
Robinson TE, Berridge KC (1993) The neural basis of drug craving: an incentive-sensitization theory of addiction. Brain research reviews 18:247-291.
Rogers JL, Ghee S, See RE (2008a) The neural circuitry underlying reinstatement of heroin-seeking behavior in an animal model of relapse. Neuroscience 151:579-588.
Rogers JL, Ghee S, See RE (2008b) The neural circuitry underlying reinstatement of heroin-seeking behavior in an animal model of relapse. Neuroscience 151:579-588.
Root DH, Melendez RI, Zaborszky L, Napier TC (2015) The ventral pallidum: Subregion-specific functional anatomy and roles in motivated behaviors. Progress in neurobiology 130:29-70.
Root DH, Fabbricatore AT, Ma S, Barker DJ, West MO (2010) Rapid phasic activity of ventral pallidal neurons during cocaine self-administration. Synapse 64:704-713.
Root DH, Ma S, Barker DJ, Megehee L, Striano BM, Ralston CM, Fabbricatore AT, West MO (2013) Differential roles of ventral pallidum subregions during cocaine self-administration behaviors. Journal of Comparative Neurology 521:558-588.
Roth BL (2016) DREADDs for neuroscientists. Neuron 89:683-694.
Roth BL, Irwin JJ, Shoichet BK (2017) Discovery of new GPCR ligands to illuminate new biology. Nature chemical biology 13:1143-1151.
Saga Y, Hoshi E, Tremblay L (2017) Roles of multiple globus pallidus territories of monkeys and humans in motivation, cognition and action: an anatomical, physiological and pathophysiological review. Frontiers in neuroanatomy 11:30.
Saga Y, Richard A, Sgambato-Faure V, Hoshi E, Tobler PN, Tremblay L (2016) Ventral pallidum encodes contextual information and controls aversive behaviors. Cerebral Cortex 27:2528-2543.
Salamone JD, Correa M (2012) The mysterious motivational functions of mesolimbic dopamine. Neuron 76:470-485.
Salamone JD, Correa M, Farrar A, Mingote SM (2007) Effort-related functions of nucleus accumbens dopamine and associated forebrain circuits. Psychopharmacology 191:461-482.
Sangha S, Diehl MM, Bergstrom HC, Drew MR (2020) Know safety, no fear. Neuroscience & Biobehavioral Reviews 108:218-230.
Seal RP, Edwards RH (2006) Functional implications of neurotransmitter co-release: glutamate and GABA share the load. Current opinion in pharmacology 6:114-119.
Serre F, Fatseas M, Swendsen J, Auriacombe M (2015) Ecological momentary assessment in the investigation of craving and substance use in daily life: a systematic review. Drug and alcohol dependence 148:1-20.
Shaham Y, Erb S, Stewart J (2000) Stress-induced relapse to heroin and cocaine seeking in rats: a review. Brain Research Reviews 33:13-33.
Shaham Y, Shalev U, Lu L, De Wit H, Stewart J (2003) The reinstatement model of drug relapse: history, methodology and major findings. Psychopharmacology 168:3-20.

Shalev U, Grimm JW, Shaham Y (2002) Neurobiology of relapse to heroin and cocaine seeking: a review. Pharmacological reviews 54:1-42.
Sharma PK, Wells L, Rizzo G, Elson JL, Passchier J, Rabiner EA, Gunn RN, Dexter DT, Pienaar IS (2020) DREADD activation of pedunculopontine cholinergic neurons reverses motor deficits and restores striatal dopamine signaling in parkinsonian rats. Neurotherapeutics:1-22.
Sharpe MJ, Marchant NJ, Whitaker LR, Richie CT, Zhang YJ, Campbell EJ, Koivula PP, Necarsulmer JC, Mejias-Aponte C, Morales M (2017) Lateral hypothalamic GABAergic neurons encode reward predictions that are relayed to the ventral tegmental area to regulate learning. Current Biology 27:2089-2100.
Siciliano CA, Noamany H, Chang C-J, Brown AR, Chen X, Leible D, Lee JJ, Wang J, Vernon AN, Vander Weele CM (2019) A cortical-brainstem circuit predicts and governs compulsive alcohol drinking. Science 366:1008-1012.
Silberman Y, Bajo M, Chappell AM, Christian DT, Cruz M, Diaz MR, Kash T, Lack AK, Messing RO, Siggins GR (2009) Neurobiological mechanisms contributing to alcohol–stress–anxiety interactions. Alcohol 43:509-519.
Simmons WK, Rapuano KM, Ingeholm JE, Avery J, Kallman S, Hall KD, Martin A (2014) The ventral pallidum and orbitofrontal cortex support food pleasantness inferences. Brain Structure and Function 219:473-483.
Simon NW, Setlow B (2012) Modeling risky decision making in rodents. In: Psychiatric Disorders, pp 165-175: Springer.
Simon NW, Gilbert RJ, Mayse JD, Bizon JL, Setlow B (2009) Balancing risk and reward: a rat model of risky decision making. Neuropsychopharmacology 34:2208.
Sinha R (2001) How does stress increase risk of drug abuse and relapse? Psychopharmacology 158:343-359.
Sinha R, Li CSR (2007) Imaging stress-and cue-induced drug and alcohol craving: association with relapse and clinical implications. Drug and alcohol review 26:25-31.
Smedley EB, DiLeo A, Smith KS (2019) Circuit directionality for motivation: lateral accumbens-pallidum, but not pallidum-accumbens, connections regulate motivational attraction to reward cues. Neurobiology of learning and memory 162:23-35.
Smith KS, Berridge KC (2005) The ventral pallidum and hedonic reward: neurochemical maps of sucrose "liking" and food intake. Journal of neuroscience 25:8637-8649.
Smith KS, Berridge KC (2007) Opioid limbic circuit for reward: interaction between hedonic hotspots of nucleus accumbens and ventral pallidum. Journal of neuroscience 27:1594-1605.
Smith KS, Berridge KC, Aldridge JW (2011) Disentangling pleasure from incentive salience and learning signals in brain reward circuitry. Proceedings of the National Academy of Sciences 108:E255-E264.
Smith KS, Tindell AJ, Aldridge JW, Berridge KC (2009) Ventral pallidum roles in reward and motivation. Behavioural brain research 196:155-167.
Smith KS, Bucci DJ, Luikart BW, Mahler SV (2016) DREADDS: Use and application in behavioral neuroscience. Behavioral neuroscience 130:137.
Smith RJ, Aston-Jones G (2012) Orexin/hypocretin 1 receptor antagonist reduces heroin self-administration and cue-induced heroin seeking. European Journal of Neuroscience 35:798-804.
Smith RJ, Laiks LS (2018) Behavioral and neural mechanisms underlying habitual and compulsive drug seeking. Progress in Neuro-Psychopharmacology and Biological Psychiatry 87:11-21.
Spear LP (2000) The adolescent brain and age-related behavioral manifestations. Neuroscience & biobehavioral reviews 24:417-463.

Spix TA, Nanivadekar S, Toong N, Kaplow IM, Isett BR, Goksen Y, Pfenning AR, Gittis AH (2021) Population-specific neuromodulation prolongs therapeutic benefits of deep brain stimulation. Science 374:201-206.
Stefanik MT, Kupchik YM, Brown RM, Kalivas PW (2013) Optogenetic evidence that pallidal projections, not nigral projections, from the nucleus accumbens core are necessary for reinstating cocaine seeking. Journal of Neuroscience 33:13654-13662.
Stephenson-Jones M (2019) Pallidal circuits for aversive motivation and learning. Current Opinion in Behavioral Sciences 26:82-89.
Stephenson-Jones M, Bravo-Rivera C, Ahrens S, Furlan A, Xiao X, Fernandes-Henriques C, Li B (2020) Opposing contributions of GABAergic and glutamatergic ventral pallidal neurons to motivational behaviors. Neuron 105:921-933.
Sternson SM, Roth BL (2014) Chemogenetic tools to interrogate brain functions. Annual review of neuroscience 37:387-407.
Stratford TR, Kelley AE, Simansky KJ (1999) Blockade of GABAA receptors in the medial ventral pallidum elicits feeding in satiated rats. Brain research 825:199-203.
Surmeier DJ, Ding J, Day M, Wang Z, Shen W (2007) D1 and D2 dopamine-receptor modulation of striatal glutamatergic signaling in striatal medium spiny neurons. Trends in neurosciences 30:228-235.
Swanson LW, Cowan WM (1975) A note on the connections and development of the nucleus accumbens. Brain research 92:324-330.
Szablowski JO, Lee-Gosselin A, Lue B, Malounda D, Shapiro MG (2018) Acoustically targeted chemogenetics for the non-invasive control of neural circuits. Nature biomedical engineering 2:475-484.
Tachibana Y, Hikosaka O (2012) The primate ventral pallidum encodes expected reward value and regulates motor action. Neuron 76:826-837.
Tindell AJ, Berridge KC, Aldridge JW (2004) Ventral pallidal representation of pavlovian cues and reward: population and rate codes. Journal of Neuroscience 24:1058-1069.
Tindell AJ, Smith KS, Berridge KC, Aldridge JW (2009) Dynamic computation of incentive salience:“wanting” what was never “liked”. Journal of Neuroscience 29:12220-12228.
Tooley J, Marconi L, Alipio JB, Matikainen-Ankney B, Georgiou P, Kravitz AV, Creed MC (2018) Glutamatergic ventral pallidal neurons modulate activity of the habenula–tegmental circuitry and constrain reward seeking. Biological psychiatry 83:1012-1023.
Torres OV, Jayanthi S, Ladenheim B, McCoy MT, Krasnova IN, Cadet JL (2017) Compulsive methamphetamine taking under punishment is associated with greater cue-induced drug seeking in rats. Behavioural brain research 326:265-271.
Tritsch NX, Granger AJ, Sabatini BL (2016) Mechanisms and functions of GABA co-release. Nature Reviews Neuroscience 17:139-145.
Turner MS, Gray TS, Mickiewicz AL, Napier TC (2008) Fos expression following activation of the ventral pallidum in normal rats and in a model of Parkinson’s Disease: implications for limbic system and basal ganglia interactions. Brain Structure and Function 213:197-213.
Vachez YM, Tooley JR, Abiraman K, Matikainen-Ankney B, Casey E, Earnest T, Ramos LM, Silberberg H, Godynyuk E, Uddin O (2021) Ventral arkypallidal neurons inhibit accumbal firing to promote reward consumption. Nature neuroscience 24:379-390.
Van Haaren F, Meyer ME (1991) Sex differences in locomotor activity after acute and chronic cocaine administration. Pharmacology Biochemistry and Behavior 39:923-927.
Vanderschuren LJMJ, Everitt BJ (2004) Drug seeking becomes compulsive after prolonged cocaine self-administration. Science 305:1017-1019.
Vanderschuren LJMJ, Minnaard AM, Smeets JAS, Lesscher HMB (2017) Punishment models of addictive behavior. Current opinion in behavioral sciences 13:77-84.

Vaswani M, Linda FK, Ramesh S (2003) Role of selective serotonin reuptake inhibitors in psychiatric disorders: a comprehensive review. Progress in neuro-psychopharmacology and biological psychiatry 27:85-102.
Venniro M, Caprioli D, Shaham Y (2016) Animal models of drug relapse and craving: from drug priming-induced reinstatement to incubation of craving after voluntary abstinence. Progress in brain research 224:25-52.
Venniro M, Banks ML, Heilig M, Epstein DH, Shaham Y (2020) Improving translation of animal models of addiction and relapse by reverse translation. Nature Reviews Neuroscience:1-19.
Venniro M, Zhang M, Caprioli D, Hoots JK, Golden SA, Heins C, Morales M, Epstein DH, Shaham Y (2018) Volitional social interaction prevents drug addiction in rat models. Nature neuroscience 21:1520.
Venniro M, Caprioli D, Zhang M, Whitaker LR, Zhang S, Warren BL, Cifani C, Marchant NJ, Yizhar O, Bossert JM (2017) The anterior insular cortex→ central amygdala glutamatergic pathway is critical to relapse after contingency management. Neuron 96:414-427.
Wakabayashi KT, Feja M, Baindur AN, Bruno MJ, Bhimani RV, Park J, Hausknecht K, Shen R-Y, Haj-Dahmane S, Bass CE (2019) Chemogenetic activation of ventral tegmental area GABA neurons, but not mesoaccumbal GABA terminals, disrupts responding to reward-predictive cues. Neuropsychopharmacology 44:372.
Wang F, Zhang J, Yuan Y, Chen M, Gao Z, Zhan S, Fan C, Sun W, Hu J (2020) Salience processing by glutamatergic neurons in the ventral pallidum. Science Bulletin 65:389-401.
Wikler A (1973) Dynamics of drug dependence: Implications of a conditioning theory for research and treatment. Archives of general psychiatry 28:611-616.
Williams DJ, Crossman AR, Slater P (1977) The efferent projections of the nucleus accumbens in the rat. Brain Research 130:217-227.
Wolffgramm J (1991) An ethopharmacological approach to the development of drug addiction. Neuroscience & Biobehavioral Reviews 15:515-519.
Wulff AB, Tooley J, Marconi LJ, Creed MC (2018) Ventral pallidal modulation of aversion processing. Brain research.
Yager LM, Garcia AF, Donckels EA, Ferguson SM (2019) Chemogenetic inhibition of direct pathway striatal neurons normalizes pathological, cue-induced reinstatement of drug-seeking in rats. Addiction biology 24:251-264.
Yoshimura M, Nishimura K, Nishimura H, Sonoda S, Ueno H, Motojima Y, Saito R, Maruyama T, Nonaka Y, Ueta Y (2017) Activation of endogenous arginine vasopressin neurons inhibit food intake: by using a novel transgenic rat line with DREADDs system. Scientific reports 7:1-10.
Zahm DS (1989) The ventral striatopallidal parts of the basal ganglia in the rat—II. Compartmentation of ventral pallidal efferents. Neuroscience 30:33-50.
Zahm DS, Heimer L (1988) Ventral striatopallidal parts of the basal ganglia in the rat: I. Neurochemical compartmentation as reflected by the distributions of neurotensin and substance P immunoreactivity. Journal of Comparative Neurology 272:516-535.
Zahm DS, Heimer L (1990) Two transpallidal pathways originating in the rat nucleus accumbens. Journal of Comparative Neurology 302:437-446.
Zahm DS, Williams E, Wohltmann C (1996) Ventral striatopallidothalamic projection: IV. Relative involvements of neurochemically distinct subterritories in the ventral pallidum and adjacent parts of the rostroventral forebrain. Journal of Comparative Neurology 364:340-362.
Zhou L, Pruitt C, Shin CB, Garcia AD, Zavala AR, See RE (2014) Fos expression induced by cocaine-conditioned cues in male and female rats. Brain Structure and Function 219:1831-1840.
Zhu C, Yao Y, Xiong Y, Cheng M, Chen J, Zhao R, Liao F, Shi R, Song S (2017) Somatostatin neurons in the basal forebrain promote high-calorie food intake. Cell reports 20:112-123.